AT MICROFICHE REFERENCE LIBRARY

A project of Volunteers in Asia

Horizontal Axis Fast Running Wind Turbines for
Developing Countries

by: W.A.M. Jansen

Published by:
    Steering Committee for Windenergy in
      Developing Countries
    P.O. Box 85
    3800 AB Amersfoort
    The Netherlands

Paper copies are $ 7.00; single copies are
available for free to research institutes in
developing countries.

Available from:
    Steering Committee for Windenergy in
      Developing Countries
    P.O. Box 85
    3800 AB Amersfoort
    The Netherlands

Reproduced by permission of the Steering Committee
for Windenergy in Developing Countries.

horizontal axis fast running wind turbines for developing countries

by W.A.M. Jansen

June 1976

HORIZONTAL-AXIS FAST RUNNING WIND
TURBINES FOR DEVELOPING COUNTRIES

by

Initials:

W.A.M. JANSEN

June, 1976

11663/3

TABLE OF CONTENTS   page

Errata: Horizontal-axis fast running wind turbines for developing countries.

page:	place:	error:	read:
2	line 16	op power	of power
4	line 23	η_β	η_B
9	line 6	Appendix I	Appendix II
15	3rd line above last line	0.25 %	1 %
20	fig. 1.9b	propeller	windmill rotor
20	3rd line above last line	page 13	page 14
20	last line		add: where for sin ϕ should be taken $\frac{r}{R}$ sin $\frac{\phi}{2}$
25	(1-58)	C_Y under line	C_Y above line
27	fig. 2.1	C. mast + pole	C. mast + sail
27	line 10	3. masts + poles	3. masts + sails
39	fig. 2.7b	moment on left side moment on right side	M_1 M_2
41	(2-17)	$Y^{'''}$	$y^{'''}$
41	(2-18)	$y = \frac{Y}{R}$	$Y = \frac{y}{R}$
41	(2-23)	$C_1 = \frac{F_m R^3}{2EI}(1-x^2)$	$C_1 = \frac{F_m R^3}{2EI}$

Summary

This report gives briefly the theories that form the basis for calcu-
lation of the design and the behaviour of a windmill. A modification
of the Prandtl model of tip losses is derived. This modification takes
the relatively heavy loading of the windmill rotor into account. It is
argumented that, in contrast with propeller design, a maximum energy
extraction is reached by enlarging the chords of the blades near the
tips. Selection, design and construction of several rotors and of a
test unit are described. Tests of steel plate rotors and so-called
sail trouser rotors are described while test results are presented
in the form of $C_p-\lambda$ and $C_Q-\lambda$ characteristics. Final conclusion is
that with simple materials high power coefficients are possible.

List of symbols

a	axial interference factor	(-)
a'	tangential interference factor	(-)
a^*	factor a for an ideal windmill	(-)
a'^*	factor a' for an ideal windmill	(-)
a_n	polynomial coefficient	(-)
A	area	(m^2)
A_1	wake cross section area	(m^2)
B	number of blades	(-)
c	chord	(m)
C_L	sectional lift coefficient	(-)
C_D	sectional drag coefficient	(-)
C_x	sectional force coefficient in x-direction	(-)
C_y	sectional force coefficient in y-direction	(-)
C_p	power coefficient	(-)
C_Q	torque coefficient	(-)
C_W	loss op power coefficient due to airfoil drag	(-)
C^*, C_1, C_2	constants	
d	diameter	(m)
D	drag force	(N)
E	elasticity modulus	(Nm^{-2})
f	plate bending	(m)
	factor in F	(-)
F	circulation reduction factor	(-)
F_c	centrifugal force	(N)
F_x	force in x-direction	(N)
F_y	force in y-direction	(N)

F_m	maximum force per unit of length	(Nm^{-1})
F_t	force in tangential direction	(N)
F_g	force of generator on force transducer	(N)
h	height of watercolumn	(m)
	thickness of steelplate	(m)
I	moment	(m^4)
l	arm length	(m)
L	lift force	(N)
M	bending moment	(Nm)
M_t	torsional moment	(Nm)
m	mass	(kg)
$\dot{m}$	mass flow	(kgs^{-1})
n	number of revolutions	(s^{-1})
	coefficient index	$(-)$
p	pressure	(Nm^{-2})
	pitch	(m)
p_o	atmospheric pressure	(Nm^{-2})
p'	pressure immediately behind the rotor	(Nm^{-2})
p	power	(Nms^{-1})
Q	torque	(Nm)
q	distance	(m)
r	radius	(m)
R	rotor radius	(m)
R_a	arching radius	(m)
Re	Reynolds number	$(-)$
s	standard deviation	$(-)$
	distance between vortex sheets	(m)
S	cable tension	(N)

s_x	sub quantity for calculation of interference factor a'	(-)
s_y	sub quantity for calculation of interference factor a	(-)
T	thrust force	(N)
	temperature	(K)
U	axial flow velocity through rotor	(ms^{-1})
U_1	axial flow velocity in fully developed wake	(ms^{-1})
V	velocity	(ms^{-1})
V_∞	undisturbed flow velocity	(ms^{-1})
v^*	swept volume	(m^3)
W	relative flow velocity through rotor	(ms^{-1})
W_b	resisting moment	(m^3)
x	direction, variable	
y	direction, variable	
	deflection	(m)
X	dimensionless variable	
Y	dimensionless variable	
α	angle of incidence	(-)
β	blade setting, blade angle	(-)
Γ	circulation	(m^2s^{-1})
Γ_∞	circulation if the number of blades were infinite	(m^2s^{-1})
η	efficiency	(-)
η_a	aerodynamic efficiency	(-)
η_β	factor for influence of number of blades	(-)
η_w	efficiency factor for bladefriction	(-)
λ	tip speed ratio	(-)

λ_r	speed ratio of element at radius r	$(-)$
ν	kinematic viscosity	$(m^2 s^{-1})$
ρ	fluid density	(kgm^{-3})
ρ_m	material density	(kgm^{-3})
ρ_{bl}	blade mass per unit of length	(kgm^{-1})
σ	solidity	$(-)$
	stress	(Nm^{-2})
σ_c	centrifugal stress	(Nm^{-2})
σ_b	bending stress	(Nm^{-2})
σ_t	total rotor solidity	$(-)$
$\emptyset v$	volume flow	$(m^3 s^{-1})$
ϕ	angle between plane of rotation and and relative flow velocity in the plane of rotation	$(-)$
ϕ_1	angle between plane of rotation and and relative flow velocity in the fully developed wake	$(-)$
τ	sheering stress	(Nm^{-2})
ψ	torsion	$(-)$
Ω	rotor angular velocity	(s^{-1})
ω	wake angular velocity	(s^{-1})

1. THEORY

In the past few years several authors translated the propeller-theory, as developed before World War II, into theories that can be used for design, calculation and prediction of the behaviour of windmills (1, 5, 8). In this chapter I have tried to expose the line of reasoning and the essential results from the above given references. Special consideration has been given to the effect of a finite number of blades, since the existing models to describe this effect were not found satisfactory.

1.1. Momentum theory

1.1.1. Axial momentum theory (1)

The simplest description of the extraction of energy from the wind is the one dimensional, incompressible, non-viscous flow model using axial momentum theory (Rankine-Froude) (see fig. 1.1.). The flow is assumed to be entirely axial with no rotational motion. Two expressions for the thrust acting upon the extracting device, may be obtained:

Continuity : $UA = U_1 A_1$ (1-1a)

Momentum theorem : $T = \dot{m} \ (V_\infty - U_1) = \rho A U \ (V_\infty - U_1)$ (1-1)

Bernoulli upwind : $p_0 + \tfrac{1}{2}\rho \ V_\infty^2 = p + \tfrac{1}{2}\rho \ U^2$ (1-2)

Bernoulli downwind: $p_0 + \tfrac{1}{2}\rho \ U_1^2 = p' + \tfrac{1}{2}\rho \ U^2$ (1-3)

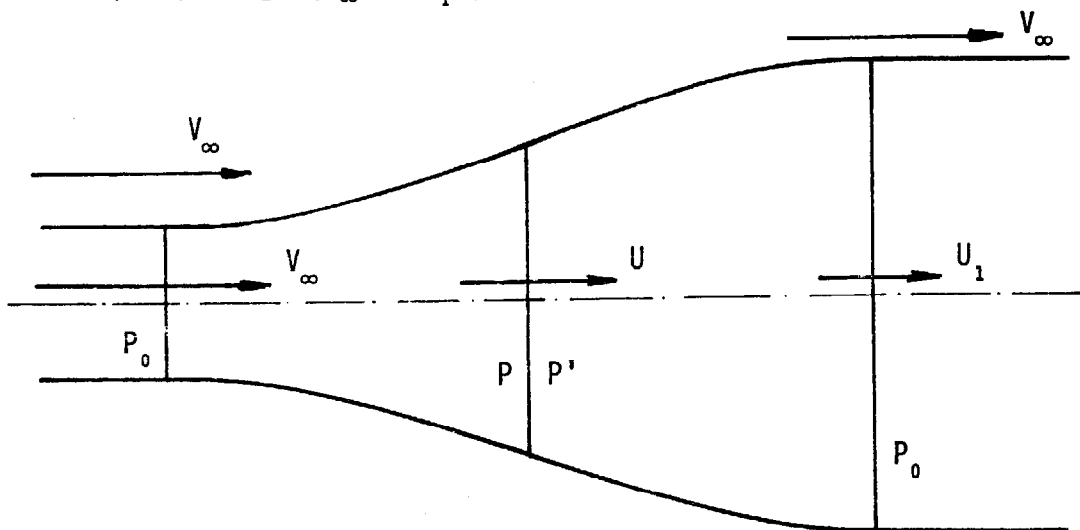thus $p - p' = \tfrac{1}{2}\rho \ (V_\infty^2 - U_1^2)$ (1-4)

Fig. 1.1.: Axial flow model

Combining equations (1-1) and (1-4) with:

$$T = A\Delta p \tag{1-5}$$

leads to: $\quad U = \dfrac{V_\infty + U_1}{2} \tag{1-6}$

The power extracted is:

$$P = \tfrac{1}{2}\dot{m} \ (V_\infty^2 - U_1^2)$$

$$= \tfrac{1}{2}\rho \ UA \ (V_\infty^2 - U_1^2) \tag{1-7}$$

If we denote $C_p = \dfrac{P}{\tfrac{1}{2}\rho \ V_\infty^3 \ A} \tag{1-8}$

and $U = (1-a) \ V_\infty$ then with (1-6) $U_1 = (1-2a) \ V_\infty$

and with (1-7) $C_p = 4a \ (1-a)^2$ (see fig. 1.1.a.) $\tag{1-9}$

which has a maximum when $a = \dfrac{1}{3}$

$$C_{p_{max}} = \dfrac{16}{27} = 0.593$$
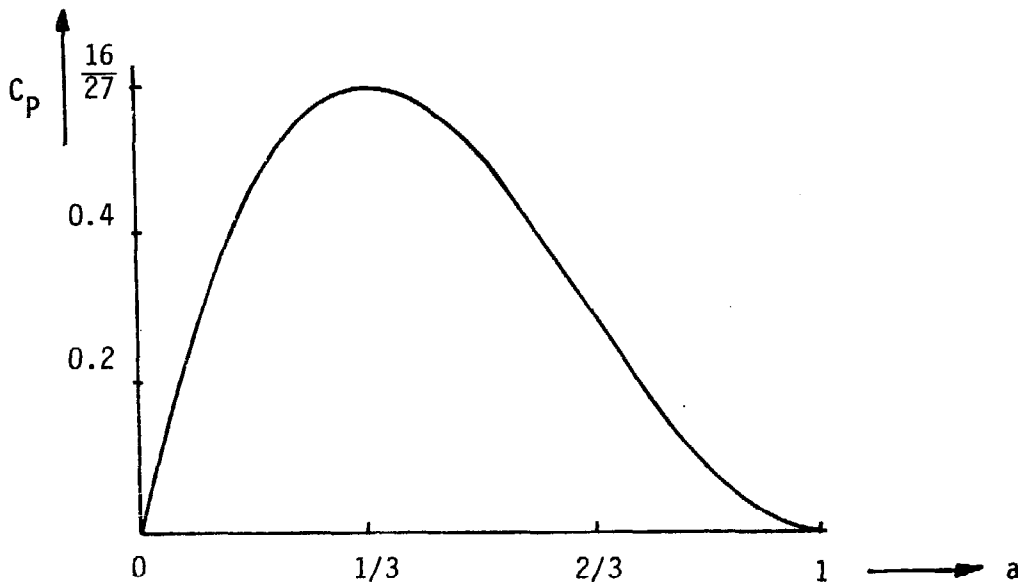
Fig. 1.1.a.:

The factor (a) is known as the axial interference factor and is a measure of the influence of the turbine on the speed of the air. Note that even if we don't know with which device we shall extract the energy, we already do know that the highest possible energy extraction requires slowing down the air to one third of its original speed.

In the used model, that gives the maximum C_p equal to $\dfrac{16}{27}$, three principle assumptions have been made:

1. The flow is entirely axial,
2. no friction occurs when the air passes the device,
3. the flow is rotationally symmetric.

If the device that extracts power from the air is a rotor, the power of
the air is transformed into torque Q and angular speed Ω. This means that,
if the angular speed cannot be infinite, extracting power (= $P = Q * \Omega$)
means generating torque.

Since generating torque implies tangential forces and thus momentum changes
in the air in tangential direction, assumption 1 is only acceptable for
very high speed devices. The higher the torque that is generated, the higher
the tangential momentum in the air downstream will be. Apart from other los-
ses that occur in reality, we here have the first reason why a C_p of 59.3%
cannot be realized in a real construction. Deviations in reality from the
second and third assumption will lead to even more losses. These losses will
be dealt with in the following paragraphs.

1.1.2. Effect of wake rotation

In describing this effect the assumption is made that upstream of the rotor
the flow is entirely axial and that the flow downstream rotates with an
angular velocity ω (r), but remains irrotational.
According to (8) this model produces unrealistic velocities near the rota-
tion axis; these can be avoided by replacing the region of high angular ve-
locities by a rigid rotating core. In the following discussion we will not
include this effect because it will not affect the results significantly.

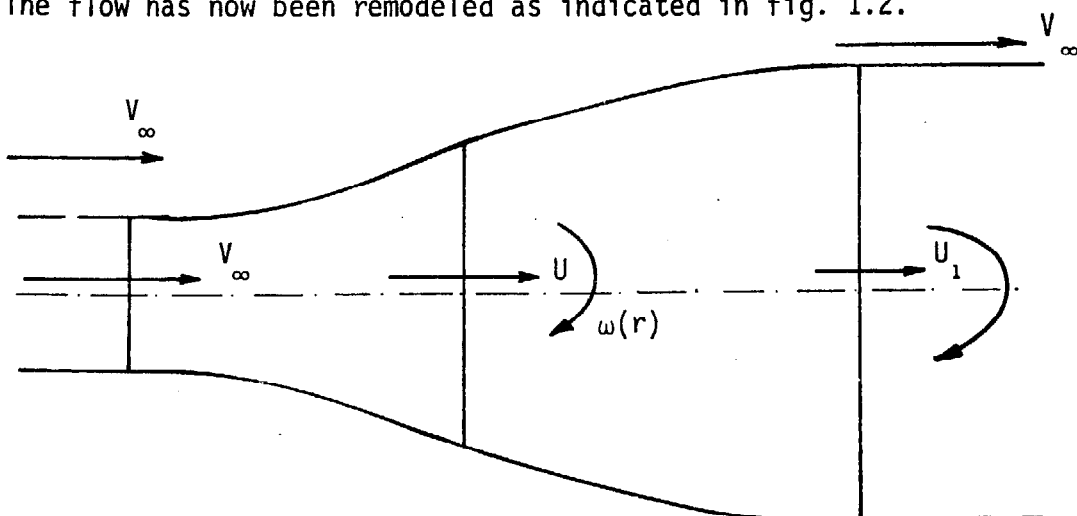The flow has now been remodeled as indicated in fig. 1.2.

Fig. 1.2.: Axial flow model with wake rotation.

One of the results of the axial flow model was that: ·

$$U = \frac{V_\infty + U_1}{2} .$$ (1-6)

According to (8) this is not correct for the model with wake-rotation; a graph presented in (8) indicates that holding on to the relation (1-6) will not result in too large an error for practical cases ($\lambda > 1.5$) (see Appendix I.).

Expressions for torque and maximum power may now be obtained by considering
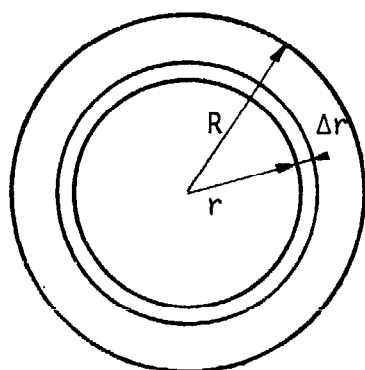

Fig. 1.3.: Annulus at radius r.

the flow through an annulus at radius r with area $\Delta A = 2\pi r \Delta r$. By changing the momentum in the air in tangential direction, tangential forces act upon the rotor:

$$\Delta F_t = \dot{m} \; (\Delta V) = \rho U \Delta A \omega r$$

$$= 2\pi \rho U \omega r^2 \; \Delta r$$ (1-10)

The torque generated in the annulus Δr is:

$$\Delta Q = 2\pi \rho U \omega r^3 \; \Delta r$$ (1-11)

And since power = torque * angular speed, the power extracted is:

$$\Delta P = 2\pi \rho \Omega U \omega r^3 \; \Delta r$$ (1-12)

The torque of the rotor becomes:

$$Q = 2\pi \rho \int_0^R U \omega r^3 \; dr$$ (1-13)

and the rotor power:

$$P = 2\pi \rho \Omega \int_0^R U \omega r^3 \; dr$$ (1-14)

To find the maximum of the expression (1-14) a relation between U and ω is needed. This relation can be found by equating the axial force on an annulus at radius r as given by the axial momentum theory to the axial force on the same annulus as may be found from considering the circulation at radius r. This is done in (1) and the result is:

$$U (V_\infty - U) = \tfrac{1}{2}\omega r (\Omega + \tfrac{1}{2}\omega)r \qquad (1\text{-}15)$$

On page 13 this result will be found in another way in dimensionless form. Defining a and a' by:

$$U = (1\text{-}a) V_\infty \qquad (1\text{-}16)$$

$$\omega r = 2a'\Omega r \qquad (1\text{-}17)$$

and

$$\lambda_r = \Omega r/V_\infty \qquad (1\text{-}18)$$

$$\lambda = \Omega R/V_\infty \qquad (1\text{-}19)$$

$$C_p = \frac{P}{\tfrac{1}{2}\rho V_\infty^{3}\pi R^2} \qquad (1\text{-}20)$$

We may obtain obtain from (1-14) and (1-15):

$$C_p = \frac{8}{\lambda^2} \int_0^{\lambda} (1\text{-}a)\, a'\lambda_r^{3}\, d\lambda_r \qquad (1\text{-}21)$$

and

$$(1\text{-}a)a = a' (1 + a')\lambda_r^{2} \qquad (1\text{-}22)$$

Now the power integral of (1-21) can be made stationary subject to the constraint of (1-22); see (1, 8). The result is a relation between a and a'.

$$a' = (1\text{-}3a)/(4a\text{-}1) \qquad (1\text{-}23)$$

This result will be used in paragraph 1.3 for design purposes.

Hence $\tfrac{1}{4} < a < \tfrac{1}{3}$. By varying a between these extremes in equations (1-13), (1-22) and (1-21), C_p for various values of λ may be obtained. The results are shown in table 1.1.

a	a'	λ_r
0.25	∞	0.000
0.26	5.5	0.073
0.27	2.375	0.157
0.28	1.333	0.255
0.29	0.812	0.374
0.30	0.500	0.529
0.31	0.292	0.753
0.32	0.143	1.154
0.33	0.031	2.619
1/3	0.000	∞

a

λ	C_p	$C_p(1-24)$
0	0.0	0.0
0.5	0.288	0.249
1.0	0.416	0.416
1.5	0.481	0.481
2.0	0.513	0.513
2.5	0.533	0.532
5.0	0.570	0.567
7.5	0.582	0.577
10.0	0.585	0.582
∞	0.592	0.592

b

Table 1.1.: a) relation between a, a' and λ_r for ideal flow and b) C_p = f(λ) for ideal flow.

For the present work it was useful to derive an approximation of C_p, as given by the formula:

$$C_{P\ approx} = \frac{16}{27} e^{-0.3538\lambda^{-1.2946}} \qquad (1-24)$$

As can be seen from the table 1.1 this approximation fits rather well for $\lambda \geqslant 1$ (error < 1 percent).

Fig. 1.4. shows C_p = f(λ) in graphical form. Keeping in mind the two assumptions in the model (rotationally symmetric and frictionless flow) this C_p may be interpreted as the characteristic of an ideal windmill.
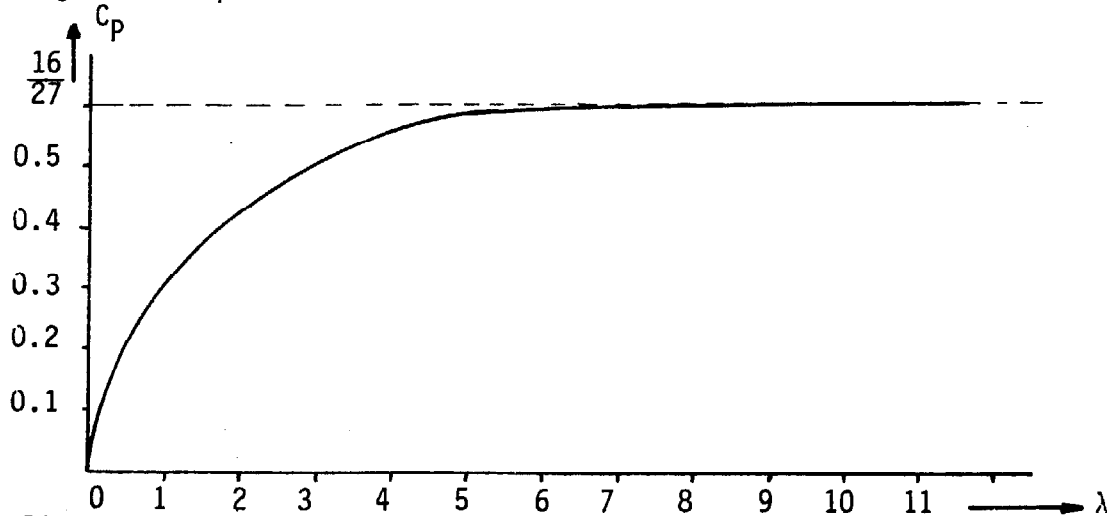

Fig. 1.4.: C_{p-max} as f(λ).

As will be seen in the next chapters, a windmill would need, apart from a frictionless medium and an infinite number of blades, an unlimited possibility of changing the blade angles and chords if a characteristic, as in fig. 1.4., were to be realized. Since this is not possible, when thinking of the horizontal-axis windmills we have in mind, it is, in contrast to the interpretation often found in other literature, better to interpret fig. 1.4. as the collection of maximum C_p-values of the characteristics of different windmills, each operating at its specific optimum λ.

1.2. Blade element theory

Since the device that extracts the energy in the momentum theory is not specified, the momentum theory cannot give information on:
- blade chords and angles;
- influence of friction;
- influence of number of blades.

The method that, when used in conjunction with the momentum theory, gives information about these aspects is called BLADE ELEMENT THEORY. The basic assumption is that the flow through the rotor occurs in non-interacting circular stream tubes.

The flow at an element Δr (see fig. 1.5.) may then be regarded as two dimensional. This opens the possibility of using the information that exists on the properties of airfoil sections, since that information is in fact strictly for two-dimensional flow.
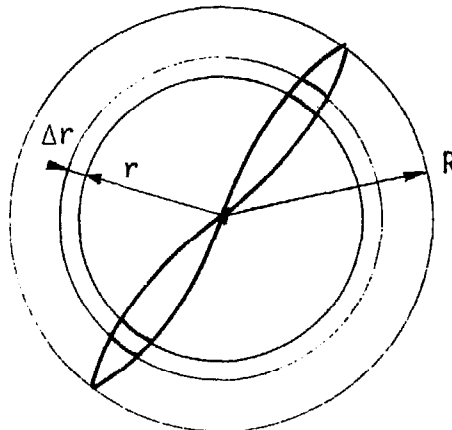

Fig. 1.5.: Rotor blade elements.

In this paragraph the flow through the circular stream tube is thought to be rotationally symmetric. Since the number of blades is always finite this assumption is not entirely valid and the formulas found here will be corrected

in the following paragraphs.

1.2.1. Effect of drag

An element at radius r in fig. 1.5. is shown in fig. 1.6. In this figure the rotational velocity is assumed to be half the value of the final rotational velocity in the wake.

Defining:

$$C_D = D/\tfrac{1}{2}\rho W^2 A \qquad (1\text{-}25)$$

$$C_L = L/\tfrac{1}{2}\rho W^2 A \qquad (1\text{-}26)$$

$$C_X = F_X/\tfrac{1}{2}\rho W^2 A \qquad (1\text{-}27)$$

$$C_Y = F_Y/\tfrac{1}{2}\rho W^2 A \qquad (1\text{-}28)$$

with:

A = $c\Delta r$ and c = blade chord,
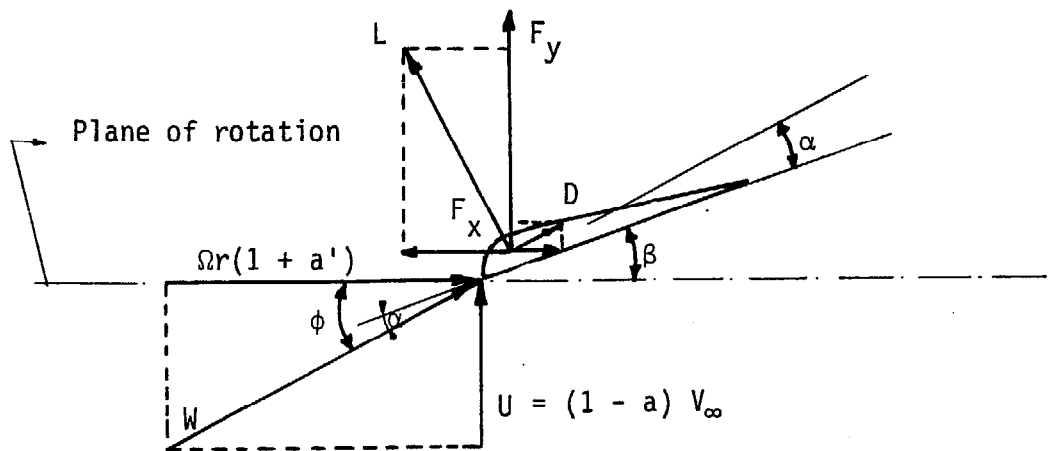

Fig. 1.6.: Velocities and forces on blade element at radius r.

the following trigonometric relations may be obtained from fig. 1.6.:

$$\alpha = \phi - \beta \qquad (1\text{-}29)$$

$$\tan\phi = \frac{1-a}{1+a'}\,\frac{V_\infty}{\Omega r} \qquad (1\text{-}30)$$

$$C_Y = C_L\cos\phi + C_D\sin\phi \qquad (1\text{-}31)$$

$$C_X = C_L\sin\phi - C_D\cos\phi \qquad (1\text{-}32)$$

Expressions may now be derived for the thrust T and torque Q of element Δr at radius r:

$$dT = B \ c \ \tfrac{1}{2}\rho W^2 C_Y dr \qquad\qquad (1-33)$$

$$dQ = B \ c \ \tfrac{1}{2}\rho W^2 C_X r \ dr \qquad\qquad (1-34)$$

where B is the number of blades. From the momentum theory (1-1) and (1-11) we already know:

$$dT = \rho(2\pi r dr) \ U \ (V_\infty - U_1) \qquad\qquad (1-1)$$

$$dQ = \rho(2\pi r dr) \ U\omega r^2 \qquad\qquad (1-11)$$

Equation (1-1) and (1-11) were derived from the momentum theory. Since this theory essentially does not include friction, we may only equate the thrust and torque of equation (1-1) and (1-11) to equation (1-33) and (1-34) if we assume $C_D = 0$.

Using definitions (1-16) and (1-17) the following equations may be derived:

$$\frac{a}{1-a} = \frac{\sigma C_L \cos\phi}{4 \sin^2\phi} \qquad\qquad (1-35)$$

$$\frac{a'}{1+a'} = \frac{\sigma C_L}{4 \cos\phi} \qquad\qquad (1-36)$$

with $\sigma = \dfrac{Bc}{2\pi r}$

Note that taking together (1-35) and (1-36) leads with (1-30) to equation (1-15) in dimensionless form of (1-22). From (8) the following elegant method for calculating the flow conditions at an element Δr at radius r is given.

Given r, c, $C_L(\alpha)$, $C_D(\alpha)$, β, V_∞, Ω, B:

A. Estimate a and a'
B. Calculate ϕ (1-30)
C. Calculate α (1-29)
D. Find C_L
E. Calculate a (1-35)
F. Calculate a' (1-36)
G. Go back to step B and repeat.

Once this iteration converges, the sectional flow properties are known and the local contributions to torque (1-34) and thrust (1-33) may be integrated

to determine the overall torque and thrust of the rotor. Note that now dQ in equation (1-34) must be interpreted as net torque and that for C_X we need equation (1-32) as a whole.

The effect of the profile drag on the C_p - λ curve of the ideal windmill (see page 10) can be found through the effect on the torque (1).

$$\text{Without drag } dQ = Bc\tfrac{1}{2}\rho W^2 C_L \sin\phi \, rdr$$

$$\text{with drag } \quad dQ = Bc\tfrac{1}{2}\rho W^2 (C_L \sin\phi - C_D\cos\phi) \, rdr$$

$$= Bc\tfrac{1}{2}\rho W^2 C_L \sin\phi \left(1 - \frac{C_D}{C_L}\cot\phi\right) rdr$$

$$\rightarrow \quad (dQ)_{\text{with drag}} = \left(1 - \frac{C_D}{C_L}\cot\phi\right)(dQ)_{\text{without drag}} \quad \rightarrow$$

equation (1-21) becomes:

$$C_p = \frac{8}{\lambda^2} \int_0^\lambda (1 - a)a'\lambda_r^3 \left(1 - \frac{C_D}{C_L}\cot\phi\right) d\lambda_r =$$

$$= C_{p\ \text{ideal}} \ (C_D = 0) - C_W$$

where $C_W = \dfrac{8}{\lambda^2} \displaystyle\int_0^\lambda (1 - a)a'\lambda_r^3 \dfrac{C_D}{C_L}\cot\phi \, d\lambda_r$ \hfill (1-37)

together with (1-30) C_W becomes:

$$C_W = \frac{8}{\lambda^2} \int_0^\lambda (1 - a)a'\lambda_r^3 \frac{C_D}{C_L}\frac{1 + a'}{1 - a}\lambda_r d\lambda_r$$

Assuming that the angle of incidence at the blade section and the form of the section itself do not vary along the blade.

$$C_W = \frac{8}{\lambda^2}\frac{C_D}{C_L} \int_0^\lambda a'(1 + a')\lambda_r^4 d\lambda_r \quad \rightarrow$$

with equation (1-22)

$$\rightarrow \quad C_W = \frac{8}{\lambda^2}\frac{C_D}{C_L} \int_0^\lambda (1 - a) a\lambda_r^2 d\lambda_r$$

With table (1.1.) it may be concluded that for $\lambda_r > 1$ under the optimum conditions $(1 - a)a$ is almost constant (error < 0.25%) and equal to 0.22. C_W now becomes:

$$C_W \approx \frac{8}{\lambda^2}\frac{C_D}{C_L} \int_0^\lambda \frac{2}{9}\lambda_r^2 \, d\lambda_r = \frac{C_D}{C_L} * \frac{16}{27}\lambda \hfill (1-38)$$

In fig. 1.7. C_p - λ curves are shown for different C_D/C_L-values. The curves should be interpreted in the way that is indicated on page 11.

1.2.2. Effect of a finite number of blades

The theories presented in the previous paragraphs, are based on the assumption that the flow through the rotor is rotationally symmetric. With a finite number of blades this assumption obviously does not hold. Another assumption is that the flow at any element is two-dimensional.

Radial acceleration and wake-induced flow at the tip may alter the assumed flow pattern. According to (8), the radial acceleration may be neglected for most wind power machines; however, the wake effects may not be neglected. Since the effects, due to the finite number of blades, result in performance losses concentrated near the tips of the blades, we speak of tip losses and we describe these effects with tip loss models.

The tip losses have been analysed by Prandtl (3). He developed a model describing the reduction of circulation due to the wake interaction at the tips. This model was derived for lightly loaded propellers with neglegible wake contraction. "Lightly loaded" should be interpreted as "giving a small change in the momentum of the flow that passes through the rotor".

The windmill is destined to produce as much power as possible. We know, from the momentum theory, that we therefore must reduce the windspeed to about one third of its original value. This means that the assumption of light loading may lead to erroneous results in calculating windmill performance.

Although this means that one of the basic assumptions of Prandtl's analysis may not be valid for the windmill, we will use here his results because it will be shown that some changes can be made that take the relatively heavy loading into account.

The tip losses are expressed by a circulation-reduction factor defined by:

$$F = \frac{B\Gamma}{\Gamma_\infty} \tag{1-39}$$

where Γ is the actual circulation of one blade at radius r, B is the number of blades and Γ_∞ is the circulation of a rotor with an infinite number of blades as calculated by the previously mentioned theory. The factor F is a function of the number of blades, tip speed ratio and radial position. It has been derived for a frictionless rotor with optimum distribution of circulation along the blades.
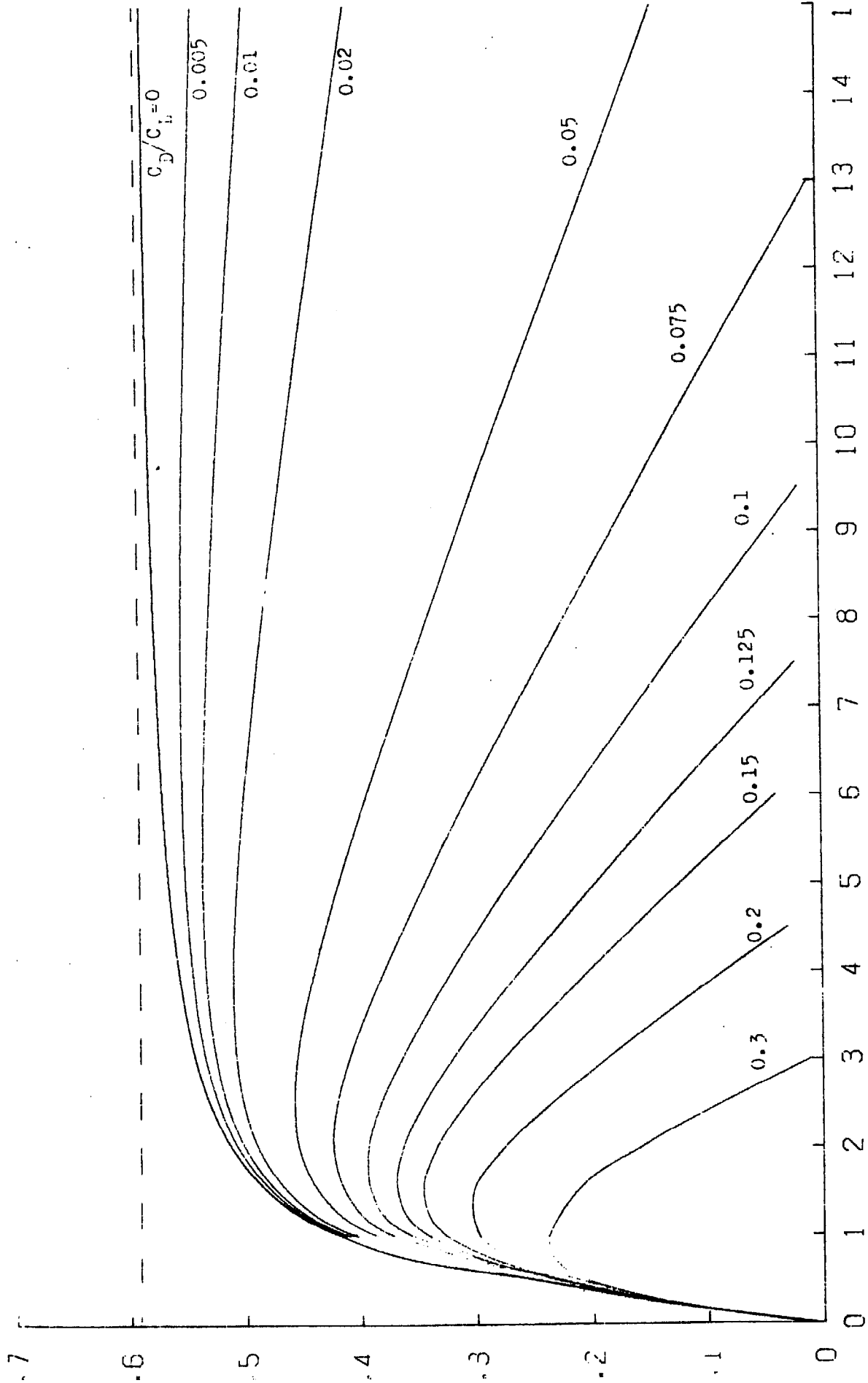
Fig. 1.7 C_P-λ characteristic of ideal windmills with B=∞

A more refined model was given by Goldstein, but we will use the Prandtl model for the following reasons:

a) The difference in results of the two models is small (8);
b) The Goldstein model is very difficult to use while the Prandtl model is relatively simple;
c) The above given considerations on the assumptions with regard to the load apply to both models.

The Prandtl model is described in (3, 5). The result is a formula for factor F:

$$F = \frac{2}{\pi} \arccos e^{-f} \tag{1-40}$$

where

$$f = \frac{B}{2} (1 - \frac{r}{R})\sqrt{1 + \lambda^2} \tag{1-41}$$

The quantity $\sqrt{1 + \lambda^2}$ came into Prandtl's model when he needed the distance between the vortex sheets in the wake of the flow. See fig. 1.8., where for a lightly loaded one bladed propeller, the vortex sheet is shown.
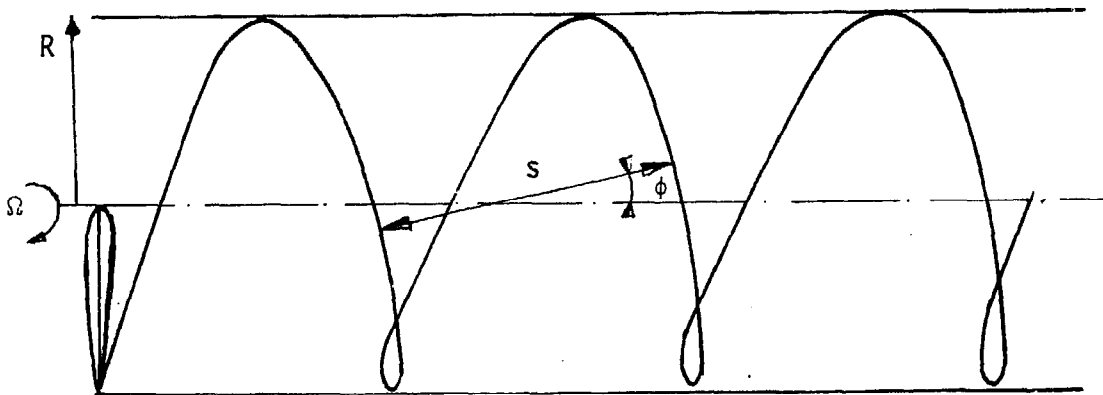

Fig. 1.8.: Vortex sheet of lightly loaded one bladed propeller.

For more blades the situation is shown in fig. 1.9a. where the distance s between the sheets is:

$$s = \frac{2\pi R}{B} \sin\phi$$

where ϕ is the angle of the vortex sheets (fig. 1.9a.) which may be interpreted as the angle ϕ in fig. 1.6.

In the non-contracting wake of the Prandtl model:

$$\sin\phi = \frac{V_\infty}{\sqrt{(\Omega R)^2 + V_\infty^2}} = \frac{1}{\sqrt{1 + \lambda^2}} \tag{1-42}$$

Writing $\frac{1}{\sin\phi_1}$ instead of $\sqrt{1 + \lambda^2}$, equation (1-41) becomes:

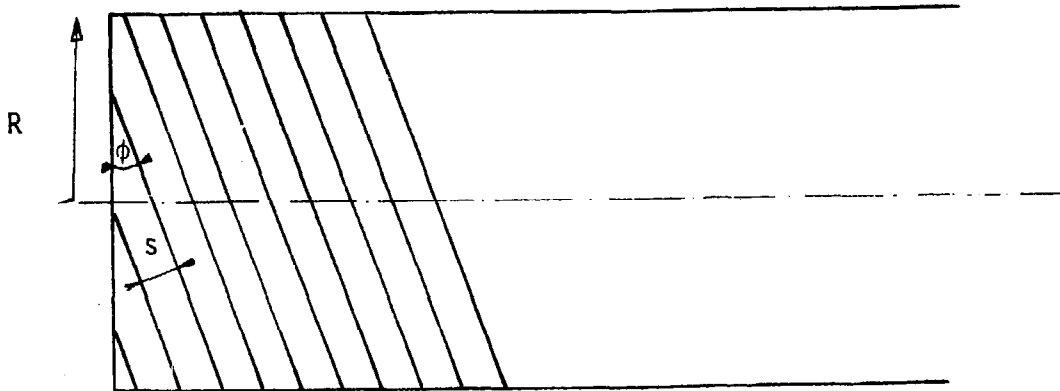$$f = \frac{B}{2} (1 - \frac{r}{R}) \frac{1}{\sin\phi_1} \qquad (1-43)$$

Fig. 1.9a.: Vortex sheets of lightly loaded multi bladed propeller.

Since the Prandtl model considers the wake of the flow we think it will be the best to take for ϕ_1 the angle that occurs in the wake of the not lightly loaded rotor (see fig. 1.9b.). Analogous to equation (1-30) this angle ϕ_1 may be calculated from:

$$\tan\phi_1 = \frac{1 - 2a}{1 + 2a} \cdot \frac{1}{\lambda_r} \qquad (1-30a)$$

According to (3, 8) the physical meaning of the tipspeed, correction is virtually that the maximum change of axial velocity, $(V_\infty - U_1)$ or $2aV_\infty$, in the slipstream only occurs on the vortex sheets and the average velocity change is only a fraction F of this velocity. Thus the axial velocity change $2aV_\infty$ becomes $2aFV_\infty$ and in a similar manner, the angular velocity change is written $2a'F\Omega$. Note that for calculating velocity changes on the blade element itself the velocity change remains $2aV_\infty$ and $2a'\Omega$ but for calculating momentums we should use $2aFV_\infty$ and $2a'F\Omega$.

Therefore (1-33) and (1-34) remain the same but in equating them to (1-1) and (1-11) we should take in (1-1) and (1-11) for U_1 and ω:

$$U_1 = (1 - 2aF) V_\infty \qquad (1-44)$$

$$\omega = 2a'F\Omega \qquad (1-45)$$

In (8) it is suggested that the correction of the velocity distribution should not only be applied to the velocity U_1 of the wake, but also to the velocity

U in the plane of the rotor, for calculating the average mass flow through an annulus.
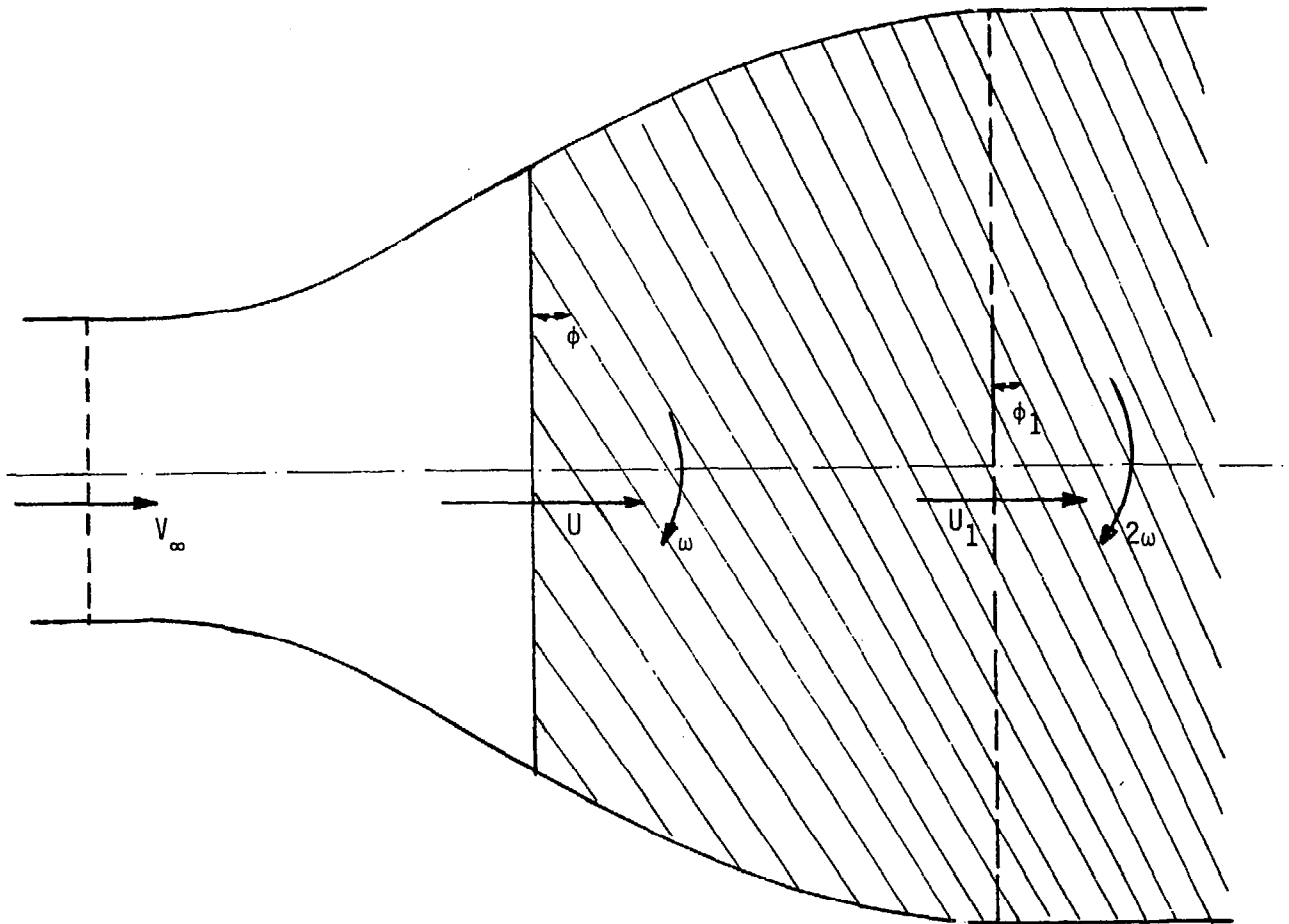
$U = (1-aF) V_\infty$

fig. 1.9b. Vortex sheets of heavy loaded multy bladed propeller.

Equating again (1-1) and (1-11) to (1-33) and (1-34) changes the relations (1-35) and (1-36): they now become

$$aF (1 - aF) = \frac{\sigma C_L \cos\phi \, (1-a)^2}{4\sin^2 \phi} \tag{1 - 47}$$

and
$$\frac{a'F (1 - aF)}{(1 - a)(1 + a')} = \frac{\sigma C_L}{4 \cos\phi} \tag{1 - 48}$$

The method for calculating flow conditions and torque contributions, as described on page 13, only changes in that for steps E and F now equations (1 - 47) and (1 - 48) should be used.

Factor F is to be calculated from (1 - 40) and (1 - 43).

Note, that in combining (1 - 47) and (1 - 48) again equation (1 - 22) may be derived. This means that the Prandtl factor F does not change the relation between interference factors a and a'. In trying to find a formula for the effect of the finite number of blades on the maximum power of the propeller as a whole, Prandtl derived an effective radius for lightly loaded optimum propellers. If the equations as derived from momentum theory are used for calculating form and angles of the blades of the windmill, the above mentioned correction may be used for calculating the maximum power. The effective radius may be calculated with

$$\frac{Re}{R} = 1 - \frac{1.386}{B} \sin\phi_1 \qquad (1 - 49)$$

Since the total power increases as the square of the radius, equation (1 - 49) may be transformed into a factor

$$\eta_B = (1 - \frac{1.386}{B} * \sin\phi_1)^2 \qquad (1 - 50)$$

For the ideal windmill $\phi_1 = \phi/2$ as was numerically calculated from (1 - 30 a) together with (1 - 30).
The calculated power was the power as if the number of blades were infinite. This power may be corrected through multiplication with the factor η_B.
In propeller theory, the propeller efficiency is defined

$$\eta = \frac{V \cdot T}{\Omega \cdot Q} \qquad (1 - 51)$$

where V is the speed of the airplane, T is the thrust, Ω is the angular speed of the propeller and Q is the necessary torque.
The tip losses diminish both torque and thrust. Since the reduction of the torque is smaller than the reduction of the thrust, there is a small drop in the efficiency of the propeller. For propellers this efficiency loss is minimized by changing the form of the blade tips (3, 5); the tips are rounded off in an elliptic form. This results in even more reduction of torque and thrust, however in such a way that the efficiency is the highest possible. Now, in windmill performance calculations, the situation is quite different.

Defining the windmill efficiency as $\eta = \frac{\Omega \cdot Q}{V \cdot T}$ leads us on very dangerous roads: if a relative reduction of the torque corresponds to a larger relative reduction of the thrust we have to conclude that the efficiency is higher. Although this might be true, the results would be bad since we would actually have designed a windmill with less than maximum power for the sake of obtaining the highest efficiency. It is therefore that the proposed efficiency be not used. Instead a coefficient should be used that relates the output to the power that is in the wind.

$$C_p = \frac{P}{\frac{1}{2}\rho V_\infty^3 A} = \frac{\Omega \cdot Q}{\frac{1}{2}\rho V_\infty^3 A} \qquad (1 - 20)$$

From this difference it immediately becomes clear that the negative effect of a finite number of blades is felt much stronger in calculating windmill power coefficients than in calculating propeller efficiencies. Although reduction of torque is accompanied by a reduction of thrust, this thrust is of no interest at all. Reducing the chords near the tips will lead to even more losses of torque and power.

Appendix III shows a schematic representation of the total energy conversion on an element at radius r in the form of a diagram as used in hydraulics.

1.3. Theoretical design for highest power coefficient.

Given some airfoil, and with the airfoil its C_D - C_L characteristic (5), we may use fig. 1.7.

As stated on page 11 and 15 the curves in this graph are best interpreted as collections of maxima of C_p-λ characteristics ; for a certain C_D/C_L-ratio we may choose from fig. 1.7 for which tipspeed ratio we will design a windmill. Neglecting for the moment the occurring tip losses, for maximum power we will choose the tipspeed ratio that shows the highest possible C_p value.

From paragraph 1.1.2. we know that a relation exists between a and a' (1 - 22) and that, for an optimum design, relation (1 - 23) must be realized between a and a'.

$$(1-a)a = a' (1+a') \lambda_r^2 \qquad (1 - 22)$$
$$a' = (1-3a)/(4a-1) \qquad (1 - 23)$$

From fig. 1.6. a trigonometric relation was derived

$$\tan \phi = \frac{1-a}{1+a} * \frac{1}{\lambda_r}$$

$$(1 - 30)$$

Having chosen the tipspeed ratio λ, the value λ_r is known for every section of the blades $(\lambda_r = \lambda r/R)$.

With relations $(1 - 22)$, $(1 - 23)$ and $(1 - 30)$ it is possible to express both interference factors a and a' as well as λ_r as a function of ϕ

$$a^* = \frac{\cos \phi}{\cos \phi + 1}$$

$$(1 - 52)$$

$$a'^* = \frac{1-\cos \phi}{2\cos \phi - 1}$$

$$(1 - 53)$$

$$\lambda_r = \frac{\sin \phi (2\cos \phi - 1)}{(1-\cos \phi)(2\cos \phi + 1)}$$

$$(1 - 54)$$

where, in order to indicate that expressions $(1 - 52)$ and $(1 - 53)$ are the desired values of a and a' for an ideal windmill, designed with theories based on the assumption of an infinite number of blades, the notations a^* and a'^* are introduced.

Since λ_r is known these relations give the optimum values of a and a'.

By equating thrust as derived from momentum theory to the thrust as derived from blade element theory, relation $(1 - 35)$ was found.

$$\frac{a}{1-a} = \frac{\sigma C_L \cos\phi}{4 \sin^2\phi}$$

$$(1 - 35)$$

Combining $(1 - 52)$ with $(1 - 35)$ leads to

$$\sigma C_L = 4 (1-\cos\phi)$$

$$(1 - 55)$$

Thus for a blade section at a known radius r and speed ratio λ_r the product of chord, number of blades and lift coefficient may be calculated. From the airfoil characteristics $C_L (\alpha)$ and $C_L (C_D)$ the value α is chosen and with equation $(1 - 29)$ the blade angle β is found.

$$\beta = \phi - \alpha \tag{1 - 29}$$

A constant angle of attack α (with minimum C_D/C_L-ratio) results in an irregular form of the blade. By varying α and therewith C_L, a small increase of C_D/C_L may be tolerated for realizing a blade form with constant or linearly varying chord. In all these design methods no consideration is given to tip losses and the expected output should therefore be corrected with the factor n_B as discussed in the last paragraph. A second method to find this same power coefficient is by making use of equation (1 - 47) and (1 - 48) for calculating the flow conditions on the blade elements in the way described on page 13. From these conditions the torque contributions from the elements may be calculated with equation (1 - 11) expressed in the factors a and a'.

$$\frac{dQ}{dr} = \rho \ (2\pi r)(1-aF)V_\infty 2a'F \ \Omega r^2 \tag{1 - 56}$$

$$\frac{\Delta C_Q}{\Delta x} = \frac{\dfrac{\Delta Q}{\frac{1}{2}\rho V_\infty^2 \pi R^3}}{\dfrac{\Delta r}{R}} = \frac{dC_Q}{dX} = \frac{1}{\frac{1}{2}\rho V_\infty^2 \pi R^2} \ \frac{dQ}{dr}$$

Thus (1 - 56) may be written dimensionless

$$\frac{dC_Q}{dx} = 8(1-aF)a'F\lambda \ x^3 \tag{1 - 57}$$

Note that a and a' are reduced by the factor F since these a and a' are not the average interference factors.
See for F equation (1 - 40), (1 - 43) and (1 - 30a).
By numerical or graphical integration C_Q may be found and multiplicating C_Q with λ yields C_p for one value of λ.
This process of iterations and integration must be performed for various λ's and the result is the C_p-λ characteristic of the windmill.
The above described method for design (1 - 55) neglects the effect of the tip losses. Thinking about what the tip loss models say about the flow we came to the conclusion that to some degree the consequences of the specific phenomena, that occur at the tips, might be compensated for by an appropriate rotor design. As earlier stated on page 18 the tip

speed correction physically means that the maximum change of axial velocity only occurs on the vortex sheets and that the average change of velocity is only a fraction F of this maximum change. If a change of axial velocity of $2aV_\infty$ is thought to occur, the average change will only be $2aFV_\infty$. From the simplest momentum models we know that the maximum power extraction is possible when the axial velocity is reduced to one third of its original value. If we want to realize this reduction we should design in such a way that the average kinetic energy in the wake flow equals that of a flow with velocity equal to one third of the wind speed. Consequently the reduction on the vortex sheets must be higher than the desired average.

Design formula (1 - 55) was derived from (1 - 35). This last relation was the result of equating thrust as found from momentum theory to thrust from blade element theory. If we want a larger reduction of the velocity on the vortex sheets, we must therefore enlarge the numerical value of factor a^* (as calculated from (1 - 52)) in the blade element part of equation (1 - 35). Taking again equations (1 - 1) and (1 - 11) we may now write, denoting by a^* the desired average interference factor as calculated in (1 - 52)

$$V_\infty(1-a^*)2a^*V_\infty = \frac{Bc}{2\pi r} \frac{V_\infty^2(1-a^*K)^2}{2\sin^2\phi\ C_\gamma}$$

$$\frac{(1-a^*)a^*}{(1-a^*)^2} = \frac{\sigma C_L \cos\phi}{4\sin^2\phi} \tag{1 - 58}$$

Factor K must be applied to the velocity change on the vortex sheets to obtain the desired average velocity reduction of the flow. If average velocity reduction would coincide with average kinetic energy reduction, then we could write 1/F for K in (1 - 58). Since in the energy the velocity is involved as a square, a reduction of the velocity change leads to a relatively greater reduction of the energy. If, in (1 - 58), we write for K=1/F, the result will be that the average velocity in the wake is one third of the undisturbed flow velocity but the remaining kinetic energy is still too high. Therefore K should even be larger than 1/F. Although we know that K should be larger than 1/F, (1 - 58) is rewritten with K=1/F as a first approximation.

$$C_L = \frac{(1-a^*)a^*F^2}{(F-a^*)^2} \cdot 4\sin\phi\tan\phi \qquad (1-59)$$

Factor F may be calculated with (1 - 41) and (1 - 43). For elements near the tip F approaches to zero. In (1 - 59) it may be seen that already at F = a ($\approx$ 1/3) the desired value of σC_L becomes infinite and if we really want the velocity change to be $2aV_\infty$ we must, for values of F<1/3, feed power to the system.

Consusions and remarks

- To describe the tip losses it is possible to use different modifications of the Prandtl model.
- The modification that seems the most realistic, is using the angle ϕ_1 of the flow in the slipstream to calculate the distance between the vortex sheets of the slip stream.
- Reduction of efficiency losses due to tip losses is realized in propeller theory by diminishing the tip chords. In windmill design not the inverse propeller efficiency but the power coefficient should be maximized. This leads to relatively large chords near the tips of the blades and only for values of F>a total compensation is possible.
- The analysis is based on two-dimensional airfoil theory. Large changes in chords along the radius lead to the situation that the model is not any longer adequate because the flow becomes essentially three- dimensional.

2. SELECTION AND DESIGN OF THE ROTORS

Windmills may be built from several materials varying from very simple to very sophistocated. Examples are cotton, wood, bamboo, steel, dacron, epoxy etc. These materials may be used in various ways. The material, together with the way it is going to be used, demands a certain level of technology. Therefore, in (6), different materials and combinations of materials were suggested for experiments:

1. thin arched steel plates (see fig. 2.1.)
2. double steel plates
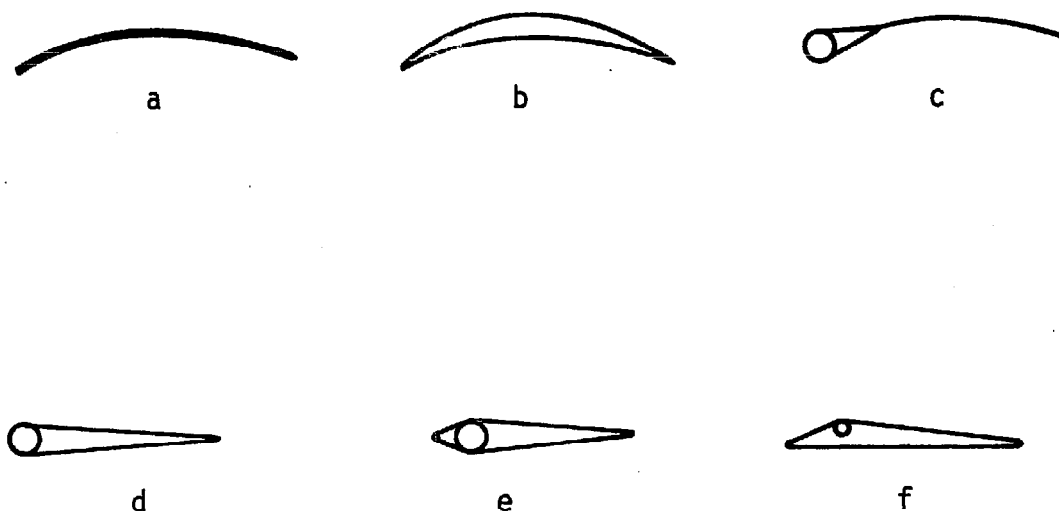3. masts + poles
4. sailwings
5. sail trousers

fig.2.1. Simple types of airfoils

a. thin steel plate   d. sail wing
b. double steel plate   e. sail trouser
c. mast + pole   f. modified sail trouser

See (6) for more information on these airfoils and the there given references.

For the following reasons the information on windmills built from these airfoils is very limited:

a. only incidentally measurements and experiments have been done and recorded

b. information on lift and drag properties of these airfoils, from which behaviour and possibilities of the windmills might be predicted, is very limited and questionable.

Therefore, as a start, comparative experiments were suggested.
To do these experiments an open wind tunnel was designed and built.
See chapter 3 for a description of the tunnel.
The windmill to be tested is placed in a free air stream. The test rotor diameters are 1.5 m (see chapter 3).
As selection critirion a high value of the power coefficient is chosen; as a secondair critirion a high speed.
With the help of the C_D/C_L-ratios from the literature study (6) and fig. 1.7. the following design speeds were selected:

mast + sail ($C_D/C_L \approx 0.2$) $\lambda_{design} = 2, 3$

steel plates and
sail trousers ($C_D/C_L \approx 0.1$) $\lambda_{design} = 2, 3, 5$

double steel and
sail wings ($C_D/C_L \approx 0.05$) $\lambda_{design} = 3, 5, 7$

The second parameter that was fixed for design was the lift coefficient.
As stated in chapter 1 paragraph 3, a fixed as well as a variable C_L-value may be chosen. In our case we fixed the value of C_L on that point of the C_L-α-characteristic that was thought to correspond with minimum C_D/C_L-ratio. (6). This resulted in the following design values for C_L:

mast + sail	C_L = 0.8
steel plate	C_L = 0.8 or 1.0
double steel plate	C_L = 1.0
sail trousers	C_L = 1.0
sail wing	C_L = 1.2

With formulas (1 - 54) and (1 - 55) it may be seen that, having fixed tip speed ratio λ and lift coefficient C_L, the value of the solidity σ at every radius may be calculated. Now one more choice must be made because the solidity includes two variables: number of blades B and chord c. For low design values of λ the solidity σ will be relatively large. Taking for these low λ-values a low number of blades leads to very large chords of the wing and has a negative influence on the maximum power coefficient (see chapter 1). Taking a high number of blades for designs with high value of λ leads to structural problems because the blades become too thin. With formulas (1 - 50) and (1 - 54) it may be seen that the influence of the number of blades on the power coefficient is relatively small for high values of λ. For these reasons the number of blades is in general lower for higher λ-values. Weighing the above mentioned effects, several rotors with different numbers of blades are proposed for experiments. A total picture of the proposed test program is given in table 2.1 on the following page.

mast + sail

$C_L = 0.8$

$\lambda = 2$ B = 4 , 6 , 8

$\lambda = 3$ B = 3 , 4 , 6

steel plate

$C_L = 0.8$

$\lambda = 2$ B = 4

$\lambda = 3$ B = 3 , 4

$\lambda = 5$ B = 2 , 3

$C_L = 1.0$

$\lambda = 5$ B = 2

double steel plate

$C_L = 1.0$

$\lambda = 3$ B = 3

$\lambda = 5$ B = 2

$\lambda = 7$ B = 2

sail trousers

$C_L = 1.0$

$\lambda = 3$ B = 2 , 3 , 4

$\lambda = 5$ B 2

sail wing

$C_L = 1.2$

$\lambda = 3$ B = 2 , 3 , 4

$\lambda = 5$ B = 2

$\lambda = 7$ B = 2

Table 2.1. Proposed test program.

During the period in which the test rotors were to be selected and
designed the effects of the number of blades was not understood in
the way explained in paragraph 1.3. and in the design formula the
number of blades was not taken into account. Therefore only basic
formulas (1 - 54), (1 - 55) and (1 - 29) were used in designing the
test rotors.

$$\lambda_r = \frac{\sin\phi(2\cos\phi - 1)}{(1-\cos\phi)(2\cos\phi + 1)} \qquad (1 - 54)$$

$$\sigma\, C_L = 4\,(1-\cos\phi); \quad \sigma = \frac{Bc}{2\pi r} \qquad (1 - 55)$$

$$\beta = \phi - \alpha \qquad (1 - 29)$$

The result of evaluating these formulas for one combination of radius
R, design-λ, design-C_L and number of blades B is that, for every radius
r on the blade, the blade setting β and the value of c is known. The
value of c is the length of the chord in the two-dimensional flow model
of the blade section. (1) suggests that this chord should be set out
perpendicularly on radius r. The way the air flows on the blades depends
on the speed ratio of the element under consideration. For values of λ_r
near zero the path of the air is largely determined by the wind speed,
while for high values of λ the path becomes totally determined by the
circumferential speed of the blade element. For low values of λ the path
thus becomes a straight line while for high values of λ the path will be
circular. Although the flow is circular we do not have to give up the
two-dimensional model: just imagine that the plane of the intersection
in two-dimensional modeling is now curved with a curvature depending
on the speed ratio of the element.
Fig. 2.2. shows the difference between setting out the chord as a
straight or as a circular line. Point 0,0 is the center of the rotor.
The point that is found with the straight line is called x1, y1 and
the point from the circular line is called x2, y2. A compromise weighing
the speed ratio of the element at radius r may be found with the following
formulas, derived from linear interpolation.

$$x3 = x2 + (x1 - x2)/(1 + \frac{3}{2}\lambda_r) \qquad\qquad (2 - 1)$$

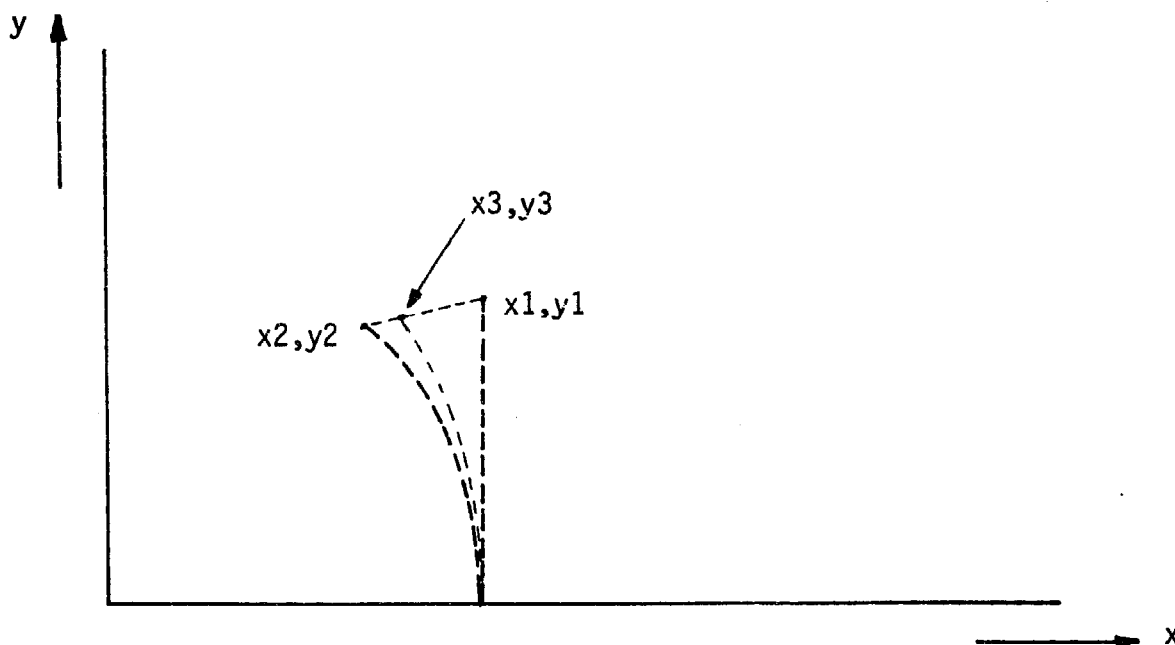$$y3 = y2 + (y1 - y2)/(1 + \frac{3}{2}\lambda_r) \qquad\qquad (2 - 2)$$

Fig. 2.2. Setting out the blade chord.

In Appendix IV results are shown for several designs. The effect of the "path correction" is highest for low design values of λ. The effects may be neglected for elements with $\lambda_r > 2$.

The results of this analysis is not a significant increase in efficiency but a reduction of the blade chord at those stations where the chord is largest. This will result in less material use and in a more simple manufacturing. In this way the general plan form of the blades of the windmill design, according to table 2.1., were derived. Appendix V shows some examples of these designs. Note that they are calculated with constant C_L-value and that the form may, if needed, be linearized as stated in paragraph 1.3.

Of the five basic airfoil types, as mentioned on page 26, until now only two have been tested. The six steel plate windmills as suggested in table 2.1. were constructed and tested. A start was made with the sail trousers; two two-bladed and one four-bladed windmills were constructed and tested.

2.1. Construction of the steel plate rotors

From (4) and (7) it was concluded that the optimum arching of a steel plate, with respect to C_D/C_L-ratio, is about 7%. With the chord c, as calculated at $r = 0.7 R$, the radius R_a, that corresponds with the calculated c and the desired value of the arching(7%), was calculated. See fig. 2.3. and table 2.2.
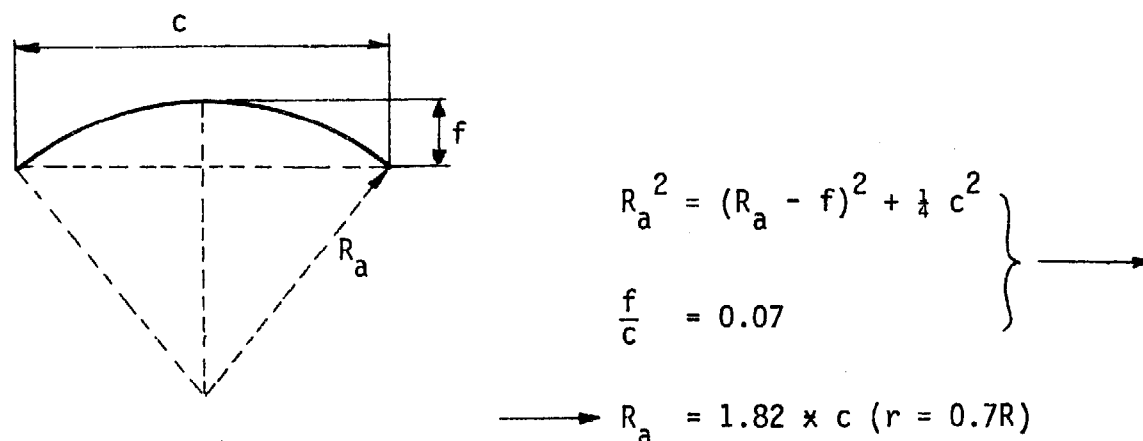
$$R_a^2 = (R_a - f)^2 + \tfrac{1}{4} c^2$$

$$\frac{f}{c} = 0.07$$

$$R_a = 1.82 \times c \quad (r = 0.7R)$$

Fig. 2.3. Calculation of the arching radius.

Steel plate (thickness = 1.5 mm) is rolled until a cilindrical form with radius R_a is realized. With $\lambda_r = \frac{r}{R} \times \lambda$ and equation (1 - 54) the angle ϕ at radius $r = 0.2 R$ and at $r = R$ are calculated. For a design with a constant C_L-value, the angle of attack α is for every radius the same. This means that the twist, which is the difference in blade angle at different radii, must be taken equal to the difference in angle ϕ. Note that the smallest r (=0.2R) is arbitrarily taken as a measure for the hub of the rotor. The twist in fact is non-linear but since it is difficult to produce such a nonlinear twist an approximation is realized in the following way. A paper model of the blade form is put on the cilinder in such a way that the axis of the cilinder makes an angle with the axis of the paper blade. From the radius R_a of the cilinder and the desired twist it may be calculated how the paper must be put on the cilinder. See fig. 2.4. When the form of the blade has been drawn in this way on the cilinder the paper may be removed and the blade may be cut out with a band-saw. In this way a blade has been produced with the

right chords and a good approximation of the blade angles. Note that the radius of the cilinder was calculated from the chord at r = 0.7R; this means that for r<0.7R the arching will be stronger. See table 2.2. where the arching at r = 0.2R is given. To be able to change the blade-setting of the blade for testing, the blades were not directly welded on a hub, but were welded on footplates that were bolted on the hub. In this way only two hubs were needed: one for the two- .and four-bladed windmills and one for the three-bladed windmills. See for example the construction on the photo of Appendix VI.
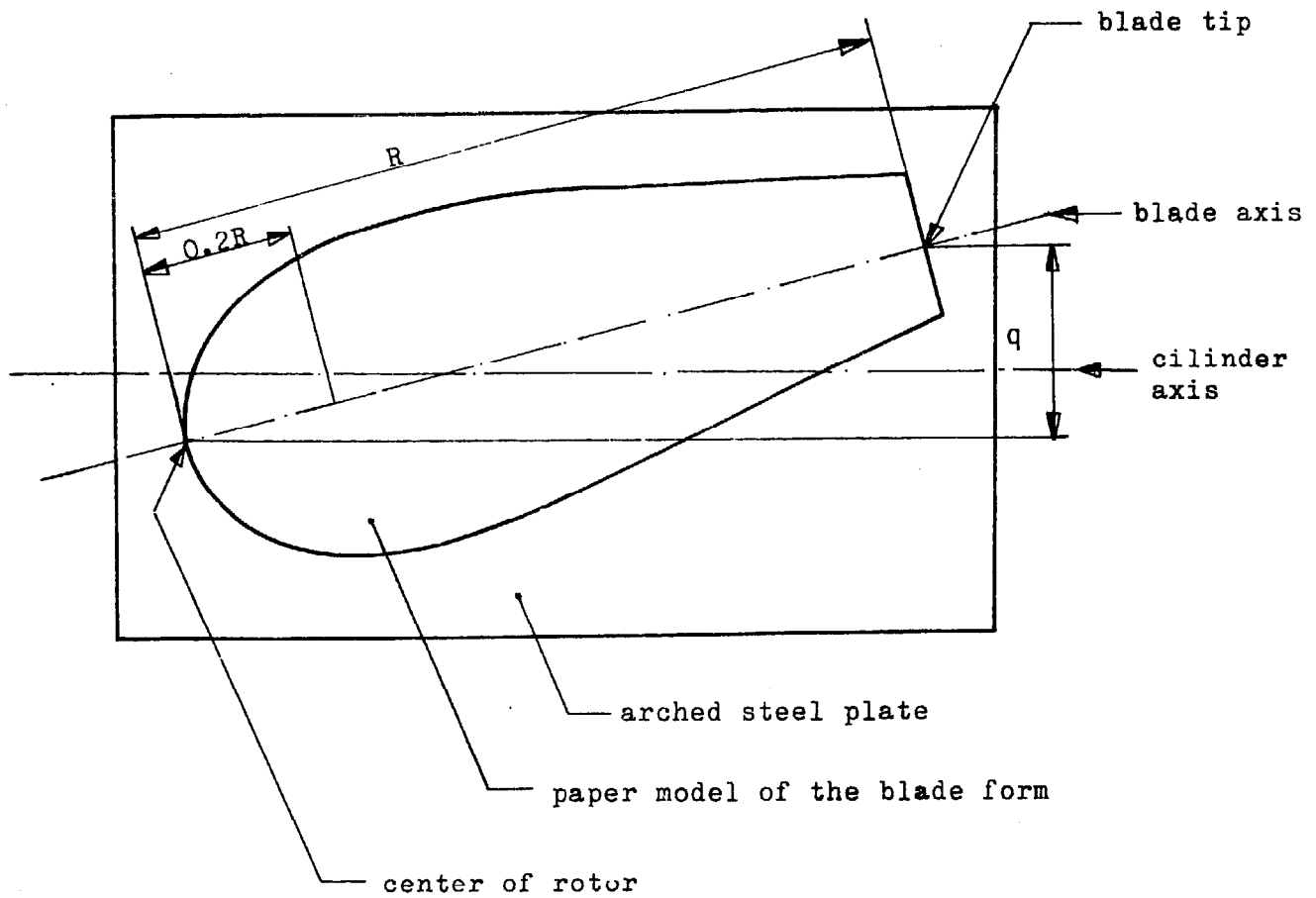
The distance q may be calculated from

$$q = \frac{R}{R-0.2R} \cdot \left\{ \phi^0(r=0.2R) - \phi^0(r=R) \right\} \cdot \frac{\pi}{180} \cdot R_a$$

Fig. 2.4. Drawing of the blade form on the arched plate.

B	C_L	λ	$\lambda_r(0.2R)$	ϕtip^0	$\phi(0.2R)^0$	$\Delta\phi^0$	c(m)	R_a(m)	arching (0.2R)%
4	0.8	2	0.533	17.71	41.40	23.7	0.34	0.619	7.8
3	0.8	3	0.800	12.30	34.30	22.0	0.22	0.401	11.3
4	0.8	3	0.800	12.30	34.30	22.0	0.18	0.328	10.3
2	0.8	5	1.333	7.54	24.68	17.14	0.14	0.255	13.7
3	0.8	5	1.333	7.54	24.68	17.14	0.09	0.164	14.9
2	1.0	5	1.333	7.54	24.68	17.14	0.11	0.200	14.3

table 2.2. Design figures for steel plates

2.2. Construction of the sail trouser rotors

Was the information on arched steel plates limited, on the sail
trousers there is no information at all. Therefore we decided to design
the sail trouser rotors in such a way that many parameters (twist, blade
angle, number of blades etc.) could, if neccessary, be varied. Since for
two- and four bladed designs one hub could be used, the construction
of a three- bladed rotor was postponed. On fig. 2.5. a sketch is shown to
illustrate the way a sail trouser rotor was constructed. On the hub angle
steels (2 or 4) were bolted; an angle steel forms the foot of a blade.
On this angle steel a socket was welded.
In this socket a tube can be fixed in such a way that later this tube may
be rotated around its axis, for twist changes. At the other end of the
tube, half of it was cut away over a length of approximately 10 cm. On
this end of the tube a tip plate was mounted that has a width equal to
the desired tip chord. The tip plate was bent at 25% of the chord
from the leading edge, in such a way that, with the tube, a thickness-
chord ratio resulted of 10%. From front and rearside of the tip plate
a leading edge and trailing edge were formed with steel cables connected
with the foot plate. Over the construction of pipe and cables the trouser
is drawn and fixed at the foot of the blade. The cable constructions
only allow linearly varying chords and blade angles. Therefore the angles
and chords, as calculated with constant C_L over the blade, were treated
in the following way.

tip plate

tube

steel cable

angle steel
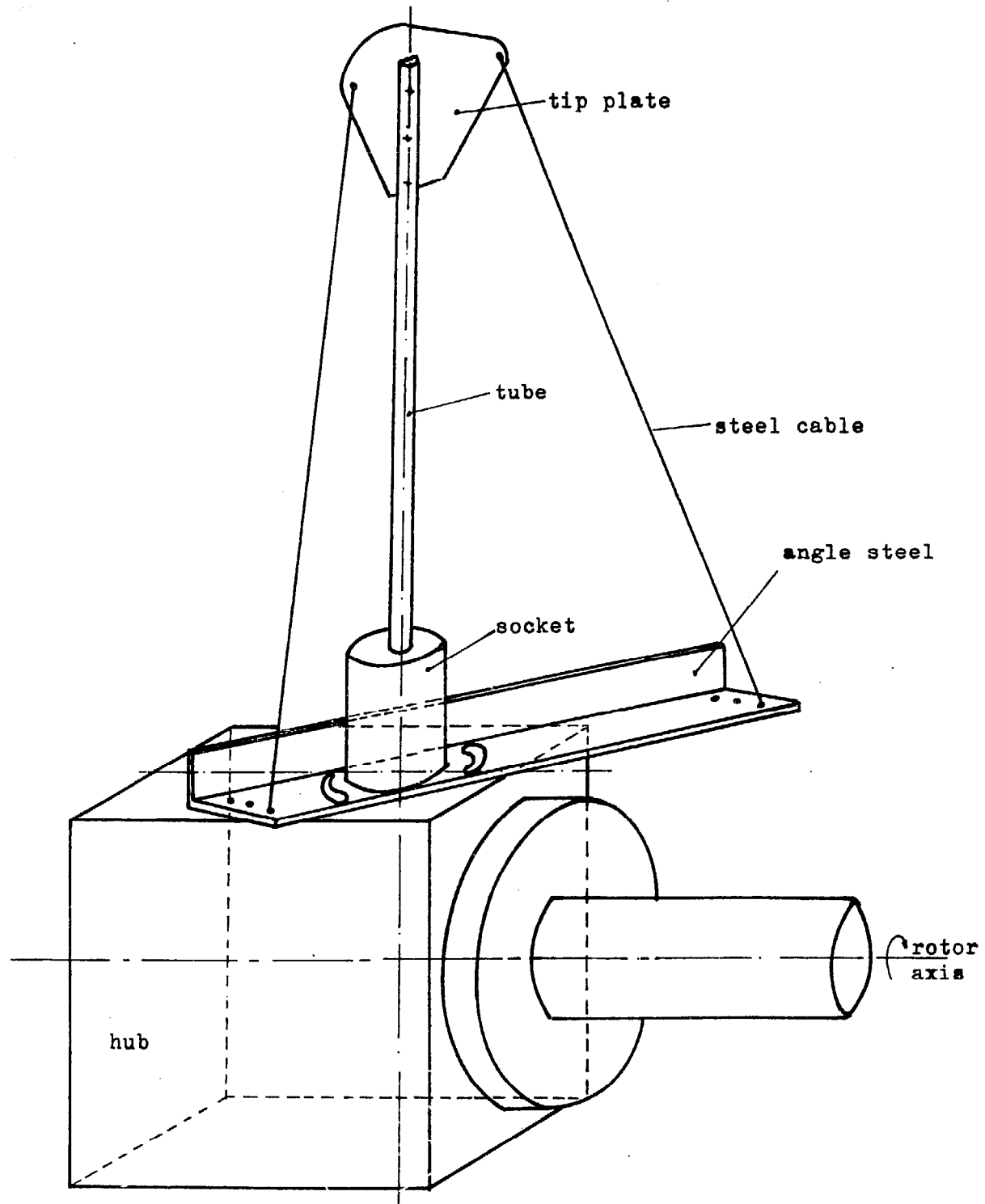
socket

rotor
axis

hub

Fig. 2.5. Sketch of the construction of a sailtrouser rotor blade mounted
on a hub on the rotor axis.

At first the chords and blade angles were linearized between the chords
and angles at radius r = 0.2R and r = R. The difference between the
desired chord and the linearized chord is rather small, but the blade
angles change so much that it may be expected that this poor approximation
will result in bad performance. The outer parts of the swept area "catch"
a relatively great part of the wind (the swept area is proportional to the
square of the radius). The aerodynamic efficiency is low at small radii,
because the speed ratio is low. A better result may be expected if the
linearization of the blade angle is done between r = 0.5R and r = R.
The change of the desired angle is small between 0.5R and R (see Appendix
VII). This results in a small twist compared to the twist as calculated
from linearization between 0.2R and R. The steel cable can be fixed at the
foot plate at different places; in this way it is possible to change the
average thickness of the blade. Two rotors were built in this way, both
designed for λ = 3 at C_L = 1.0. One rotor has four and one has two blades.
With two blades of the four bladed rotor it was possible to redesign
the blade angles in such a way that another two bladed rotor was available
for $\lambda \approx$ 4.5. The actual setting of the blades may be found in chapter 4
together with the test results.

2.3. Stress analysis

The blades of a wind mill must be strong enough to resist two loads:
centrifugal forces and bending moments. It will be shown in this paragraph
that during operation the roots of the blades only have to resist the
centrifugal forces and that the root tensions due to bending moments are
relatively low. For when the rotor is not in operation, the bending moments
must be calculated for storm conditions.

2.3.1. Centrifugal forces

The blade is modeled in the way indicated in fig. 2.6. The blade model has
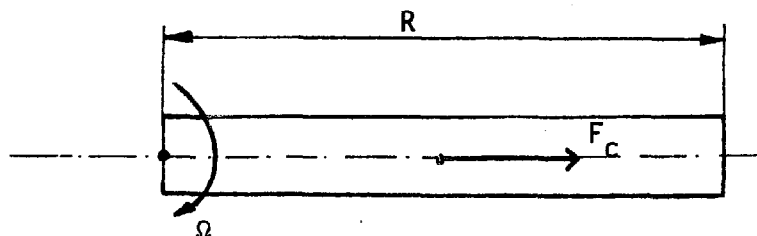a constant cross-sectional shape.

Fig. 2.6. Model of centrifugal load.

The centrifugal force is then

$$F_c = m\Omega^2 r = \rho_m \, A \, R \, \frac{\lambda^2 V_\infty^2}{R^2} \cdot \frac{R}{2} = \rho_m A \frac{\lambda^2 V_\infty^2}{2} \qquad (2-3)$$

$$\sigma = \frac{F_c}{A} = \rho_m \frac{\lambda^2 V_\infty^2}{2} \qquad (2-4)$$

ρ_m = density of construction material

A = cross-sectional area

Ω = rotor angular speed

σ = stress at the root of the blade

For a given material (wood, steel, etc.) the material properties ρ_m and σ-permissible are known and λ_{max} may be written as $f(V\infty)$

$$\lambda_{max} = \frac{1}{V_\infty} \sqrt{\frac{2\sigma_{perm}}{\rho_m}} \qquad (2-5)$$

For normal steel $\rho_m = 7.85 \times 10^3$ (kg/m^3)

and if σ_{perm} is taken $160 * 10^6$ (Nm^{-2})

the construction is safe against centrifugal loads if

$$\lambda_{max} < \frac{200}{V_{max}} \qquad (2-6)$$

2.3.2. Bending moments during operation

From chapter 1 we know the thrust on an element Δr

$$\Delta T = \rho(2\Pi r \Delta r) \, U \, (V_\infty - U_1) \qquad (1-1)$$

This indicates that the thrust is approximately a linear function of r. Then ΔT may be approximated by

$$\Delta T = \left(\frac{r}{R}\right) \Delta T_{max} = \left(\frac{r}{R}\right) \cdot F_m \; \Delta r \qquad (2-7)$$

The load on a blade under operating conditions may be modeled as shown in fig. 2.7a. Fig. 2.7b shows an element of this blade and the forces and moments acting upon it.
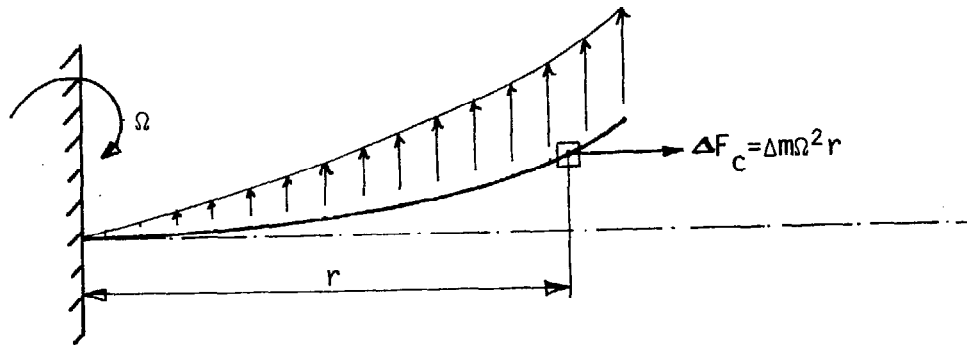

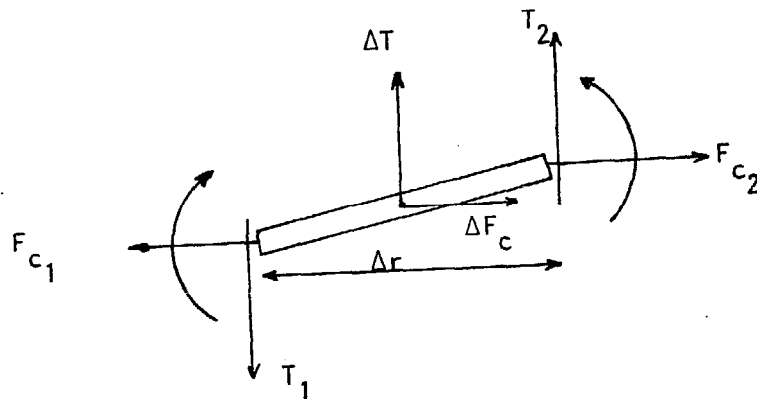fig. 2.7a. Load on blade under operating conditions

fig. 2.7b. Forces and moments acting upon a blade element Δr at radius r.

$$M_1 - M_2 - T_2 \, \Delta r + F_{c_2} \, \Delta y' - \frac{\Delta T \Delta r}{2} + \frac{\Delta Fc \Delta y}{2} = 0 \tag{2-8}$$

$$\frac{\Delta M}{\Delta r} = - T_2 + F_{c_2} \frac{\Delta y}{\Delta r} - \frac{\Delta T}{2} + \frac{\Delta Fc}{2} \, \frac{\Delta y}{\Delta r} \tag{2-9}$$

$$\frac{dM}{dr} = - T_2 + F_{c_2} \, y' \tag{2-10}$$

$$T_2 = \int_r^R \left(\frac{r}{R}\right) F_m \, dr = \frac{Fm}{2R} (R^2 - r^2) \tag{2-11}$$

With $\rho_{b1} = \dfrac{m_{blade}}{R}$ $\tag{2-12}$

F_{c_2} becomes

$$F_{c_2} = \int_r^R \rho_{b1} \, \Omega^2 \, r \Delta r = \frac{\rho b1 \Omega^2}{2} (R^2 - r^2) \tag{2-13}$$

Combining (2-10), (2-11) and (2-13) gives

$$\frac{dM}{dr} = - \frac{F_m}{2R} (R^2 - r^2) + \frac{\rho b1 \Omega^2}{2} (R^2 - r^2) \, y' \tag{2-14}$$

The differential equation for elastic bending:

$$\frac{d^2 y}{dr^2} = y'' = \frac{M}{EI} \tag{2-15}$$

differentiating (2-15) gives

$$\frac{dM}{dr} = E \, I \, y''' \tag{2-16}$$

Equating $\frac{dM}{dr}$ from (2-14) to (2-16) results in a third order differential equation with not constant coefficients

$$EIY''' - \frac{\rho b l \Omega^2}{2} (R^2 - r^2) \, y' = - \frac{Fm}{2R} (R^2 - r^2) \qquad (2\text{-}17)$$

writing

$$y = \frac{Y}{R} \qquad (2\text{-}18)$$

$$\text{and} \quad X = \frac{r}{R} \qquad (2\text{-}19)$$

with $\frac{d}{dX} = (\quad)'$ $\qquad (2\text{-}20)$

equation (2-17) becomes

$$Y''' - \frac{\rho_{bl} \Omega^2 R^4}{2 \, EI} (1 - X^2) \, Y' = - \frac{F_m R^3}{2EI} (1 - X^2) \qquad (2\text{-}21)$$

with $C_1 = \frac{\rho_{bl} \Omega^2 R^4}{2EI}$ $\qquad (2\text{-}22)$

and $C_1 = \frac{F_m R^3}{2EI} (1 - X^2)$ $\qquad (2\text{-}23)$

$$Y''' - C_1 (1 - X^2) \, Y' = - C_2 (1 - X^2) \qquad (2\text{-}24)$$

Conditions:

at $X = 0$: $Y = 0$, $Y' = 0$ $\qquad (2\text{-}25)$
at $X = 1$: $M = 0 \rightarrow Y'' = 0$ $\qquad (2\text{-}26)$

For this differential equation no analytical solution is available and until now no numerical evaluation has been made by us.
When from equations (1-24) - (1-26) $Y''(0)$ is found the bending moment at the root may be calculated with (2-15) and the root stresses may be calculated with

$$\sigma_b = \frac{M}{W_b} \qquad\qquad (1\text{-}27)$$

Where W_b is the resisting moment of the root section.

In (9) it is stated that during operation the centrifugal forces will offset the bending loads on the blade and that the centrifugal force as dealt with in paragraph 2.3.1, is the main load. From figure 2.7 it can be seen that this offsetting depends on the angular speed. It is suggested that the above mentioned numerical evaluation be made to find out below which design tipspeed ratio the centrifugal forces. It is expected however, that no problems will arise.

2.3.3. Bending moments for storm conditions

During a storm, when the windmill is not operating, the blades must resist wind speeds of, for example, 40 m/s. The thrust on a blade element then is

$$\Delta T = \frac{1}{2} \rho V_\infty^2 c \Delta r C_D \qquad\qquad (2\text{-}28)$$

where C_D is the drag coefficient.
The bending moment becomes

$$M = \frac{1}{2} \rho V_\infty^2 \int_0^R C_D c r dr \qquad\qquad (2\text{-}29)$$

As an example the following figures are given

λ =10, B = 1, c = 0.1 m, R = 0.75 m c and C_D may be taken constant over the blade span, and the value of C_D is 2. Then M becomes

$$M = \frac{1}{2} \times 1.3 \times 1600 \times 2 \times 0.1 \times \frac{1}{2} 0.75^2 = 58.5 \text{ Nm}$$

With equation (2 - 27) the bending stresses, for storm conditions, may be calculated

operating:

$$\sigma_b = \frac{M}{W_b} = \frac{M}{\frac{1}{6} ch^2} = \frac{6 \times 58.5}{0.1 \times 1.5^2 \times 10^{-6}} = 156 \times 10^7 \text{Nm}^{-2} = 1560 \text{ Nmm}^{-2}$$

not operating: $T_c = \frac{\rho_m}{2} \lambda^2 v_\infty^2 = 628 \text{ Nmm}^{-2}$

This enormous root stress shows the importance of the protections of windmills against storms. The advantage of constructions built with sails is obvious: the sails may be taken off or reefed in such a way that the blade area is reduced. The calculations above were made for a hypothetic device that was designed for a high speed as λ = 10.
To get an impression of the stresses that must be expected for relatively slow running windmills, another example is given. One of the rotors that we built and tested has the following properties:

B = 4

λ = 2

c = 340 mm (=average chord)

c = 280 mm (=chord at root)

h = 1.5 mm (thickness)

ρ_m = 7850 kgm^{-3}

V = 15 ms^{-1} (operating conditions)

40 ms^{-1} (storm conditions)

R = 0.75 m

E = 0.21 * 10^{12} Nm^{-2}

$\rho_{bl} \approx 4$ kgm^{-1}

Centrifugal forces

$$\sigma_c = \frac{\rho_m}{2} \lambda^2 V_\infty^2 \qquad\qquad (2 - 4)$$

at λ = 2 σ_c = 3.5 Nmm^{-2}

at λ = 3 σ_c = 8 Nmm^{-2}

Centrifugal forces for operating in a storm

$$\sigma_c = \frac{\rho_m}{2} \lambda^2 V_\infty^2 \qquad\qquad (2 - 4)$$

at λ = 2 σ_c = 25.1 Nmm^{-2}

at λ = 3 σ_c = 56.5 Nmm^{-2}

Bending forces for storm conditions when the windmill is not operating

$$M = \frac{1}{2} \rho V_\infty^2 \int_0^R C_D c r \, dr \qquad\qquad (2 - 29)$$

$$M \approx \frac{1}{2} \rho V_\infty^2 C_D c_{average} \times \frac{1}{2} R^2$$

$$= \frac{1}{2} \times 1.3 \times 1600 \times 2 \times 0.34 \times \frac{1}{2} \times 0.75^2 = 199 \text{ Nm}$$

$$\sigma_b = \frac{M}{W_b} = \frac{M}{\frac{1}{6} c h^2} = \frac{6 \times 199}{0.28 \times 1.5^2 \times 10^{-6}} = 1.9 \times 10^9 \text{ Nm}^{-2} = 1900 \text{ Nmm}^{-2}$$

2.3.4. Cable tension calculations

Like in the previous analysis, the load on the blade of a sail trouser rotor is supposed to vary linearly with the radius. See fig. 2.8.a. and equation (2 - 7)

From chapter 1 we know that the maximum energy to be extracted is

$$P = C_p\frac{1}{2} \rho V_\infty{}^3 \Pi R^2 = \frac{8}{27} \rho V_\infty{}^3 \Pi R^2 \qquad (2 - 27)$$

This is possible if the axial speed of the flow through the rotor was

$$U = (1-a)V_\infty = \frac{2}{3} V_\infty \qquad (2 - 28)$$

The thrust to be expected is therefore something in the order of

$$T = \frac{P}{U} = \frac{\frac{8}{27}\rho V_\infty{}^3 \Pi R^2}{\frac{2}{3} V_\infty} = \frac{4}{9}\rho V_\infty{}^2 \Pi R^2 \qquad (2 - 29)$$

and for an element Δr per blade

$$\Delta T = \frac{4\rho V_\infty{}^2}{9B} 2\Pi r \Delta r \qquad (2 - 30)$$

If the load is supposed to be carried fully by the leading edge cable, the deflection and tension S of the cable may be calculated in the following way. See fig. 2.8.a. and b.
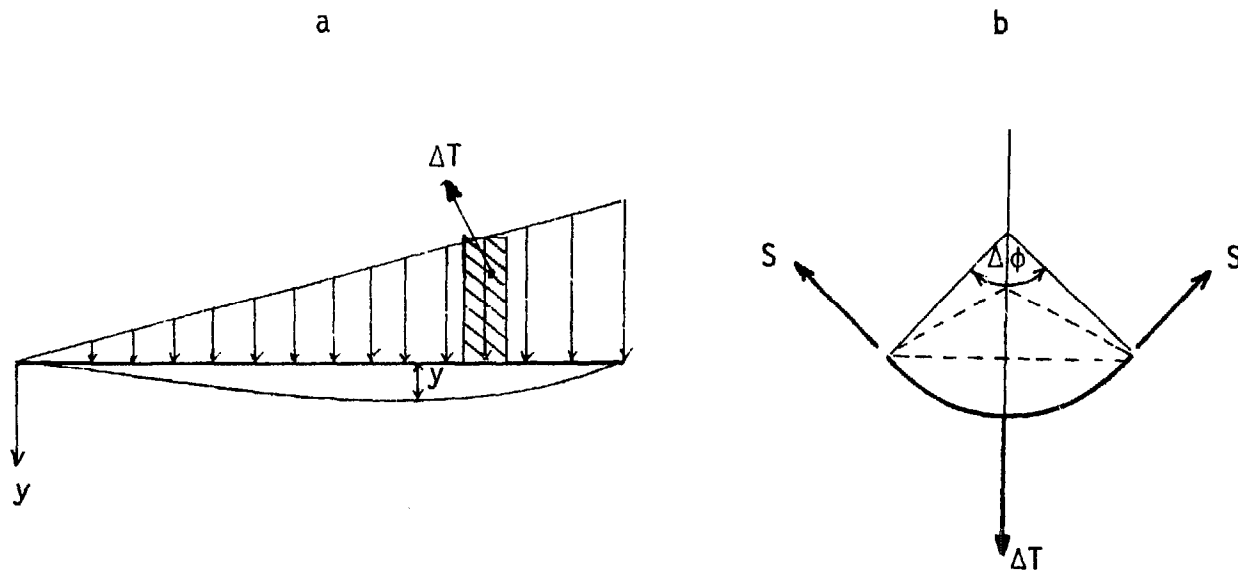
a

b

fig. 2.8. Cable tension model.

$$\Delta T = S \Delta \phi = \frac{4}{9} \frac{\rho V_\infty^2}{B} \; 2 \Pi r \Delta r \qquad (2 - 34)$$

$$\frac{d\phi}{dr} = \frac{8 \Pi \rho V_\infty^2}{9 B S} \; r \qquad (2 - 35)$$

$$\phi = \frac{4 \Pi \rho V_\infty^2}{9 B S} \; r^2 + C_1 = C^x r^2 + C_1 \qquad (2 - 36)$$

For small values of y (see fig. 2.8.a) $\tan\phi \approx \sin\phi \approx \phi$.
(2 - 36) may now be written

$$\frac{dy}{dr} = C^x r^2 + C_1 \qquad (2 - 37)$$

integration of (2 - 37) gives

$$y = \frac{1}{3} C^x r^3 + C_1 r + C_2 \qquad (2 - 38)$$

Conditions: r = 0   y = 0
$$\qquad (2 - 39)$$
              r = R   y = 0

Combining (2 - 38) with (2 - 39) yields

$$y = \frac{C^x}{3}(r^3 - R^2 r) \qquad (2 - 40)$$

The maximum deflection occurs if y'= 0. This happens when r becomes
$R/\sqrt{3}$. The maximum deflection is then

$$y_{max} = \frac{8 \Pi \rho V_\infty^2 R^3}{81 \sqrt{3} \; B S} \qquad (2 - 41)$$

If for y_{max} we take arbitrarily a value of 1 percent of the blade span, the needed tension S for the leading edge cable may be caculated with

$$S = 100 \quad \times \frac{8\pi\rho V_{\infty}^2 R^2}{81\sqrt{3}\ B} \qquad (2 - 42)$$

In our sail trouser constructions, the tube, as described in 2.2., is placed at 25 percent of the chord from the leading edge. If a balance of bending moments is desired, the trailing edge cabletension should be taken one third of the value of the leading edge cable tension.

With the desired cable tension the diameters of the cables may be chosen. In this way the cable diameter for the 4-bladed windmill was chosen 2.5 mm and for the 2-bladed windmill 3.5 mm.

2.3.5. Tube torsion

Suppose that the total force on the trouser blade construction acts on the tip of the blade at the leading edge and the that the thrust, as may be calculated by integrating (2 - 33), is representative for the load on the blade. The torque acting on the tube may then be calculated with

$$M_t = \frac{c_{tip}}{4} \int_0^R \frac{4}{9} \frac{\rho V_{\infty}^2}{B} \cdot 2\pi r dr = \frac{c_{tip}}{9} \frac{\rho V_{\infty}^2}{B} \pi R^2 \qquad (2 - 43)$$

With the following set of equations the torsion ψ and the shearing stress τ may be calculated

$$\psi = \frac{M_t R}{GI_p} \qquad (2 - 44)$$

$$\tau = \frac{M_t}{W_t} \qquad (2 - 45)$$

where

$$G = 0.385 \ E \tag{2 - 46}$$

$$I_p = \frac{\pi}{32} \ (d_{out}^4 - d_{in}^4) \tag{2 - 47}$$

$$W_t = \frac{\pi}{16} \ (d_{out}^3 - d_{in}^3) \tag{2 - 48}$$

To illustrate these calculations results are given for the two bladed sail trouser rotor.

Given:

$$c_{tip} = 0.06 \ m$$

$$\rho \quad = 1.3 \ kgm^{-3}$$

$$V_\infty \quad = 15 \ ms^{-1}$$

$$R \quad = 0.75 \ m$$

$$B \quad = 2$$

$$d_{in} \quad = 21 \times 10^{-3} m$$

$$d_{out} = 21.8 \times 10^{-3} m$$

$$E \quad = 0.21 \times 10^{12} \ Nm^{-2}$$

the torsion ψ and the sheering stress τ become

$$\psi = 0.3^o$$

$$\tau = 8 \ Nmm^{-2}$$

Conclusions and remarks

- A more accurate interpretation of the calculated chords is given.
  This does not result in a significant increase of the power coefficient
  but leads to less material use and a more simpel manufacture
- A simple method for manufacture of twisted, arched steel plates is
  given. Six rotors were built of blades that were manufactured with
  this method.
- First designs of sail trouser blades are made and two rotors were
  made according to these designs.
- Calculation of stresses in windmill rotors is complex even if
  a static analysis were sufficient. For static loads no strength
  problems are expected. It is thought however that, in connection
  with expected fatigue problems, also an analysis with dynamic loads
  should be made. This analysis was not possible within the scope of
  this work.
- The static load on the blades under normal conditions is low but a
  storm will destroy each windmill that is not protected in some way.
- Stress calculations for the components of the sailtrouser frame are
  simple and no strength problems are expected.

3. WIND TUNNEL AND MEASURING INSTRUMENTATION

In this chapter the test unit and the objective of several parts of
the used instrumentation are explained. The used instrumentation is
specified in Appendix VIII. At the end of this chapter a survey is
given of the necessary relations for calculating the desired quanti-
ties λ, C_p and C_Q from the measured quantities.

3.1. The wind tunnel

To test the rotors, a wind tunnel was built as is schematically shown
in fig. 3.1. A 2.2 m diameter, 45 kW fan is driven bij a direct
current motor. The power for this motor is generated by a socalled
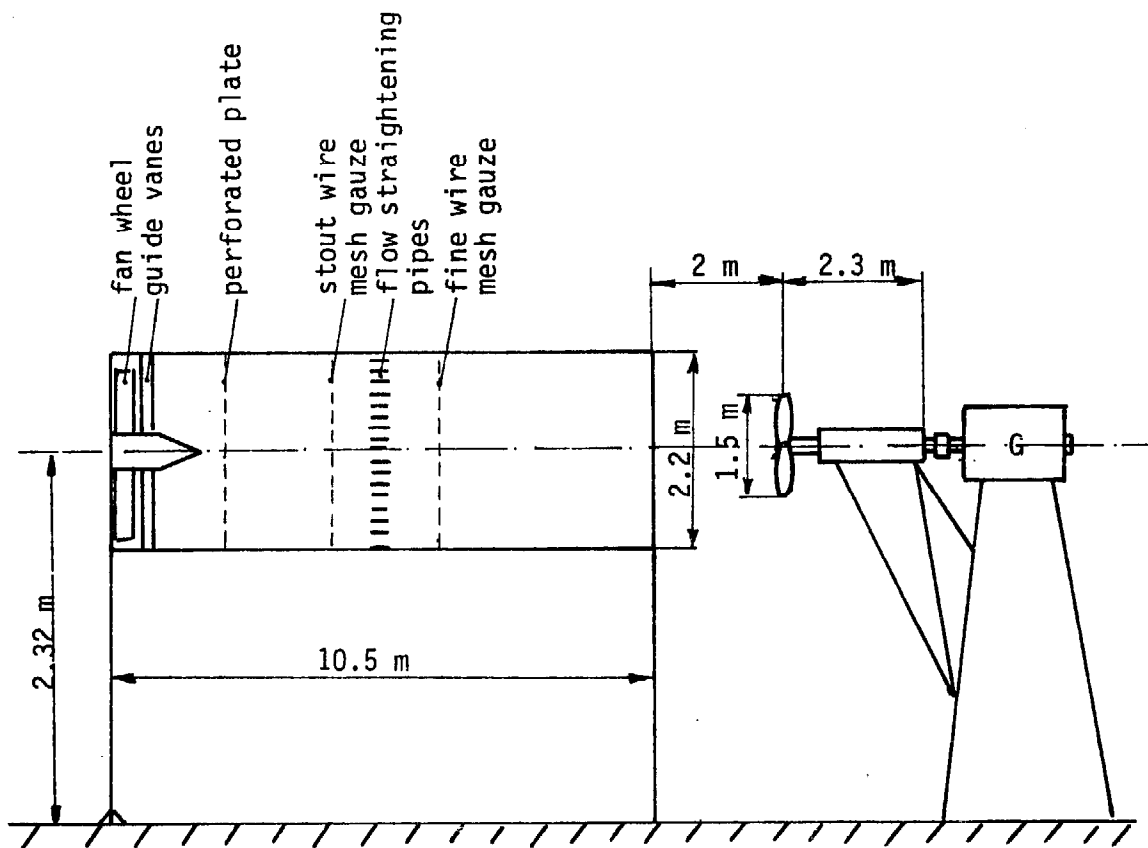
Fig. 3.1. Wind tunnel

Ward-Leonard set. In this way a stepless adjustable fan speed is
obtained and the flow velocity may be stepless adjusted between
zero and maximum. As indicated in fig. 3.1. the air passes several
objects before leaving the tunnel. The objective of these vanes,
gauzes and pipes is to eliminate rotational movements and velocity
differences in the air. Thus a free airstream is generated of 2.2 m
diameter. The velocity range is from 0 to 15 meters per second.
The velocity variations over the cross sectional area, in the free
airstream after the tunnel, are less than two percent of the average
velocity and the flow is entirely axial. In this airstream the wind-
mill is placed at 2 m distance from the tunnel opening. Tests have shown
that at this distance from the opening only a few centimeters of the
boundery between moving and not-moving air have interfered with each
other and that the velocity distribution of the flow that passes the
rotor area is still the same as in the tunnel opening. Other measurements
have shown that, when the windmill is operating, the velocity distribution
in the tunnel-opening is not affected by the presence of the windmill
2 m down stream. It is therefore assumed that the flow is sufficiently
similar to the wind in open air.
To prove that the finite dimensions of the free airstream have
no influence on the test results, the following experiment was done.
A simple four bladed steel plate rotor was built with diameter equal
to half the diameter of the windmills to be tested. This rotor was tested
at 2 m distance from the opening of the tunnel. Then a tube, with diameter
equal to half the wind tunnel diameter, was placed in the wind tunnel
opening in such a way that an airstream was generated with similar flow
conditions but half the diameter of the original airstream. In this
small diameter flow once more the 0.75 m diameter test rotor was tested
under the same flow conditions, as in the large diameter airstream, at
a distance of 1 m from the opening. See fig. 3.2.
As shown in fig. 3.3. the differences between the test results were not
significant and it was concluded that the behaviour of the small rotor
was not influenced by doubling the flow diameter. We therefore concluded
that for the 1.5 m diameter rotors the same test results will be found
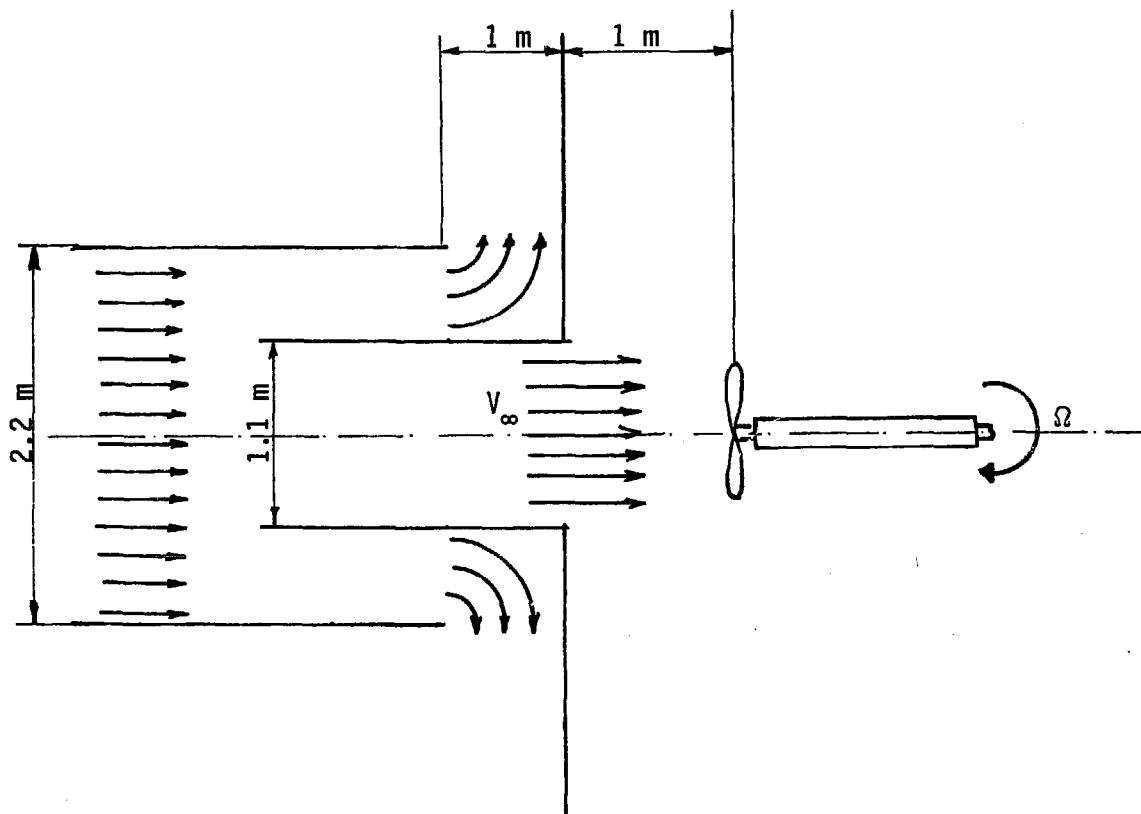in a 2.2 m as in a 4.4 m diameter free air stream.

Fig. 3.2. Reduced tunnelopening.

The ratio between the rotor swept area of the 0.75 m diameter rotor
and the cross sectional area of the free airstream of 2.2 m diameter
is 0.12. This ratio is such that this situation will yield the same
results as if the rotor were placed in a flow of infinite diameter.
This means that, with respect to the rotor diameter / air stream
diameter ratio, the test set up is representative for the atmospheric
wind.

A flow property that might affect the energy transformation by the
rotor is the degree of tubulence of the flow. From the construction
of the tunnel it is obvious that the flow is strictly not laminar.
The occurring turbulence is of a rather small scale due to the fine
wire gauzes. The natural winds are also rather turbulent but the
degree of turbulence as well as its scale is different in different
situations. Therefore no special arrangements were made to influence
nor to measure the degree or the scale of the turbulence. From the
blade chords of the rotors and the rotor speeds the Re-numbers for
the flow on the blade sections at 0.7 R were calculated as a function
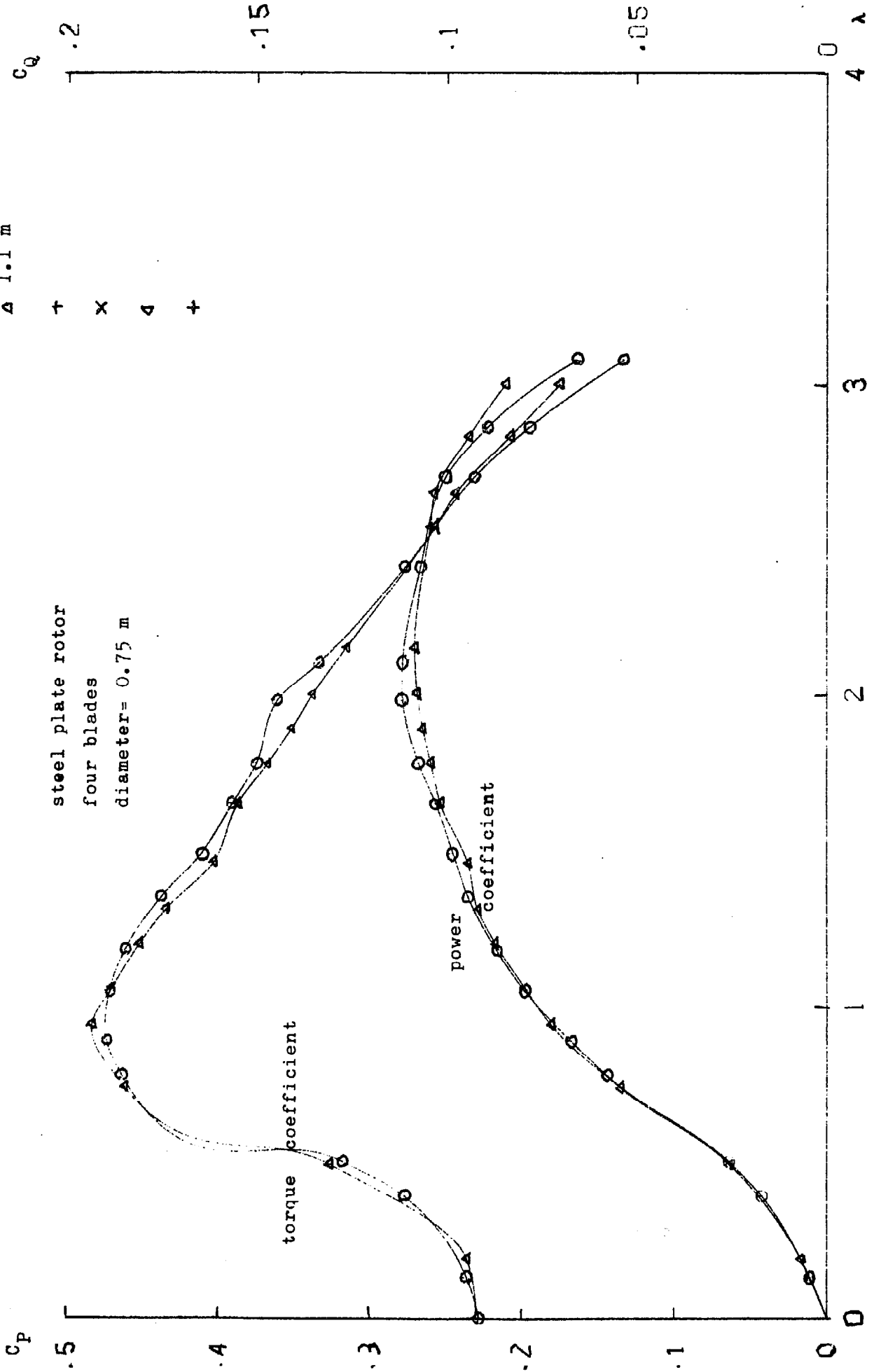of V_∞. See table 3.1. For the used airfoil sections the boundary

Figure 3.3

layer flow is estimated to be turbulent above Re = 10^5.
It may be expected that the turbulence of the free air stream from
the tunnel has only a very small effect on the performance of the
rotors, as V_∞ in the experiments was about 13 m s^{-1}.

airfoil	design	B	Re(r=0.7R)
steel plate	2	4	$3.5 \times 10^4 \times V_\infty$
"	3	4	$2.6 \times 10^4 \times V_\infty$
"	3	3	$3.4 \times 10^4 \times V_\infty$
"	5	3	$2.2 \times 10^4 \times V_\infty$
"	5	2	$3.2 \times 10^4 \times V_\infty$
sail trouser	3	4	$2.0 \times 10^4 \times V_\infty$
"	3	2	$4.1 \times 10^4 \times V_\infty$

Table 3.1. Re-numbers for several rotors as $f(V_\infty)$ at r=0.7R.

3.2. Regulation and measurements of power output and input.

As shown in fig. 3.1. the rotor is mounted on a shaft that is supported
by a tube. This axis is connected with a D.C. generator by means of an
elastic coupling. The field voltage of this generator may be adjusted
stepless between 0 and 240 = V while the resistive load that is
applied may be adjusted between 0.27 Ω and 3.6 Ω. In this way it is
possible to choose any number of revolutions between zero and maximum
for measurements and it is possible to find the total C_p-λ characte-
ristic.
The generator is mounted in bearings in such a way that the generator
as a whole is free to rotate around its axis except for the fact that
a support arm prevents a rotation. The torque that is generated by the
windmill is found by measuring the force that this arm of the generator

excerts on a force transducer as shown in fig. 3.4. Note that by calcu-
lating from this force the torque, the losses in the generator bearings
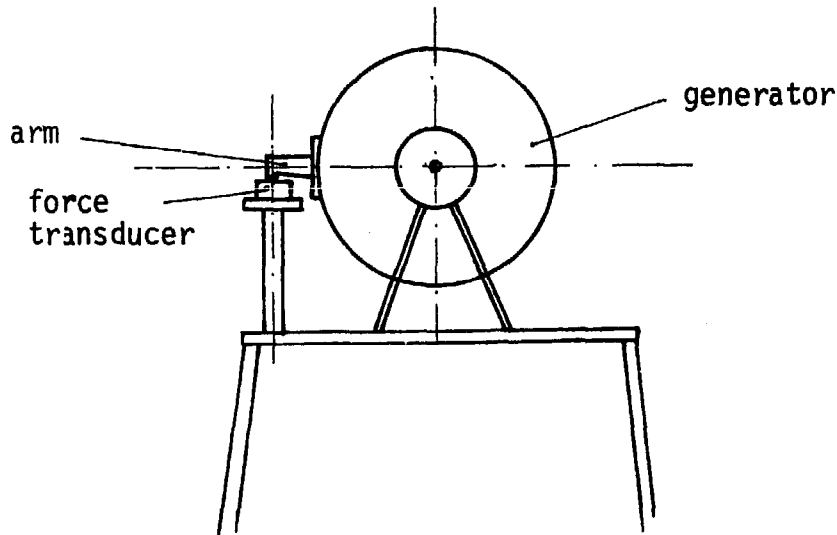and brushes are included.

Fig. 3.4. Measuring the torque

The force transducer is of the strain gauge type. The low voltage
output of this transducer is amplified and then converted into a
frequency. This is done with a voltage to frequency converter that
generates 1000 pulses per second per volt. By counting these pulses
during 10 seconds an integration of the signal is realized. In this
way the average of the varying output signal is measured; the variations
are caused by the generator acting together with the force transducer as
a mass spring system. During the same 10 seconds that the torque signal
is integrated, the number of revolutions is counted (6 pulses per
revolution during 10 seconds gives the number of revolutions per minute).
As explained in paragraph 3.1. the flow velocity may be adjusted by
means of the field voltage of the D.C. current generator that feeds the
motor of the fan. The power input for the windmill is

$$P_{in} = \frac{1}{2} \rho V_\infty^3 \pi R^2 \qquad\qquad (3 - 1)$$

Before the rotor tests were started the velocity field in the tunnel opening was measured and it was concluded that the highest local deviation was less than two percent of the average velocity.

The velocity is measured with help of a Pitot-tube; the pressure difference from this Pitot-tube is measured with a Betz-manometer. The Pitot-tube is placed in the tunnel 2 m before the opening at a spot where the velocity of the flow is equal to the average velocity in the tunnel opening. To be able to calculate the exact value of the air density the temperature and pressure of the air in the laboratory are measured and with these the air density is calculated.

3.3. Formulas for calculation of the tipspeed ratio, power coefficient and torque coefficient from the measuring data.

The pressure difference ΔP from the Pitot-tube is read from the manometer in mm water column. If h is the height of this column then

$$V_\infty = \sqrt{\frac{2\rho_w gh}{\rho_{air}}} \qquad (3 - 2)$$

$$\rho_{air} = \rho_{air}\ (t=0^oC,\ p=760\ mm\ Hg) \times \frac{273}{T} \times \frac{p}{760} \qquad (3 - 3)$$

where T = absolute temperature and p = air pressure in mm Hg

The tipspeed ratio λ is

$$\lambda = \frac{\Omega R}{V_\infty} = \frac{2\pi nR}{60V_\infty}$$

and the torque Q is

$$Q = F_g \times 1 = \delta \times \Delta NP \times 1 \qquad (3 - 5)$$

where ΔNP = number of counted pulses

1 = length of arm on generator that excerts a force on the force transducer.

δ = coefficient found from calibrating the force transducer including amplifier and voltage to frequency converter.

F_g = force as measured by the force transducer. See fig. 3.4.

C_P and C_Q may be calculated with

$$C_P = \frac{2\pi nQ}{\frac{60}{2}\rho V_\infty^3 \pi R^2} \qquad (3 - 6)$$

$$C_Q = \frac{Q}{\frac{1}{2}\rho V_\infty^2 \pi R^3} \qquad (3 - 7)$$

3.4. Calculation of the error in the power coefficient

$$C_P = \frac{Q\Omega}{\frac{1}{2}\rho V_\infty^3 \pi R^2} = \frac{Q\Omega}{\frac{1}{2}\rho (\frac{2\Delta p}{\rho})^{3/2} \pi R^2} \qquad (3 - 8)$$

Neglecting the error in ρ as calculated by (3 - 3) and the error in R, we may write

$$C_P = C \times \left(\frac{F_g \times 1 \times n}{(\Delta p)^{3/2}}\right) \qquad (3 - 9)$$

The error in factor δ in equation (3 - 5) is very small and will be neglected.

$$C_P = C \times (\Delta NP \times 1 \times n \times \Delta p^{-3/2}) \qquad (3 - 10)$$

$$dC_p = \frac{\partial C_p}{\partial \Delta NP}\ d(\Delta NP) + \frac{\partial C_p}{\partial T}\ dl + \frac{\partial C_p}{\partial n}\ dn + \frac{\partial C_p}{\partial \Delta p}\ d\Delta p \qquad (3-11)$$

Differentiating C_p in the way indicated in (3 - 11) and deviding equation (3 - 11) by C_p as given in (3 - 10) gives

$$\frac{\Delta C_p}{C_p} = \frac{\Delta(\Delta NP)}{\Delta NP} + \frac{\Delta l}{l} + \frac{\Delta n}{n} - \frac{3}{2}\ \frac{\Delta(\Delta p)}{\Delta p} \qquad (3-12)$$

ΔNP is the difference between the pulses as counted at some speed where we want to measure the torque and the pulses as counted when the rotor torque is zero. The error in ΔNP is estimated in the following way. The arm of the generator was lifted 10 times from and placed on the force transducer; because the generator is out of balance, a force acts always on the transducer, even if no torque is applied to the generator.

In this way 10 times the force on the transducer was measured by counting during 10 seconds the pulses as generated by the voltage to frequency converter. Of the results of these 10 measurements, the standard deviation s was calculated. As maximum error in NP 2s was used. Before every experiment the number of pulses NP must be counted and the number of pulses as counted for one torque measuring must be diminished with this initial number. Therefore the error in ΔNP might be 4s. The experiment as explained above resulted in s=40. Thus $\Delta(\Delta NP) = \pm 160$.

Δl is estimated 1 mm

Δn is maximum 1 rev/min

$\Delta(\Delta p)$ is estimated 0.2 mm water column

One of the rotors was tested and the following figures were measured.

Δp = 10.7 mm water column

ΔNP = 49000 pulses

n = 444 rev/min

l = 300 mm

With (3 - 12) the relative error in C_p can now be calculated

$$\frac{\Delta C_p}{C_p} = \frac{160}{150660} + \frac{1}{300} + \frac{1}{400} + \frac{3}{2}\frac{0.2}{10.7} = 0.0032+0.0033+0.0025+0.028=0.037$$

C_p as calculated from the above given figures with the equations in paragraph 3.3. is 0.36. With the relative error of 0.037 this result is to be interpreted as

$$C_p = 0.36 \pm 0.013$$

From the above given analysis it is concluded that the error in C_p is mainly due to the error in measuring Δp of the Pitot-tube. The influence of this error is about ten times higher than the error in each of the other ones and causes 75 percent of the possible error in C_p. Since all our measurements until now are done at the same flow velocity, the maximum C_p values of the other rotors will also include a maximum relative error of about 0.037.

Conclusions and remarks

- A test unit has been built for testing rotor models with diameters of 1.5 m.
- Experiments have shown that, with the chosen rotor-airstream diameter ratio, the finite dimensions of the free airstream have no significant influence on the test results.
- It is expected that the test results are representative for the behaviour of the same rotors in an atmospheric wind except for two aspects: degree of turbulence and the constancy of the flow. Comparative experiments should be carried out as soon as possible.
- Re-number of the flow on the blades, calculated with the chord of the blades at $r=0.7R$ at $V_\infty=13$ ms^{-1}, vary for optimum λ between 2.6×10^5 and 5.3×10^5.
- Flow velocity in the test unit may be adjusted between zero and 15 ms^{-1} and the load on the windmill may be adjusted in such a way that every point of the C_p-λ curve of the rotor can be tested.
- Maximum relative error in the maximum C_p values will be about 3.7 percent.

4.   ROTOR TESTS

Various rotors were tested with several configurations and blade-settings. The objective of every test was to find experimentally the C_p-λ and C_Q-λ characteristics of the rotor. These characteristics present the properties of the rotors in a form that allows comparison of these properties.

4.1.   Steel plate rotors

In chapter 2 the selection and design of these rotors was motivated and explained. In (6) a C_L-α characteristic of an arched steel plate is shown. Though this arched steel plate is not symmetric, it is thought that with this information a first choice of the angle of incidence α can be made. For a non-symmetrical arched plate the value of α is 3^0 for C_L = 0.8 and 4^0 for C_L = 1.0.
If the angle ϕ between the relative velocity and the plane of the rotor were known then it would be possible with

$$\beta = \phi - \alpha \qquad\qquad (1-29)$$

to calculate the desired blade setting β. The angle ϕ is only known for the ideal flow and may, for optimum energy extraction, be calculated with (1-54). The result is shown in Appendix VII where ϕ ideal is shown as $f(\lambda_r)$. Using these values for ϕ a design value for β is found for the blade element at r = 0.7R. Table 4.1. shows the chosen values of β.
The first rotor test showed a maximum C_p value at a smaller blade setting than the design value. We therefore concluded that the design value of α should be taken a little higher. For rotor 2 and 3 the angle of incidence α was taken 4^0. This proved to be incorrect as will be seen from the test results of rotor 2 and 3.

	λ	B	C_L	α^0	$\lambda_r(r=0.7R)$	$\phi(r=0.7R)$	$\beta_0(r=0.7r)$
1.	2	4	0.8	3	1.4	23.7	21
2.	3	3	0.8	4	2.1	17.0	13
3.	3	3	0.8	4	2.1	17.0	13
4.	5	2	0.8	3	3.5	10.6	7
5.	5	2	0.8	3	3.5	10.6	7
6.	5	2	1.0	4	3.5	10.6	7

Table 4.1. Determination of the blade setting

The rotors were tested in the following way. The blades of a rotor
were set at the value of β_0 from table 4.1. For about ten values of the
number of revolutions between zero and maximum, measurements were done
and C_p, C_Q and λ were calculated. Then the blade setting β was changed
a few degrees in an arbitrary direction and again the rotor was tested.
If the maximum value of C_p proved to be higher, the change of β was
repeated in the same direction, else β was changed in the opposite
direction. In this way a rotor was tested for several blade settings,
including the optimum one. This was done with each of the six rotors.
The results are shown on the next pages in fig. 4.1. up to and inclu-
ding 4.6.
Of the rotors that are designed for $\lambda = 5$ the leading edges were
rounded off and the trailing edges were sharpened. Fig. 4.7 shows
the effect of this measure on one of the rotors.

The marked points in fig. 4.1 - 4.7 are actual measuring results.
Different marks indicate different rotor tests as specified in the
figures. Fig. 4.8 shows the collection of the C_p-λ curves of the six
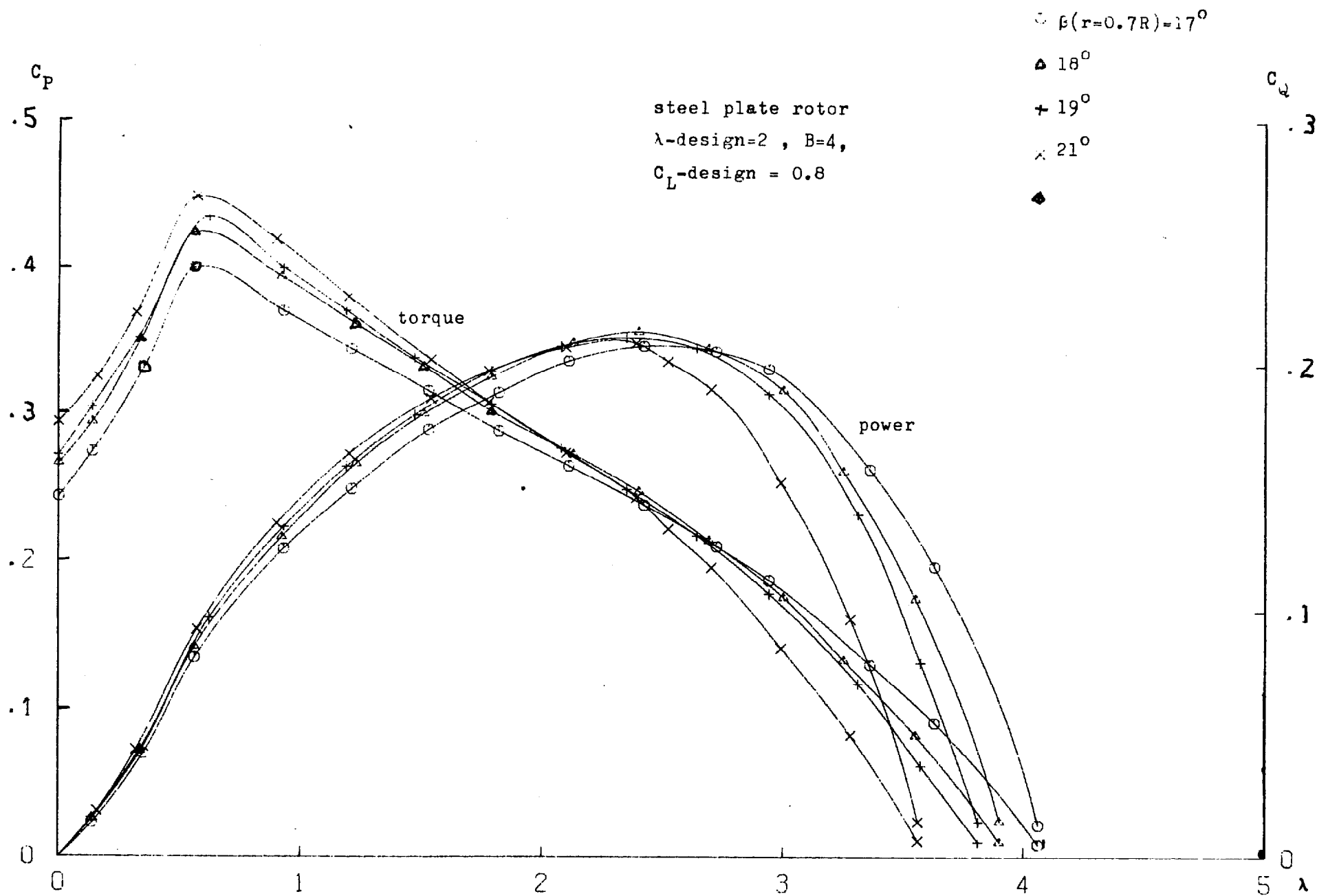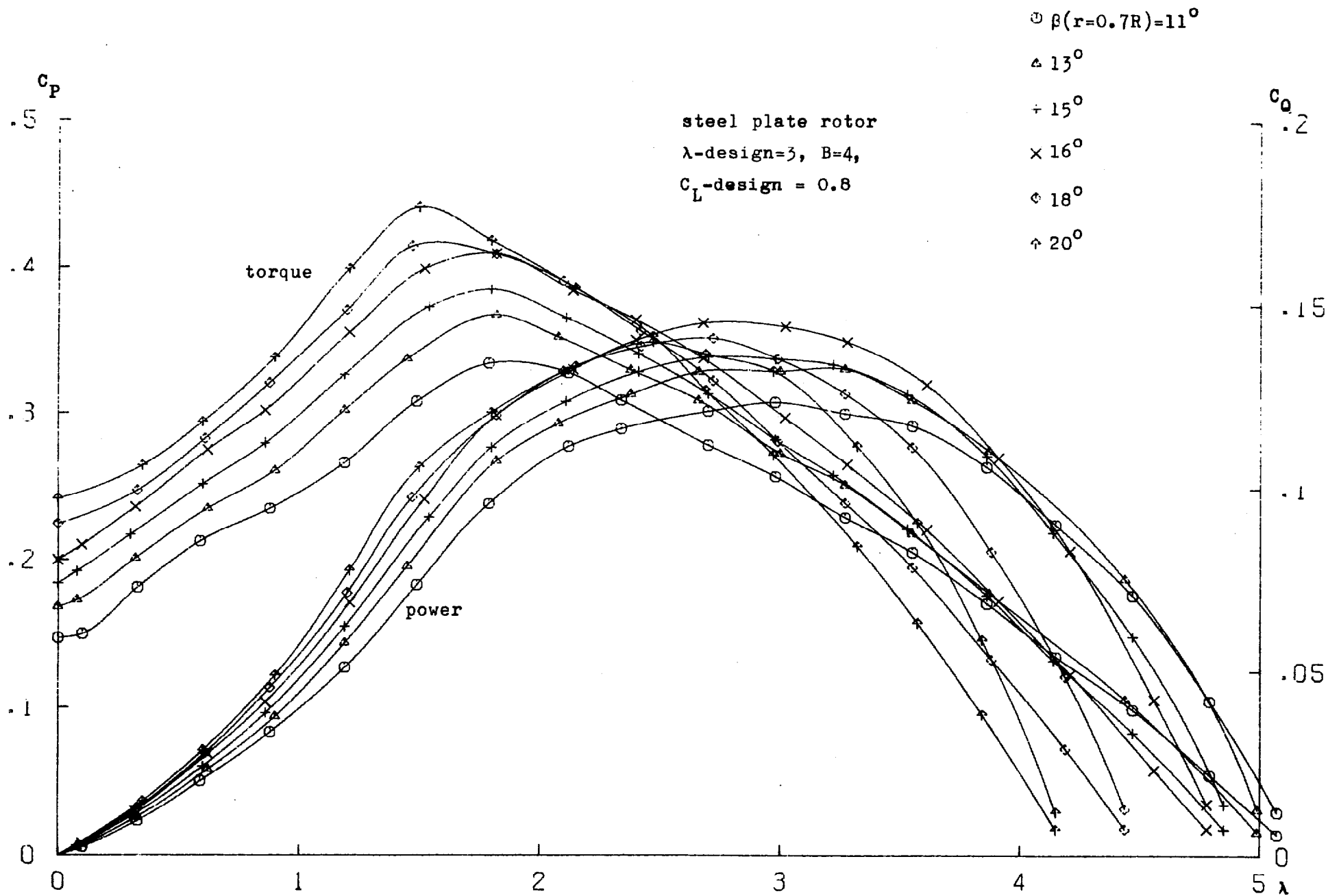steel plate rotors at their optimum blade settings.

C_P

.5

.4

.3

.2

.1

0

C_Q

.3

.2

.1

0

steel plate rotor
λ-design=2 , B=4,
C_L-design = 0.8

$\beta(r=0.7R)=17^{\circ}$
$\triangle$ 18°
$+$ 19°
$\times$ 21°

torque

power

0   1   2   3   4   5 λ

-62-
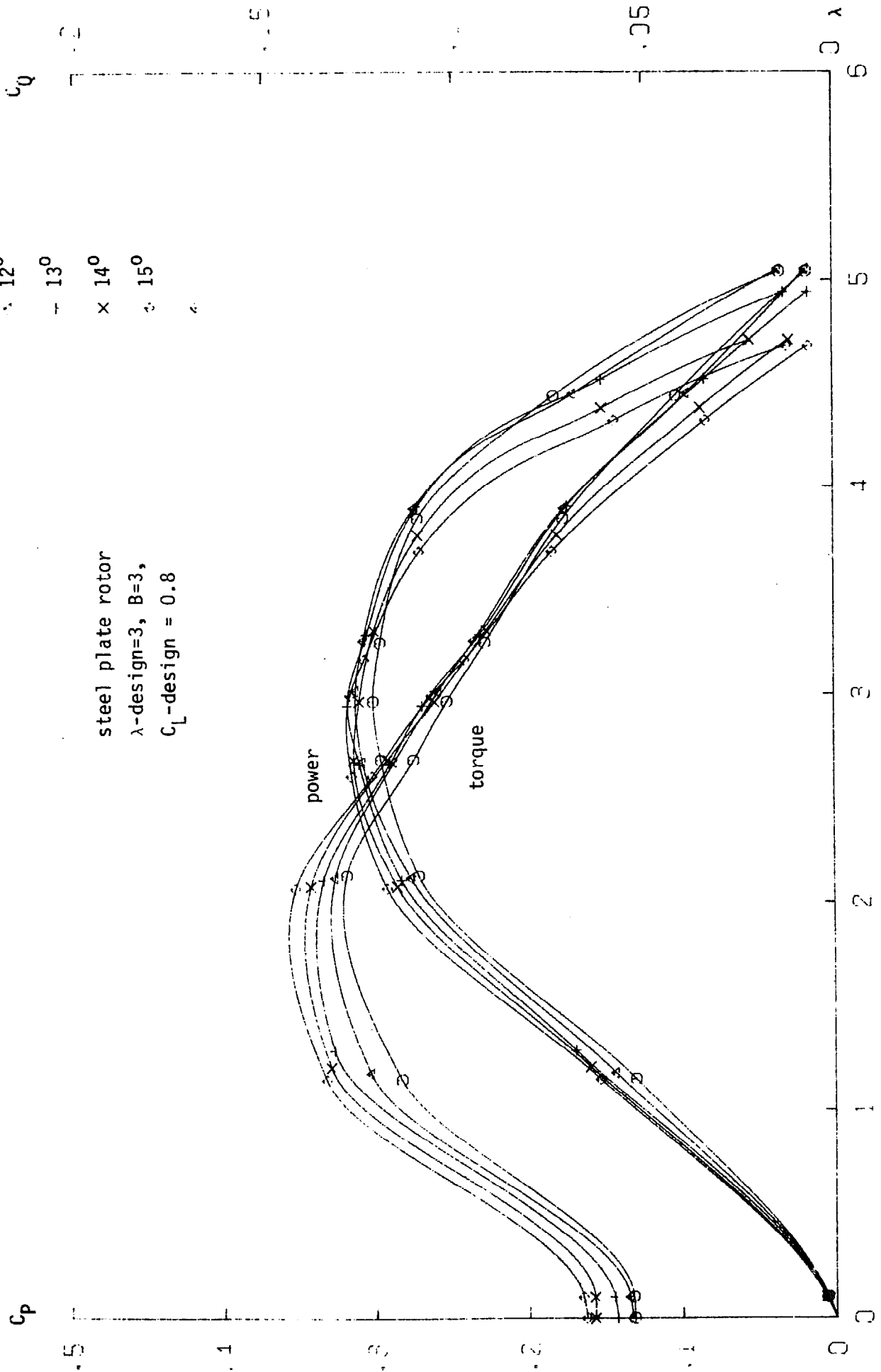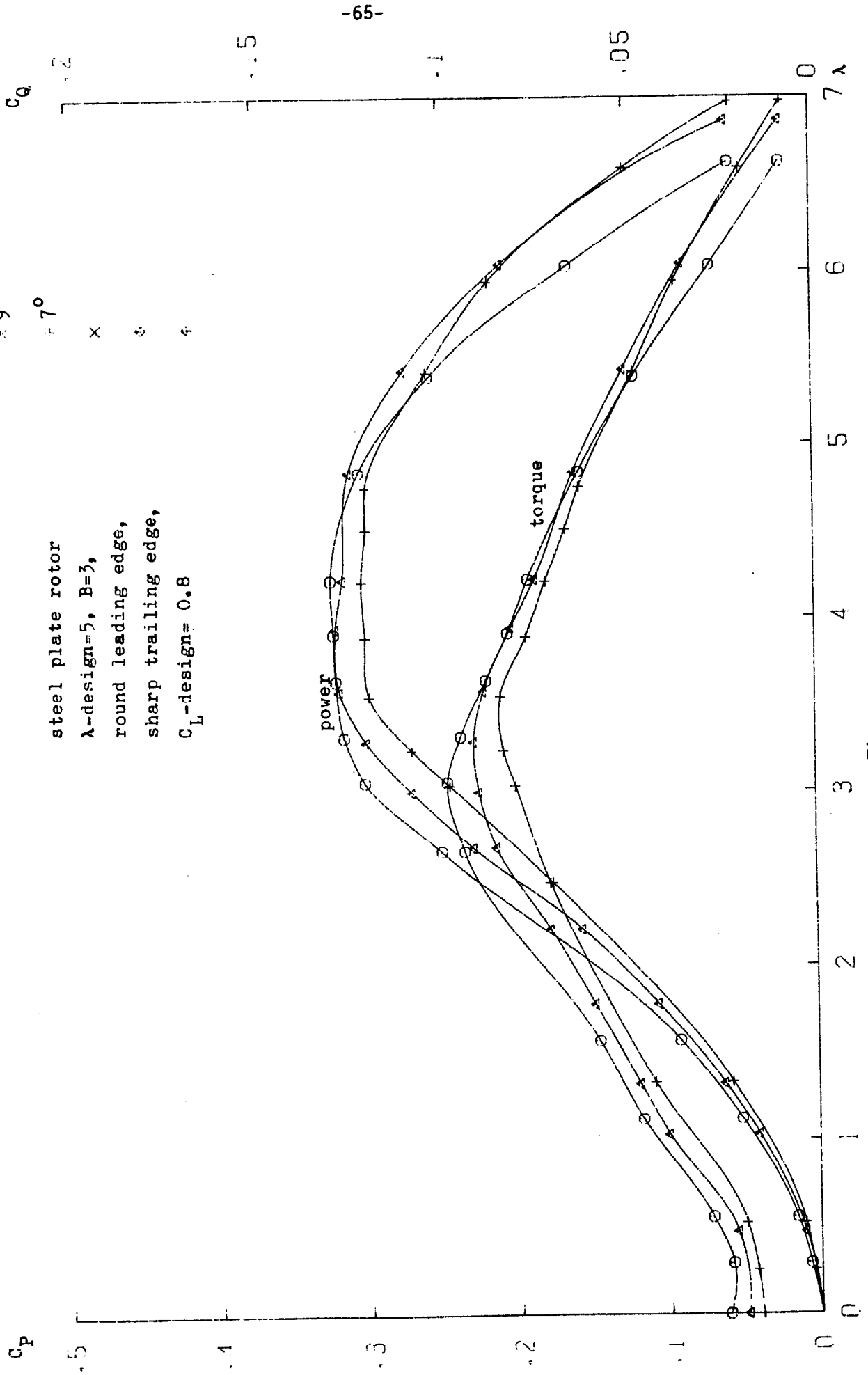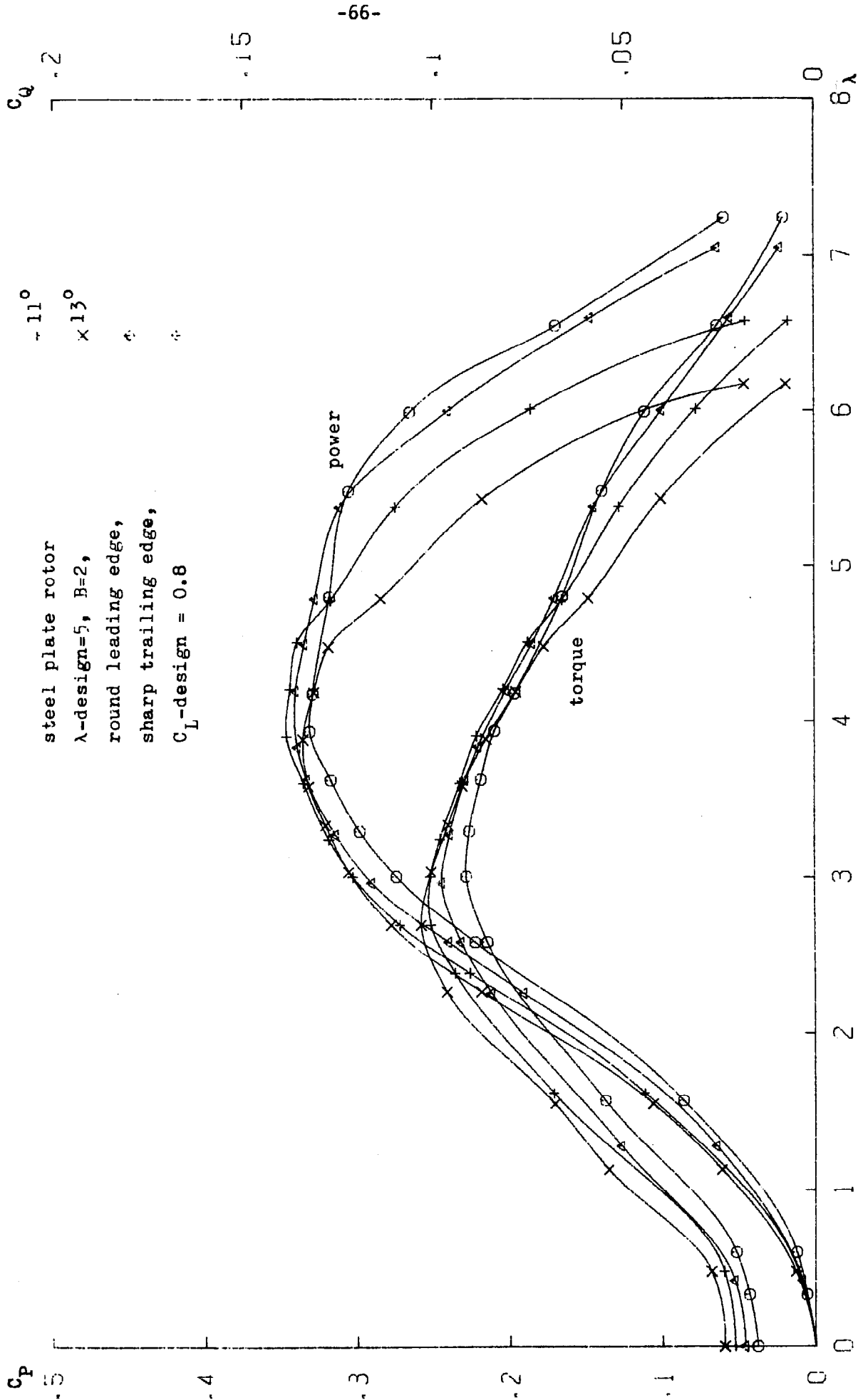
Figure 4.1

Figure 4.2
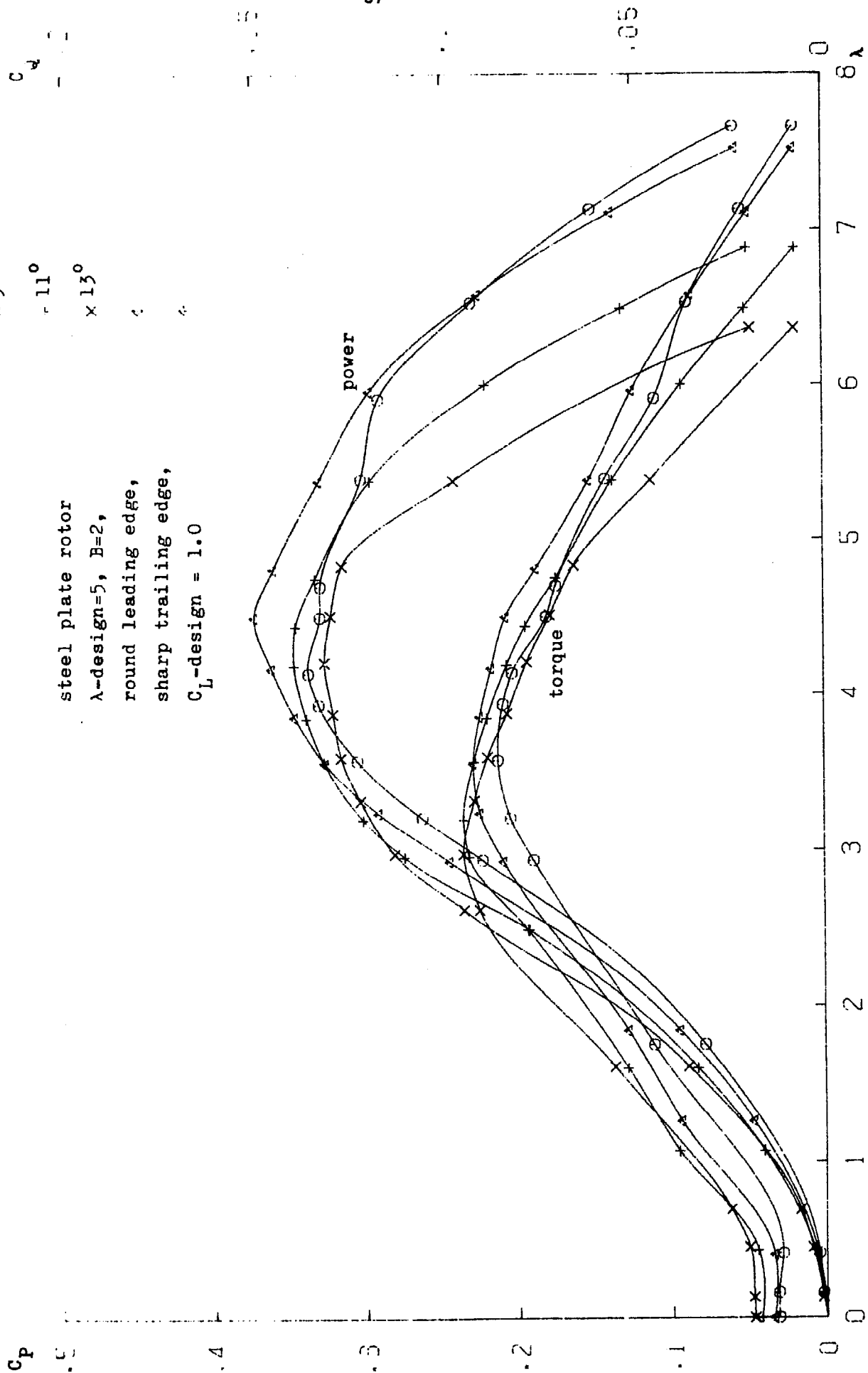
Figure 4.1
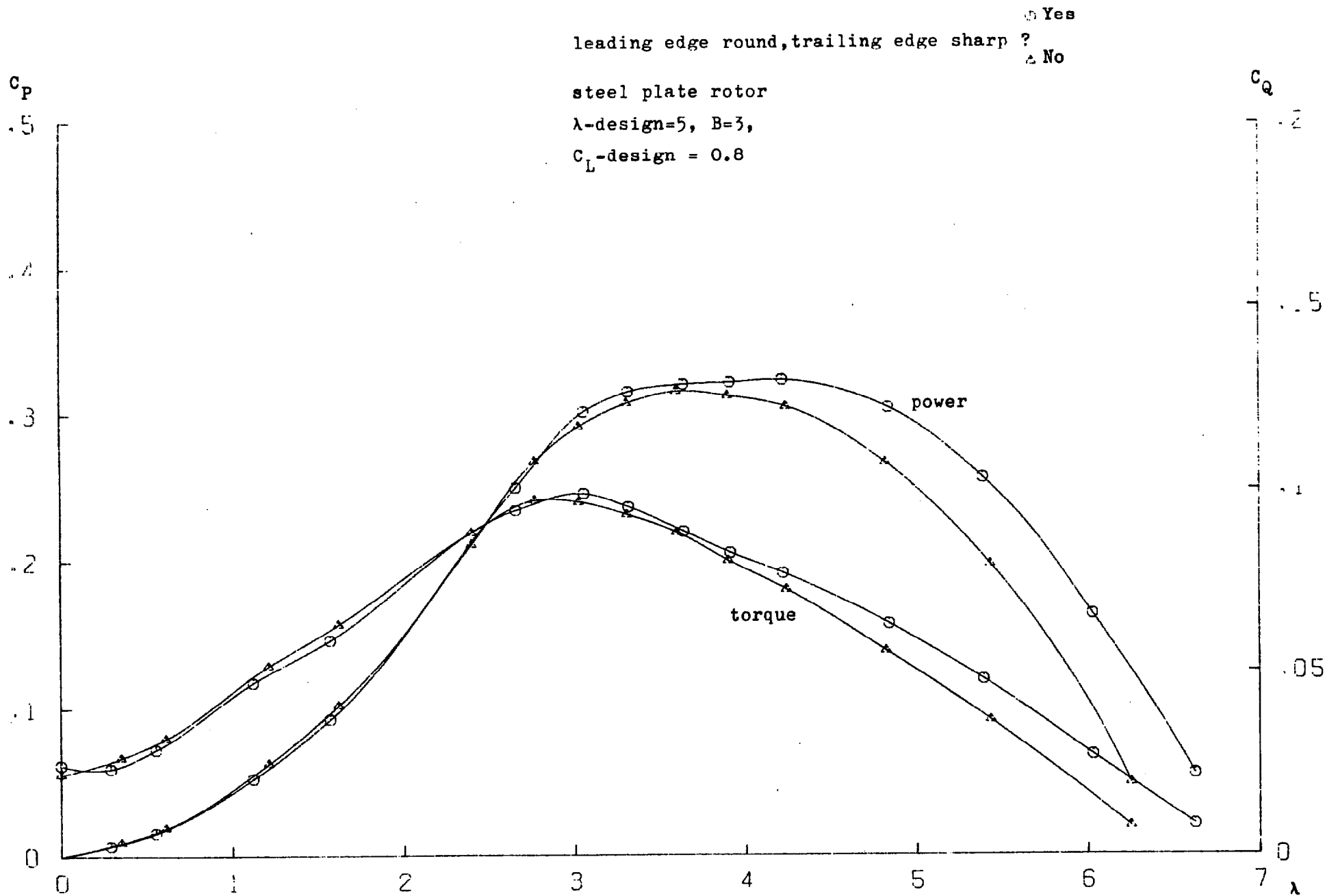
Figure 4.4

Figure 4.5

Figure 4.6

Figure 4.7

Collection of $C_p-\lambda$ curves of the tested
steel plate rotors at optimum blade setting

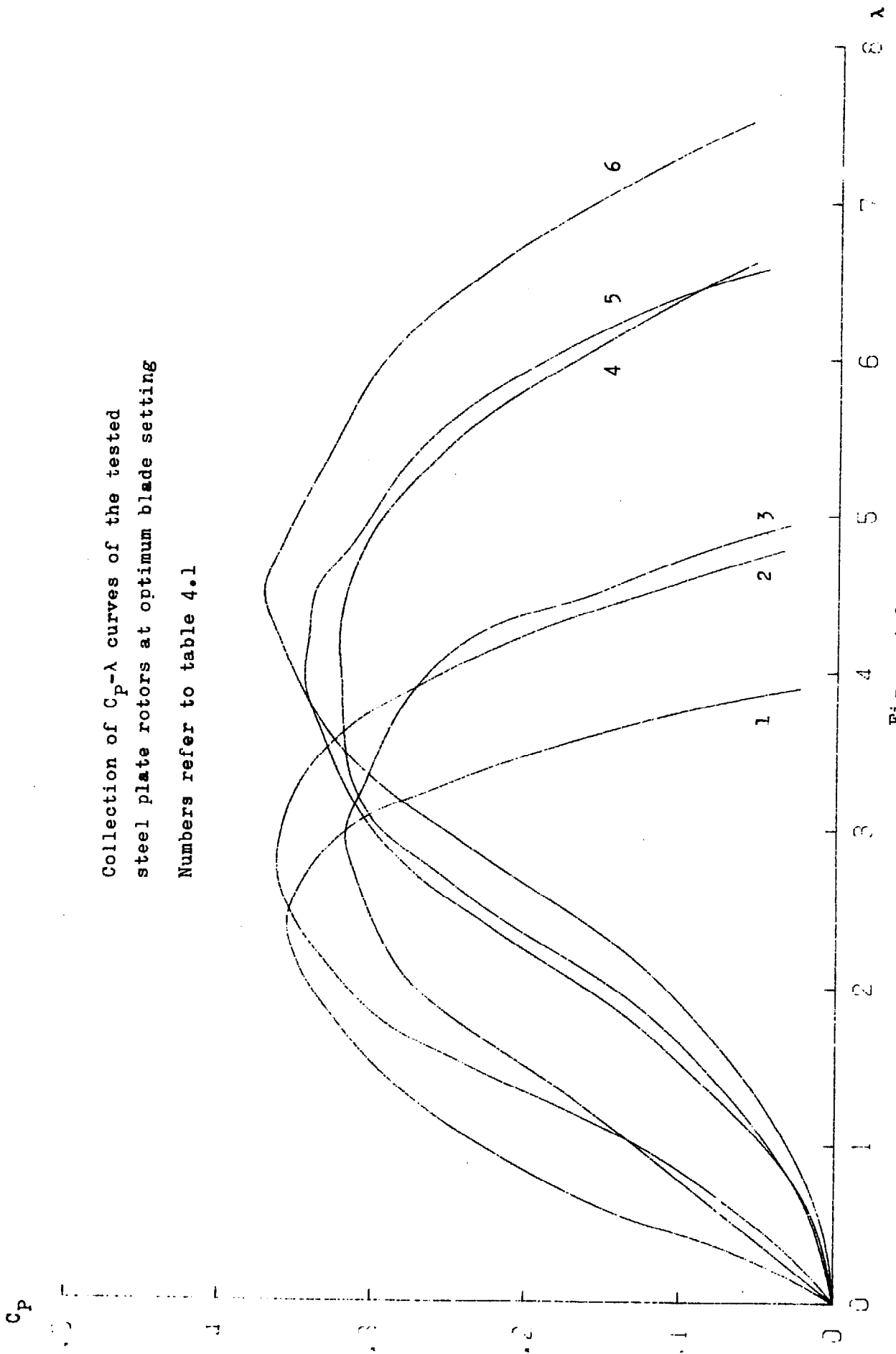Numbers refer to table 4.1

Figure 4.8

4.2.   Sail trouser rotors

The design of the form of the sail trouser blades was described in paragraph 2.1. The following blades are available:

- 4 blades, thickness 10 percent, maximum thickness at 25 percent
  of chord from leading edge; chords are linearized and are given
  by the formula: c = 0.25 - 0.19r
  Twist and blade setting are stepless adjustable. Average thickness
  can be influenced.
  These four blades will be referred to as ST-1.
- 2 blades, thickness 10 percent, maximum thickness at 25 percent
  of chord from leading edge, chords are linearized and are given
  by the formula: = 0.456 - 0.338r.
  Twist and blade setting are stepless adjustable. Average thickness
  can be influenced.
  These two blades will be referred to as ST-2.

With ST-1 a four bladed rotor (λ =3) and a two bladed rotor (λ =4.5)
were built and tested.
As explained in paragraph 2.1 the twist is linearized between
r = 0.5R and r = R. At 5 places between 0.5R and R the angle ϕ was
calculated (see Appendix VII) and with linear regression the best
straight line through these points (r, ϕ) was determined.
From this linear function ϕ = constant x r, the difference between
the blade angle of an element at the blade foot and of an element
at r=0.72 m was calculated; this difference is called the twist. It
is estimated that the desired lift coefficient will be realized by
the following angle of incidence

$$C_L = 1.0 \quad \text{at} \quad \alpha = 4^o$$

The blade setting β may now be calculated with equation (1 - 29).

$$\beta = \phi - \alpha \qquad\qquad\qquad (1 - 29)$$

In this way the desired blade settings and twists were calculated
and the results are given in table 4.2. The rotors are numbered
7, 8 and 9; numbers 1 until 6 were used for the steel plate rotors
of paragraph 4.1.

	λ	B	blade type	twist(foot-0.72 m)	β(foot)
7	3	4	ST-1	15.0^o	24°
8	3	2	ST-2	15.0^o	24°
9	4.5	2	ST-1	11.4^o	16°

Table 4.2. Design settings of the blades of the sail trouser rotors.

The sail trouser rotors were tested in the following way.
The four bladed design for λ = 3 was set according to table 4.2. and
tested in the same way as the steel plate rotors: at different
points between zero and maximum number of revolutions, the necessary
quantities were measured and C_p, C_Q and λ were calculated. Then the
blade setting was changed by 2 degrees and again the rotor was measured.
In this way the curves in fig. 4.9. are obtained. Then the twist was
changed by a few degrees while the blade angle at the tip was kept
the same as the tip blade angle that corresponds with the best C_p-λ
curve of fig. 4.9.
Again the rotor was measured and results are shown in fig. 4.10.
Twist changes only resulted in a small drop of C_p and therefore the
second design (ST-2-blades, λ=3, B=2) was only tested for several
blade settings with constant twist. Results are shown in fig. 4.11.
The third design (St-1-blades, λ=4.5, B=2) was tested the same way
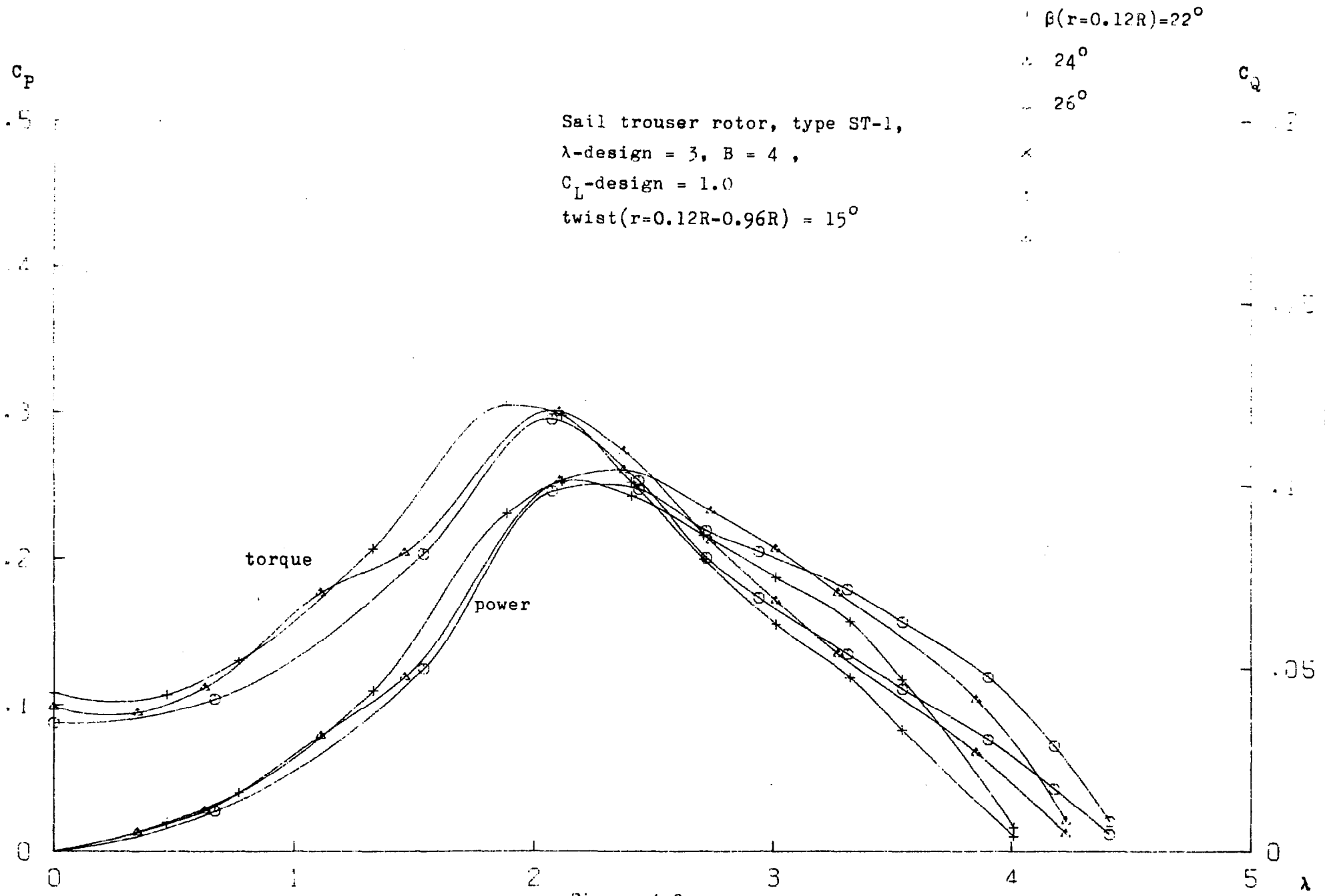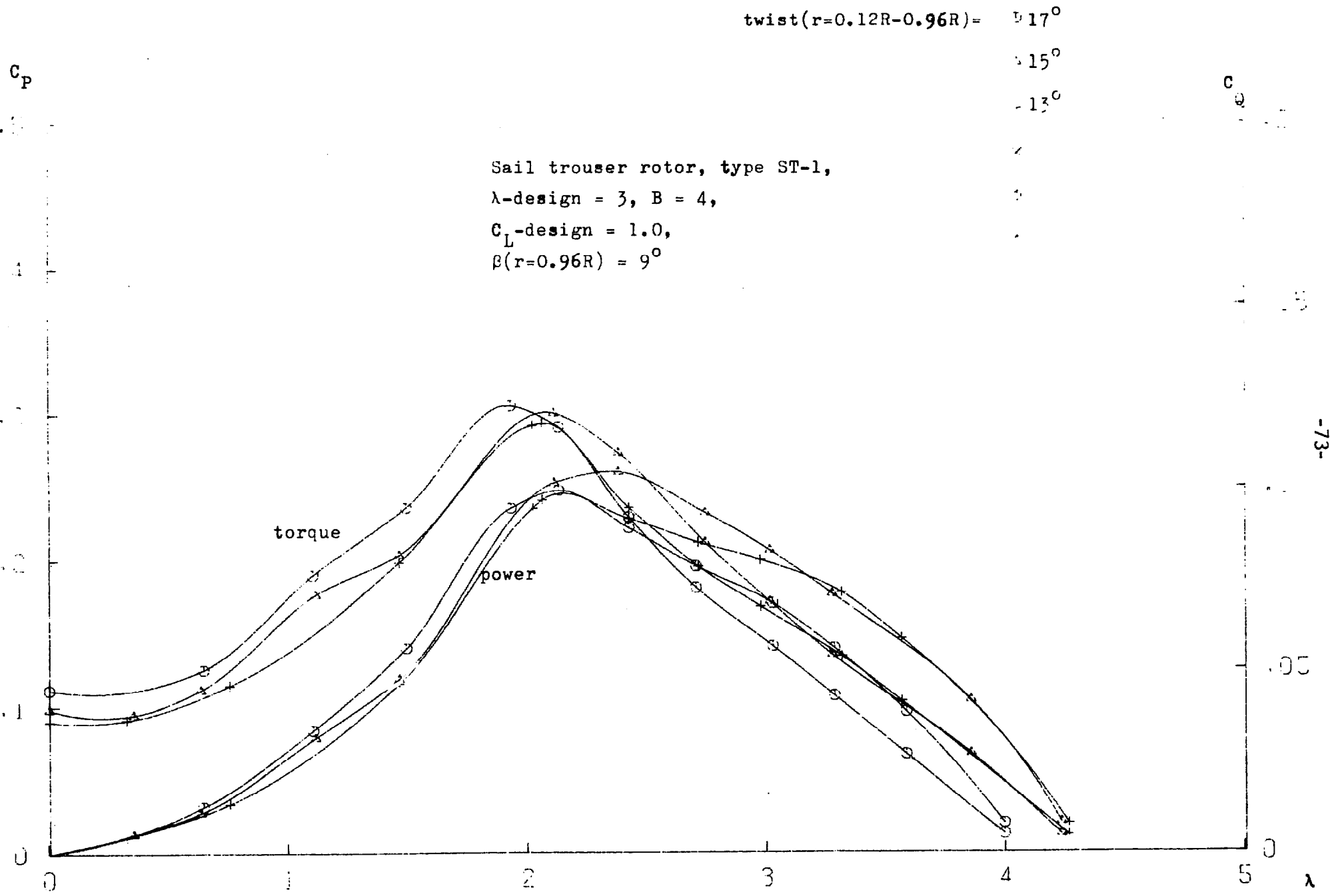and results are shown in fig. 4.12.

Figure 4.9

Figure 4.10

Figure 4.11

Figure 4.12

Sail trouser rotor, type ST-1 ,
λ-design = 4.5 , B = 2 ,
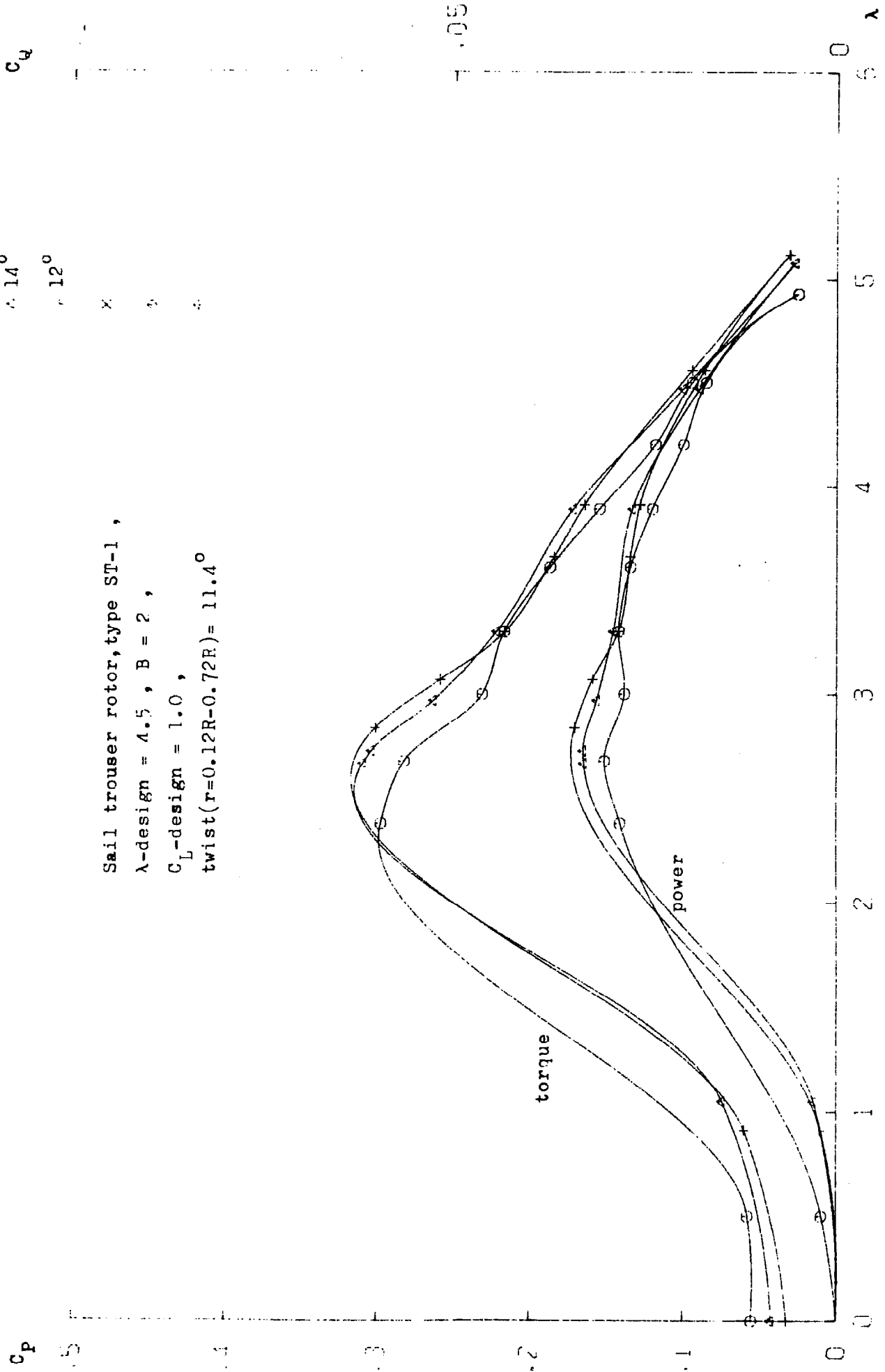C_L-design = 1.0 ,
twist(r=0.12R-0.72R)= 11.4°

β(r=0.12R)=16°

14°

12°

4.3. Interpretation and discussion of the test results

Table 4.3. shows a survey of the test results. Rotor numbers refer to the numbers as used in table 4.1. and 4.2.

rotor number	1	2	3	4	5	6	7	8	9
λ-design	2	3	3	5	5	5	3	3	4.5
β-design	21	13	13	7	7	7	24	24	16
C_P-maximum	0.36	0.37	0.32	0.32	0.34	0.37	0.26	0.22	0.17
λ-optimum	2.5	3	3	4	4	4.5	2.4	2.1	2.8
β-optimum	18	16	13	11	11	9	24	22	12
C_{Pmax} at β-design	0.35	0.33	0.32	0.30	0.31	0.32	0.26	0.20	0.15
λoptimum at β-design	2.4	3	3	4	4	4.1	2.4	2.1	2.7
$C_{Q(\lambda=0)}$ at β-optimum	0.160	0.080	0.057	0.025	0.021	0.014	0.043	0.037	0.009
$C_{Q(\lambda=\lambda_{opt})}$ at β-optimum	0.144	0.123	0.107	0.080	0.085	0.082	0.108	0.105	0.060

Table 4.3. Survey of the test results of steel plate rotors
number (1 - 6) and of sail trouser rotors number (7 - 9)

Comparison of the values of λ-design with the optimum values of λ shows a remarkable effect: for the rotor designed for $\lambda=2$ the optimum value of λ is higher than the design value, for λ-design = 3 the optimum value is equal to the design value, while for the other rotors the optimum value is lower. An explanation may be found in fig. 1.7. We interpreted the curves in fig. 1.7. as collections of maxima of C_P-λ curves that may be realized with fixed blade chords and blade settings. Although this interpretation is very helpful in selecting the design-λ, a more accurate interpretation is that one ideal curve (for one specific C_D/C_L-ratio) is the collection of points of different rotors that have

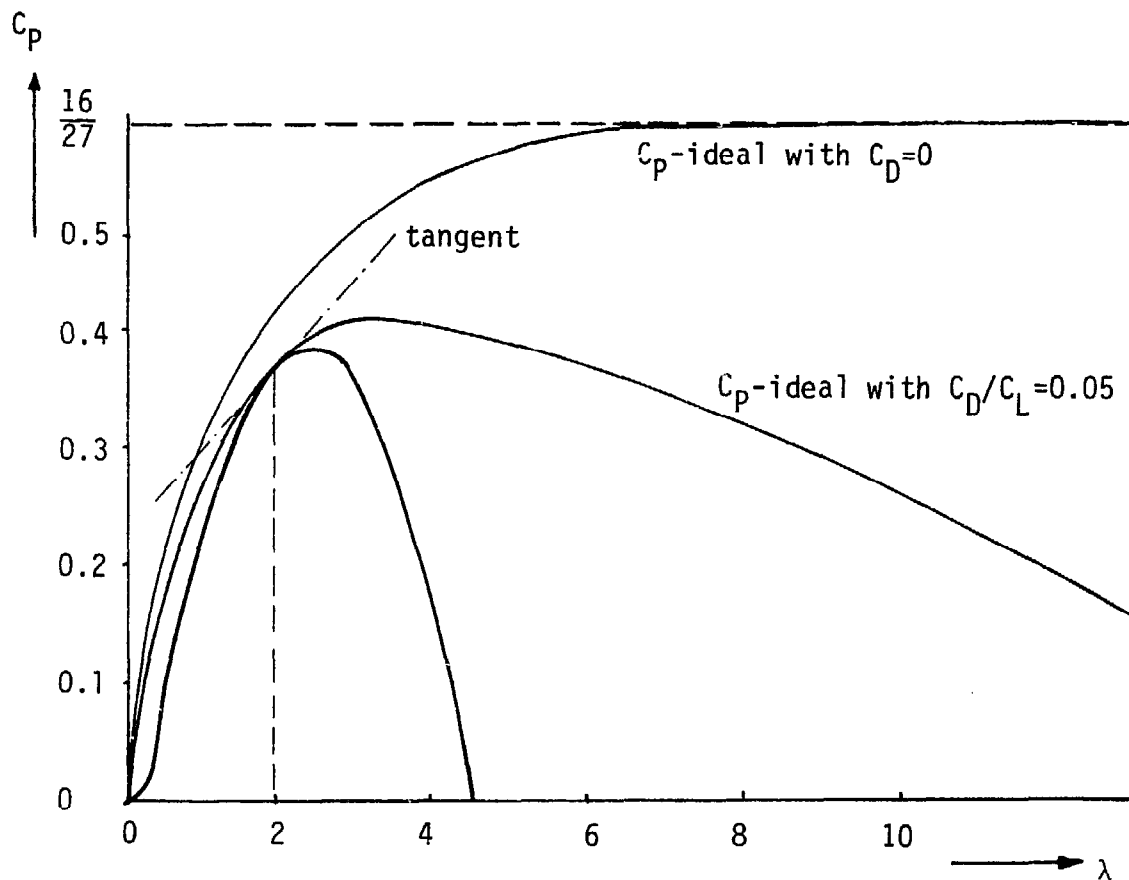'in that point a tangent common with the tangent of the ideal curve. See fig. 4.13.

Fig. 4.13. Interpretation of ideal C_p-λ curves.

Only if this tangent is zero the λ-optimum will be equal to λ-design. If λ-design is not chosen at λ where C_p-ideal (fig. 4.14) is maximum, then a tangent of zero is impossible for λ = λ-design, since this would imply that the design would have operating points outside the ideal C_p-λ curve. This is not possible because the ideal curve gives the maximum possible C_p-values for one specific C_D/C_L-ratio. In our design (λ = 2, B = 4) we assumed C_D/C_L=0.1. This assumption leads with fig. 1.7. to a choice of λ-design = 2. The C_D/C_L-ratio of 0.1 is too pessimistic, as will be seen further on in this paragraph. It will there be argumented that the true C_D/C_L-ratio is probably closer to 0.05. For this value ideal C_p-λ curves are drawn in fig. 4.13 and 4.14. The maximum value of this curve is reached between λ = 2.5 and λ = 3. This explains the differences in deviations of λ-optimum from λ-design: λ-design = 2 leads to a rotor with an optimum value of λ
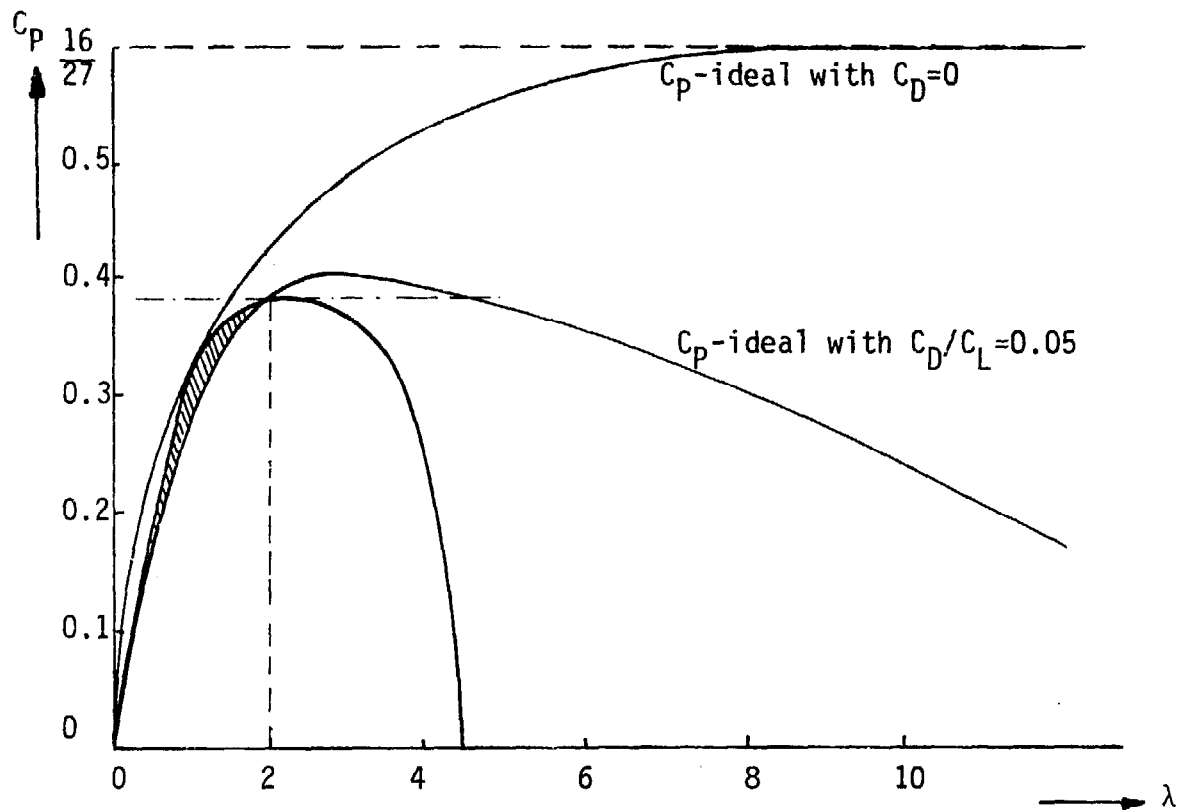
Fig. 4.14. Operating points outside the ideal C_p-curve are impossible.

higher than two because the tangent is possitive. See fig. 4.1. For λ-design = 3 this tangent is $\approx$ 0 and λ-design = λ-optimum while for λ-design > 3 the tangent is negative and therefore λ-optimum <λ-design. Comparison of β-design with β-optimum shows differences that may be influenced by both the angle of incidence α and the angle ϕ between the relative velocity and the rotor plane. The only steel plate rotor that shows a lower value for β-optimum than β-design is number 1.

This may be understood from the fact that for this rotor λ-optimum is higher than λ-design. Appendix VII shows that for higher λ-value the angle ϕ is lower and with equation (1 - 29) we can see that β will indeed be lower. The difference in λ-optimum between rotors with number 2 and 3 is insignificant as may be seen from fig. 4.3.: the difference between results of the rotor at β = 15° and β = 13° is smaller than the possible error as calculated in paragraph 3.4.

Comparison of C_p-maximum and λ-optimum at β-design with C_p-max and λ-optimum at β-optimum leads to the conclusion that the designed rotors were only slightly improved by correcting experimentally the blade setting.

For comparison of the measured C_p-values with theoretically possible C_p-values table 4.4. shows C_p-values calculated for different C_D/C_L-ratios and with different models. The C_p-values are calculated in the following way. For the optimum λ of the rotor, C_p-ideal ($C_D=0$) is calculated with (1 - 24). This value is diminished with the result of (1 - 38) and the result is multiplied with the value η_B from (1 - 50) C_p in table 4.4 indicates that η_B was calculated with the original model of Prandtl. See equation (1 - 50) and take $\sin\phi_1 = \dfrac{1}{\sqrt{1+\lambda^2}}$.

C_{Pm1} indicates that for this calculation the Prandtl model is modified by taking in equation (1 - 50) for ϕ_1 the angle ϕ. C_{Pm2} indicates that (1 - 50) was used with angle ϕ_1 as explained under equation (1 - 50). When considering the figures in table 4.4. it is absolutely essential to keep in mind that

- the measured values of C_p are measured at a real rotor, with a hub, with linearizations of for example the blade angles and with other concessions that have been made to the ideal design.
- the maximum relative error in C_p is smaller than 4 percent (see paragraph 3.4.)
- the calculated C_p-values are values to be reached with a theoretical design that is only approximated by our real constructions.

From the table we have drawn the following conclusions.

- Only the second modification of the Prandtl model and the assumption that $C_D/C_L = 0.05$ result in a calculated C_p-value that is higher than the measured C_p-value.
- Results with the sail trousers suggest that the C_D/C_L-ratio of the used sail trouser blades is higher than 0.1 but lower than 0.15. It is expected that the minimum C_D/C_L-ratio is 0.1, as was estimated for the design.

steel plates				$C_D/C_L = 0.05$			$C_D/C_L = 0.075$			$C_D/C_L = 0.1$		
λ-design	λ-opt	B	C_P-measured	$C_{P_{Pr}}$	$C_{P_{m1}}$	$C_{P_{m2}}$	$C_{P_{Pr}}$	$C_{P_{m1}}$	$C_{P_{m2}}$	$C_{P_{Pr}}$	$C_{P_{m1}}$	$C_{P_{m2}}$
2	2.5	4	0.36	0.348	0.382	0.419	0.319	0.351	0.385	0.291	0.320	0.351
3	3	4	0.37	0.361	0.391	0.422	0.326	0.352	0.381	0.290	0.314	0.345
3	3	3	0.32	0.332	0.370	0.411	0.300	0.334	0.371	0.267	0.298	0.331
5	4	3	0.32	0.347	0.377	0.408	0.300	0.326	0.353	0.254	0.275	0.298
5	4	2	0.34	0.305	0.347	0.392	0.264	0.300	0.339	0.223	0.253	0.286
5	4.5	2	0.37	0.313	0.348	0.388	0.262	0.294	0.328	0.214	0.240	0.268
Sail trousers				$C_D/C_L = 0.1$			$C_D/C_L = 0.15$					
3	2.4	4	0.26	0.291	0.320	0.351	0.235	0 258	0.283			
3	2.1	2	0.22	0.188	0.246	0.315	0.169	0.202	0.238			
4.5	2.8	2	0.17	0.223	0.266	0.314	0.141	0.160	0.181			

Table 4.4. Measured and calculated C_P-values.

Conclusions and remarks

- Comparison of test results with calculation results suggest that the Prandtl model is best used when modified in the way explained under equation (1 - 50) of chapter 1.

- C_D/C_L-ratio of the arched steel plates is probably 0.05 while C_D/C_L-ratio of sail trousers is minimum 0.1.

- Fig. 1.7. is a good help in selecting λ-design values. The optimum λ of a rotor designed for this selected value will only be equal to λ-design if λ-design corresponds with the value of λ that shows, for a chosen C_D/C_L-ratio, the highest C_p-value in fig. 1.7. If a specific design speed is the first criterion for selecting a rotor, this speed is to be translated in λ-design by the definition of λ ($\lambda = \Omega R/V_\infty$). Though the optimum value of λ will not necessarily be the same as λ-design, selection of another value for λ-design will not lead to a higher C_p-value at the design speed of the rotor.

- With rotors built from simple materials high power coefficients are possible.

- Deviations of blade angles from the ideal values result in small performance losses.

- Only the four bladed design for $\lambda = 2$ results in a rotor with a starting torque that is higher than the torque at maximum C_p. This property makes the design very suitable for constant torque loads: the same wind-speed that can start this rotor is enough for speeding up this rotor to the number of revolutions where C_p-maximum is reached. All other rotors would, under a constant torque load, need a higher wind speed for starting than is needed for working at λ-optimum.

5. SUMMARY OF CONCLUSIONS AND RECOMMENDATIONS

- To describe the tip losses it is possible to use different modifications of the Prandtl model.
- The modification that seems the most realistic, is using the angle ϕ_1 of the flow in the slipstream to calculate the distance between the vortex sheets of the slipstream.
- Reduction of efficiency losses due to tip losses is realized in propeller design by diminishing the tip chords. In windmill design not the inverse propeller efficiency but the power coefficient should be maximized. This leads to relatively large chords near the tips of the blades.
- A more accurate interpretation of the calculated chords is given. This does not result in a significant increase of the power coefficient but leads to less material use and a more simple manufacture.
- Calculation of stresses in windmill rotors is complex even if a static analysis were sufficient. For static loads no strength problems are expected. It is thought however that, in connection with expected fatigue problems, also an analysis with dynamic loads should be made. This analysis was not possible within the scope of this work.
- The static load on the blades under normal conditions is low but a storm will destroy each windmill that is not protected in some way.
- Stress calculations for the components of the sailtrouser frame are simple and no strength problems are expected.
- It is expected that the test results are representative for the behaviour of the same rotors in an atmospheric wind except for two aspects: degree of turbulence and the constancy of the flow. Comparative experiments should be carried out as soon as possible.
- Experiments have shown that, with the chosen rotor-airstream diameter ratio, the finite dimensions of the free airstream have no significant influence on the test result.
- Re-number of the flow on the blades, calculated with the chord of the blades at $r = 0.7R$ at $V_\infty = 13$ ms^{-1}, vary for optimum λ between 2.6×10^5 and 5.3×10^5.
- Flow velocity in the test unit may be regulated between zero and 15 ms^{-1} and the load on the windmill may be regulated in such a way that every point of the C_p-λ curve of the rotor can be tested.

- Maximum relative error in the maximum C_p value will be around 3.7 percent.
- Comparison of the test results with calculation results suggest that the Prandtl model is best used when modified in the way explained under equation (1-50) of chapter 1.
- C_D/C_L-ratio of the arched steel plates is probably 0.05 while C_D/C_L-ratio of sail trousers is minimum 0.1.
- Fig. 1.7. is a good help in selecting λ-design values. The optimum λ of a rotor designed for this selected value will only be equal to λ-design if λ-design corresponds with the value of λ that shows, for a chosen C_D/C_L-ratio, the highest C_p-value in fig. 1.7. If a specific design speed is the first criterion for selecting a rotor, this speed to be translated in λ-design by the definition of λ ($\lambda = \Omega R/V_\infty$). Though the optimum value of λ will not necessarily be the same as λ-design, selection of another value for λ-design will not lead to a higher C_p-value at the design speed of the rotor.
- With rotors built from simple materials high power coefficients are possible.
- Deviation of blade angles from the ideal values result in small performance losses.
- Only the four bladed design for $\lambda = 2$ results in a rotor with a starting torque that is higher than the torque at maximum C_p. This property makes the design very suitable for constant torque loads: the same windspeed that can start this rotor is enough for speeding up that rotor to the number of revolutions where C_p-maximum is reached. All other rotors would, under a constant torque load, need a higher wind speed for starting than is needed for working at λ-optimum.

LITERATURE

(1) Beurskens, J., Houet, M., Varst, P. v.d.
    Wind energy (in Dutch), diktaat no. 3323,
    Eindhoven University of Technology, Eindhoven, Netherlands,
    April 1974, 161 pp.

(2) Dobbinga, E.
    Some theory on airscrews (in Dutch), diktaat D 16,
    Delft University of Technology, Delft, Netherlands,
    March 1971, 95 pp.

(3) Durand, W.F.
    Aerodynamic Theory, volume IV, Dover Publications, Inc., 1965.

(4) Eiffel,
    The resistance of air and aviation, experiments at the Laboratory
    in Champs du Mars (in French), Paris, Dunod, 1910.

(5) Hul, F.A.J.R. v. 't,
    Fast running wind turbines, aerodynamics, (in Dutch), Twente Uni-
    versity of Technology, dept. of mechanical engineering, group
    mechanization, Netherlands, 1975.

(6) Jansen, W.A.M.
    Literature survey horizontal axis fast running wind turbines for
    developing countries, March 1976, 44 pp.

(7) Schmitz, F.W.
    Aerodynamics of flying models, measurements at airfoil sections I,
    (in German), Luftfahrt und Schule, Reihe IV, volume I (1942).

(8) Wilson, R.E., Lissaman, P.B.S.
    Applied aerodynamics of wind power machines,
    Oregon State University, U.S.A., May 1974, 106 pp.

(9) Park J.
    Symplified Windpower Systems for Experimenters,1975,Helion
    Sylmar, California, 80pp.
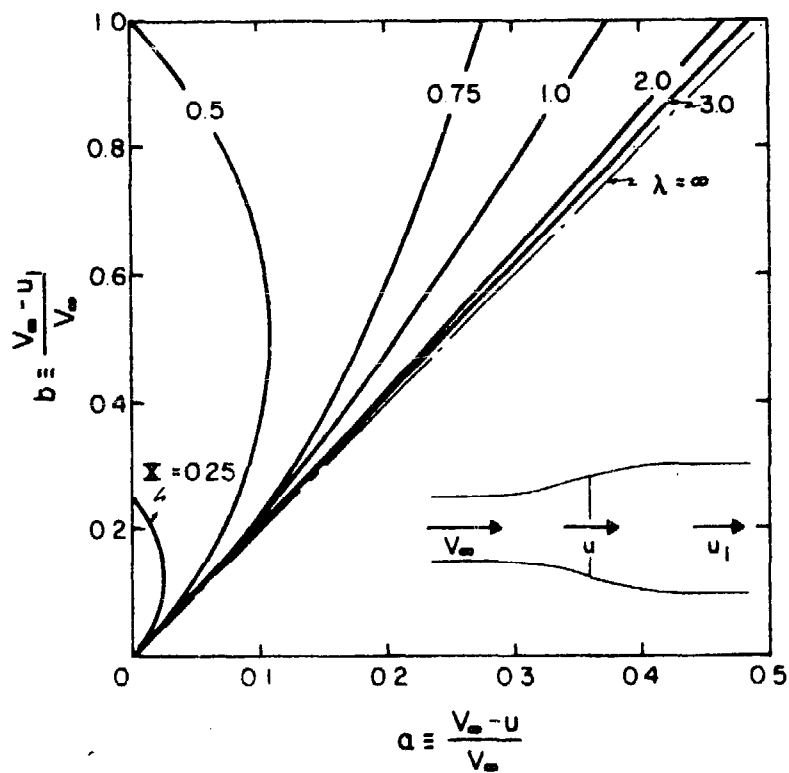
Effect of Tip Speed Ratio on the Induced Velocities for Flow with an Irrotational Wake.

Schematic representation of energy conversion on blade element Δr at radius r
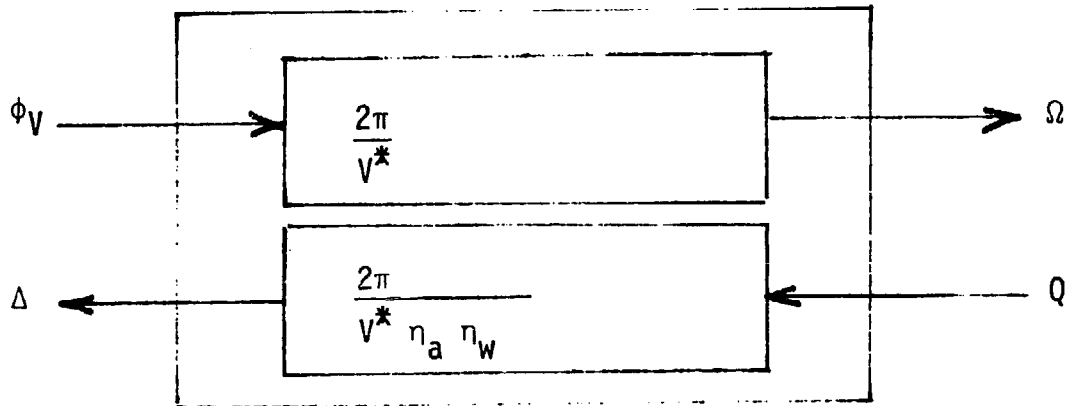
$\phi_V = V_\infty \cdot 2\pi r \Delta r \quad ;$

$\Delta = 0.5\rho V_\infty^2 \quad ;$

$C_p = \dfrac{P_{out}}{P_{in}} = \dfrac{\Omega \cdot Q}{\Delta \cdot \phi_V} = n_a \cdot n_w = \dfrac{P}{0.5\rho V_\infty^3 A} \quad ;$

$n_a = \dfrac{(1-a)^2}{\sin\phi} \cdot \sigma C_L \lambda_r \quad ;$

$\lambda_r = \dfrac{\Omega r}{V} \quad ; \quad \sigma = \dfrac{Bc}{2\pi r} \quad ;$

$n_w = (1 - \dfrac{C_D}{C_L} \cot\phi) \quad ;$

$\tan\phi = \dfrac{(1-a)}{(1+a')\lambda_r} \quad ; \quad \alpha = \phi - \beta \quad ; \quad C_L = f(\alpha) \quad ; \quad C_D = f(\alpha) \quad ;$

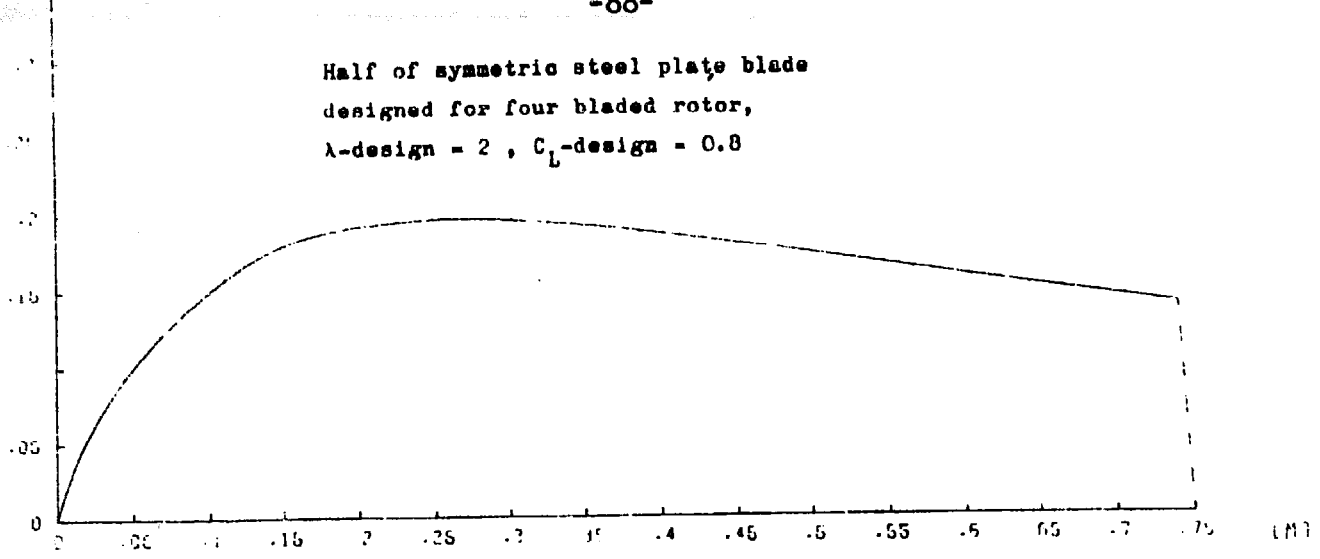$V^* = \dfrac{(2\pi r)(2\pi r \Delta r)}{\lambda_r} = P_{aer} \cdot (2\pi r \Delta r) \quad ;$

$a = \dfrac{2S_y F + F - \sqrt{F^2 + 4S_y F(1-F)}}{2(S_y + F^2)} \quad ; \quad S_y = \dfrac{\sigma C_L \cos\phi}{4\sin^4\phi} \quad ;$

$a' = \dfrac{1}{\dfrac{F(1-aF)}{S_x(1-a)} - 1} \quad ; \quad S_x = \dfrac{\sigma C_L}{4\cos\phi} \quad ;$

$F = \dfrac{2}{\pi} \arccos e^{-f} \quad ; \quad f = \dfrac{B}{2}(1 - \dfrac{r}{R}) \dfrac{1}{\sin\phi_1} \quad ; \quad \phi_1 = \dfrac{\phi}{2} \quad ;$

Half of steel plate blade
B = 2, λ-design = 5, C_L= 0.8

--------------- straight path
--.--.--.--. circular path
——————— compromise

Half of steel plate blade
B = 3 , λ-design = 5 , C_1=0.8

Half of steel plate blade
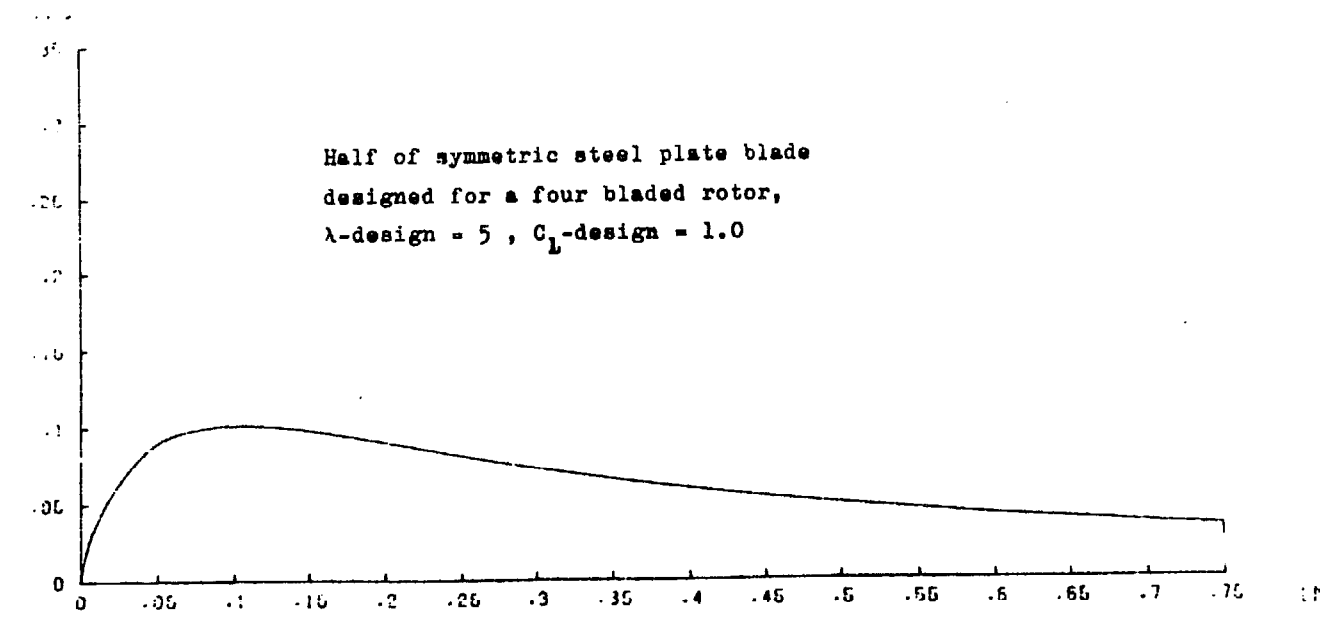B = 4, λ-design = 2, C_L= 0.8
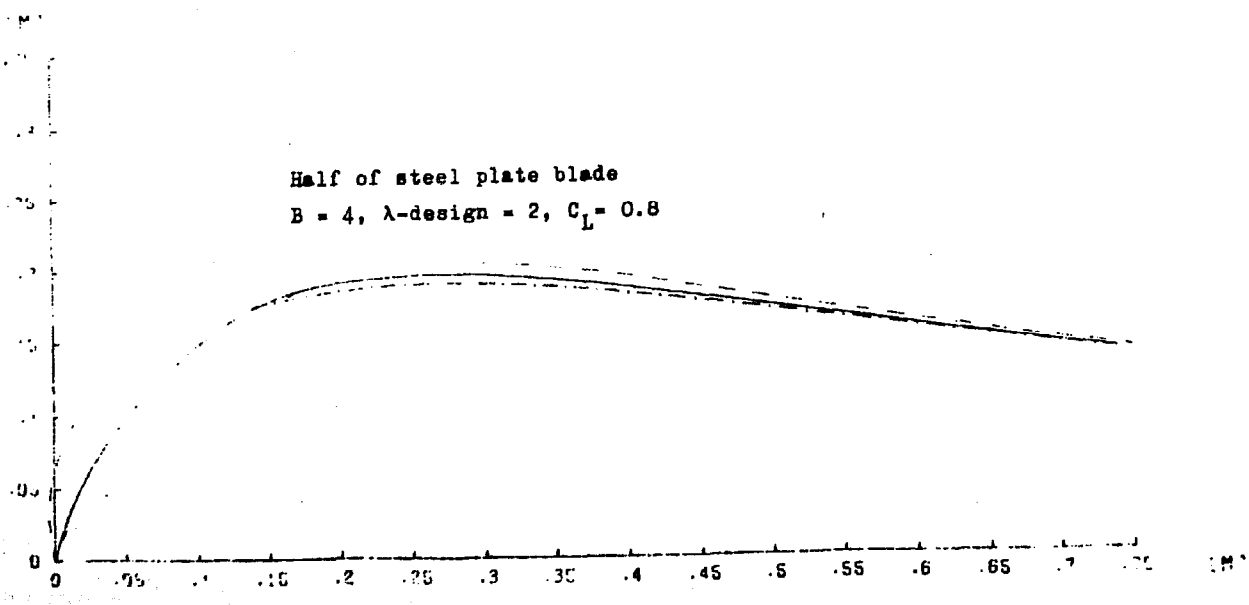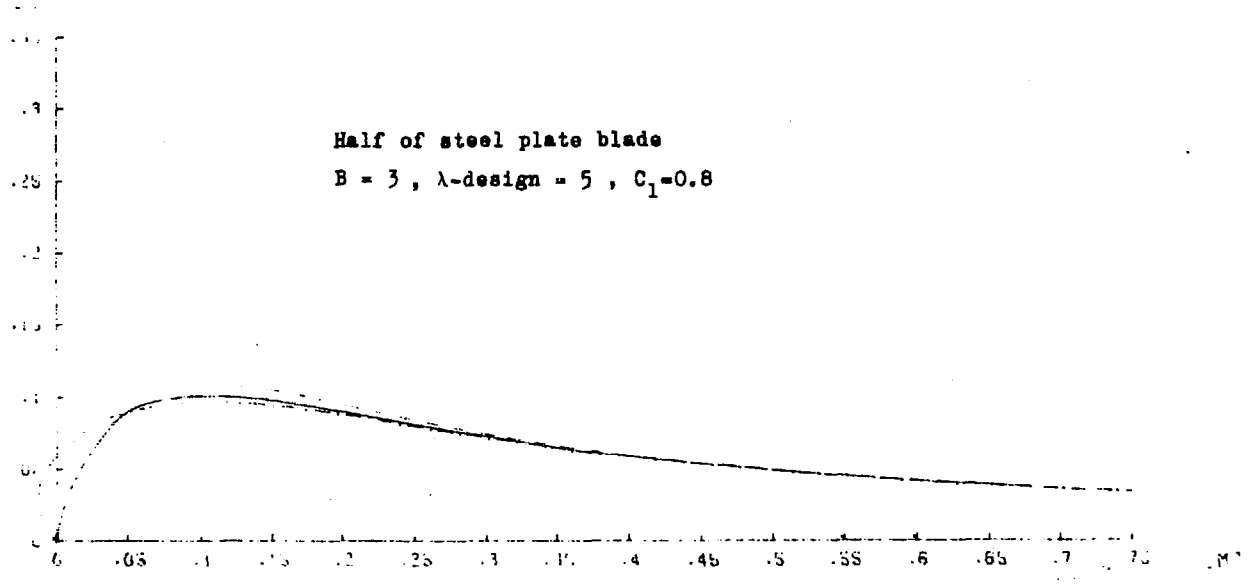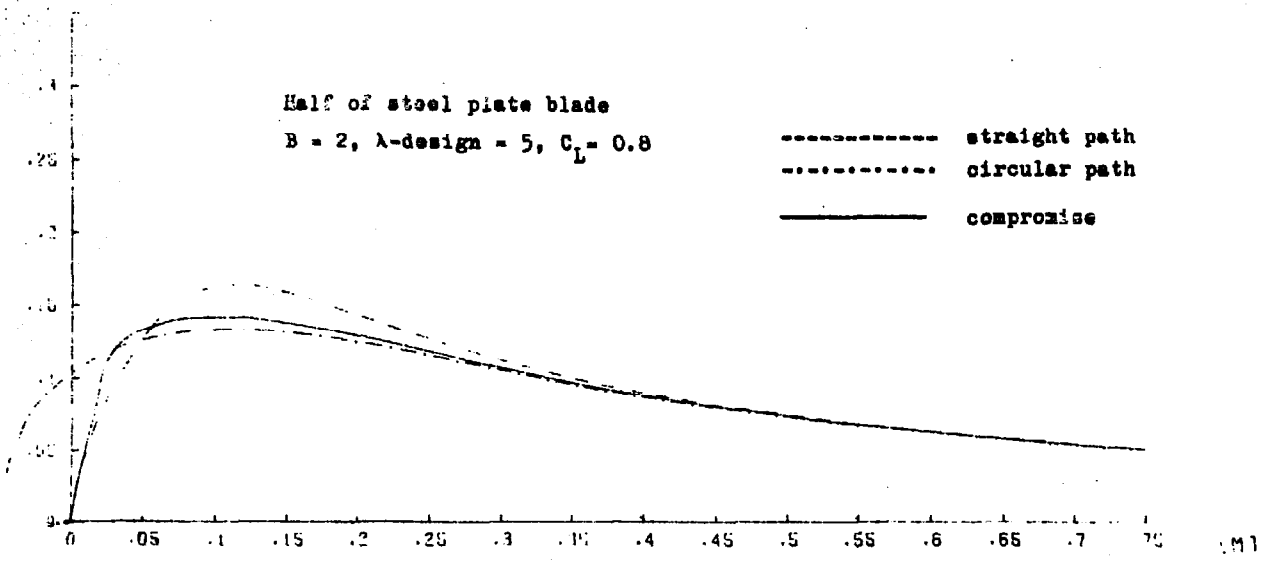
Half of symmetric steel plate blade
designed for four bladed rotor,
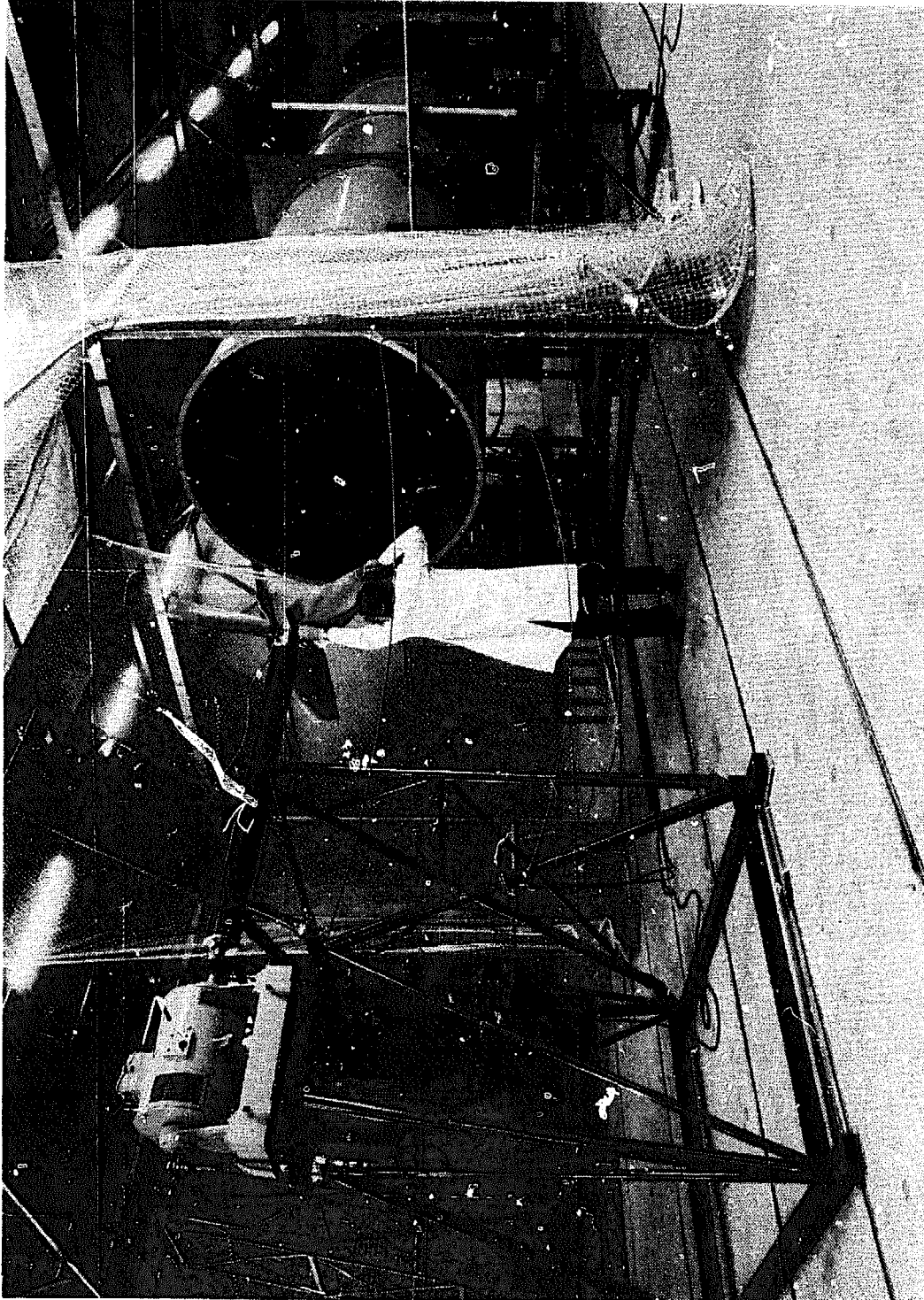λ-design = 2 , C_L-design = 0.8

[M]

Half of symmetric steel plate blade
designed for a four bladed rotor,
λ-design = 3 , C_L-design = 0.8

[M]
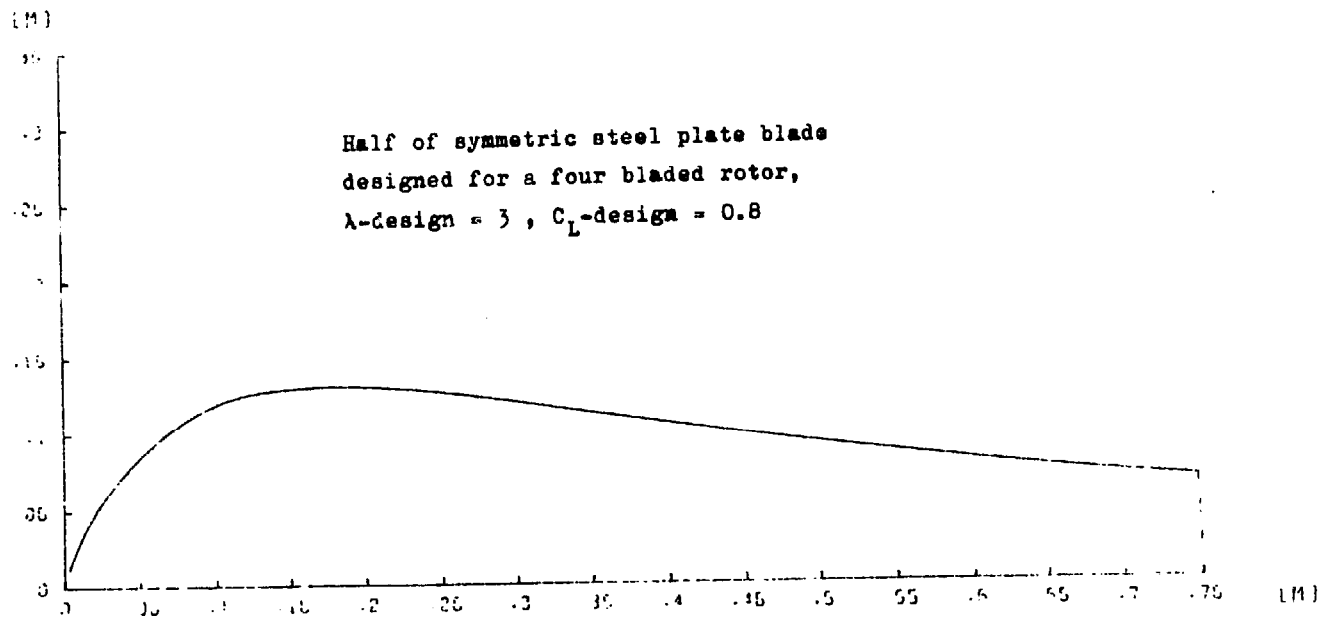
Half of symmetric steel plate blade
designed for a four bladed rotor,
λ-design = 5 , C_L-design = 1.0

[M]

$$\lambda_r = \frac{\sin\varphi(2\cos\varphi - 1)}{(1-\cos\varphi)(2\cos\varphi + 1)}$$

λ_r	φ
10.00	3.807
9.75	3.904
9.50	4.006
9.25	4.113
9.00	4.227
8.75	4.347
8.50	4.473
8.25	4.607
8.00	4.750
7.75	4.902
7.50	5.063
7.25	5.236
7.00	5.420
6.75	5.618
6.50	5.831
6.25	6.060
6.00	6.308
5.75	6.577
5.50	6.870
5.25	7.190
5.00	7.540
4.75	7.926
4.50	8.353
4.25	8.827
4.00	9.357
3.75	9.954
3.50	10.630
3.25	11.402
3.00	12.290
2.75	13.322
2.50	14.534
2.25	15.975
2.00	17.710
1.75	19.830
1.50	22.460
1.25	25.773
1.00	30.000
0.75	35.420
0.50	42.290
0.25	50.642
0.00	60.000
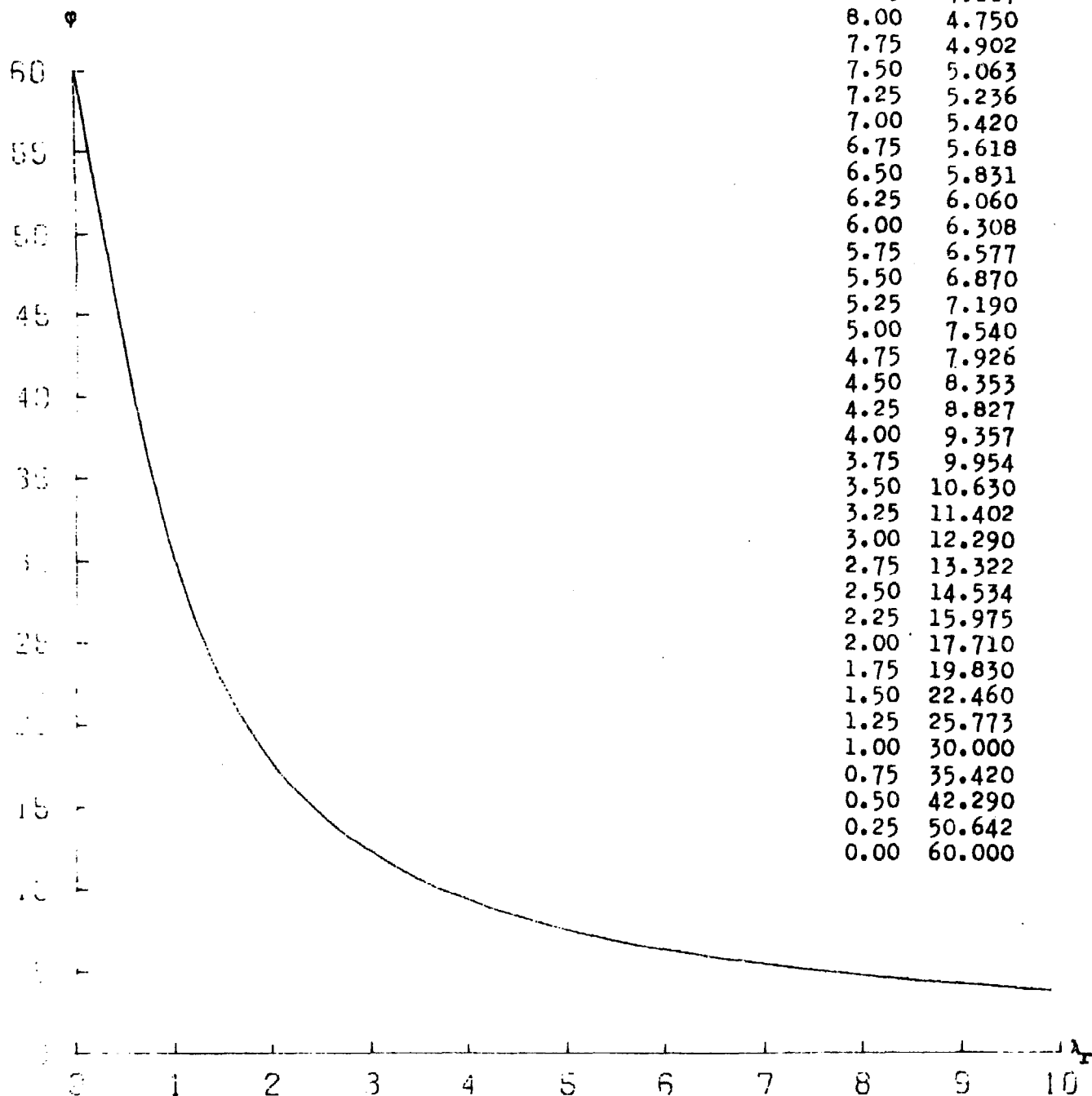
Angle φ between relative velocity and plane of the rotor versus the speed ratio of an element at radius r for a windmill with a flow equal to the flow of an ideal windmill.

List of used instruments.

- Electronic Counter (6 digits), Hewlett/Packard, 5532A

- Electronic Counter (4 digits), Venner Electronics Ltd, TSA 6634

- Static/Dynamic strain indicator, Peekel N.V. , 540 DNH

- Voltage to frequency converter, Dymec, DY-2211A/B

- Force transducer, H.B.M., range 0-10 kg, U1

- Force transducer, Iweco, range 0-100 kg, ED335

- Oscilloscope, Hewlett/Packard, 130C

- Digital volt meter, Teletec Airtronic, TE 350

- Betz micro manometer, van Essen

- Pitot tube, Iweco

- Photo-electric cell, v.d. Heem

- Amplifier, v.d. Heem, 9818

- Barometer, System Paulin A.B.

- Laboratory thermometer.